الجمهورية الجزائرية الديمقراطية الشعبية
République Algérienne démocratique et populaire

وزارة التعليم العالي والبحث العلمي
Ministère de l'enseignement supérieur et de la recherche scientifique

جامعة سعد دحلب البليدة
Université SAAD DAHLAB de BLIDA

كلية التكنولوجيا
Faculté de Technologie

قسم الإلكترونيك
Département d'Électronique

Final Project Dissertation

Presented by

Mr. AZZEDINE BOUTELHIG

In Partial Fulfillment of the Requirements for the Master in Electronic Engineering (Automation)

Title

Study and sizing of a stand-alone Photovoltaic Water Pumping System (PVPS) optimal design for typical installation in Ghardaia region

Supervised by: Dr. Amar Hadj Arab

June 2012

Acknowledgements

I would like to first acknowledge my advisor, Dr. Amar Hadj Arab, Director of research, Photovoltaic laboratory, CDER - Algiers, for his support and advice throughout my research work and his feedbacks are incorporated in this thesis.

I would like to express my sincere gratitude to my professors Dr. A. Guessoum, Dr. H. Salhi, Dr. B. Kazed and Dr. A. Naamane, from the department of electronic, Blida University, for their constant advices. I would like to thank my colleague and friend, Yahia Bakelli, from our Photovoltaic Water Pumping laboratory, URAER-Ghardaia, for reviewing together the work steps and a number of ideas generated from our numerous discussions are incorporated in this thesis. Special word of appreciation and thanks are the best contributors to Dr. S. Chader Kerdjou, Director of Applied Research Unit for Renewable Energies, Ghardaia, for her assistance and willingness to help me out during various stages of my project. Also, thanks to my other good colleague, Idriss Hadj Mahammed for his kind cooperation and fruitful advices. Thanks to thesis committee for reviewing and evaluation.

Finally, to my parents, my sisters, and my friends - many thanks for much support the whole way through, especially my wife for her constant encouragement and support during the year of my graduate work.

Azzedine BOUTELHIG
June 2012

ملخص:
يتضمن هذا العمل حوصلة لدراسة وقياس نظام ضخ الماء بالطاقة الشمسية , ويتكون هذا النظام من مضخة شمسية قدرتها القصوى (0.9 كيلووات) , مزودة بمولد كهرو ضوئي و المتكون من (6x2) لوحة شمسية نموذج Isofoton (110/24) .ومن خلال هذه الدراسة نطمح لتحقيق ثلاث اهداف رئيسية : الهدف الأول , هو كيفية التعامل مع مراحل قياس الضخ الشمسي لتحديد القدرة القصوى للمولد الكهرو ضوئي, الهدف الثاني هو كيفية تحليل نموذج رياضي للاستغلال الأمثل للطاقة و الهدف الثالث فيتضمن كيفية دراسة لمختلف برامج تعقب نقطة الاستطاعة القصوى باستعمال نظام السيطرة المعتمدة على نظرية المنطق الغامض و الشبكات العصبية .
وقد ثبتت النتائج المسجلة لمختلف التجارب القياسية في المخبر و المحاكاة ببرنامج Matlab ان الغاية قد تحققت في الشكل و الإنتاج .

كلمات المفاتيح: قياس , ضخ الماء بالطاقة الشمسية , الشبكات العصبية , المنطق الغامض

Résumé : Dans ce présent travail, une étude et dimensionnement d'un système de pompage photovoltaïque autonome (PVPS) ont été réalisés. Le système mentionné est composé d'une pompe solaire immergé Grundfos (0.9 kW), couplée directement à un générateur de (2x6) modules photovoltaïques Isofoton (110/24). Trois objectifs principaux sont considérés dans ce projet, le premier s'intéresse auxétapes de dimensionnement pour déterminer la puissance crête du générateurphotovoltaïque et sa configuration. Le second est d'identifier un nouveau modèlemathématique pour une exploitation optimal de l'énergie produite par le Générateur, tandis que le troisième objectifdiscutes des différentalgorithmes du MPPT, dont lequel un schémautilisantl'intelligence artificielle en l'occurrence (ANFIS) et (FLC) a été étudié. Les résultats obtenues des tests de caractérisation du PVPS et avec simulation Matlab montre que le système est optimisé en configuration et cout est peut être l'objet d'une installation prototype dans la région de Ghardaïa.
Mots clés : Dimensionnement ; PVPS ; model. Optimal, caractérisation, prototype

Abstract: In the present work, a study and sizing of a stand-alonephotovoltaic water pumping system (PVPS) has been carried out. The mentioned (PVPS) consists of a direct coupling submersible DC pump Grundfos (0.9 kW), poweredby (2x6) Isofoton (110/24) PV modules. Three main objectives are considered in this thesis, the first part deals with the dimensioning steps to determine the PV generator peak power and design, the second part investigates a new mathematical model for an optimal PV array energy output exploitation, while the third part includes discussion of various MPPT algorithms and control methods, where a proposed design using Adaptative Neuro-Fuzzy Inference System (ANFIS) and Fuzzy Logic Control (FLC) has been studied. The recorded results following the characterization tests of the different system parts and through Matlab simulation averred that the system is optimallyoptimized in size and cost and may be a subject for a typical installation in the Ghardaia region.

Keywords :Sizing, standalone, PVPS, model, optimal, ANFIS, FLC, characterization

List of acronyms and abbreviations

PVPS: Photovoltaic Water Pumping System

PV:Photovoltaic

Si: Silicon

Ge: Germanium

AM: Air Mass

I-V Characteristics: Current versus Voltage curve

I_{sc}: Short Circuit

V_{oc}: Open Voltage Circuit

P-V Characteristics; Power versus Voltage curve

MPPT: Maximum Power Point tracking

MPP: Maximum Power Point

FF: Fill factor

STC: Standard Test Conditions

SOC: Standard Operating Conditions

T_{cell}: Temperature of PV cell junction

T_{amb}: AmbientTemperature

NOCT: Nominal Operating cell Temperature

MFs: Membership Functions

GMF: Gaussian Membership Function

GBMF: generalized Bell Membership Function

RMSE: Root Mean Square error

ANFIS: Adaptative Neuron-Fuzzy Inference based System

FLC: Fuzzy Logic Controller

FIS; Fuzzy Inference System

Vs: Versus

Table of Contents

.

List of figures

List of Tables

Foreword

Climate change, global warming and issues of energy are some of the biggest challenges for humanity in the 21st century. Energy is so important for everyone, and in fact, taking control of the world's supply of oil is one of the most important agenda, for almost biggest consumer countries. The world is getting divided into two groups: the countries that have access to oil and natural gas resources and those that do not. In contrast, renewable energy resources are ubiquitous around the world. Especially, PV has a powerful attraction because it produces electric energy from a free inexhaustible source, the sun, using no moving parts, consuming no fossil fuels, and creating no pollution or greenhouse gases during the power generation. Together with decreasing PV module costs and increasing efficiency, PV is getting more pervasive than ever. Algeria is favorable area to start early with renewable energies. A great solar potential covering the whole south region throughout the year and a huge ground water are two essential sources to encourage the photovoltaic water pumping system installations.Finally, Iwish that this thesis serves the interests of other students who are interested in photovoltaic field for PV water pumping system applications and provides encouragement towards more advanced senior project, Masteror Doctorate's thesis research.

Azzedine BOUTELHIG
PV Water Pumping Laboratory
Applied Research Unit for Renewable Energies
Ghardaia, Algeria

Introduction

The Geographic location of Algeria north the equator, favorites the solar energy usages in water pumping, mainly in remote arid and semi-arid areas , as Oued Righ oasis in Righ basin and M'Zab valleys in Ghardaia basin. Indeed, in these desert regions, the availability of solar radiation and the abundance of underground water sources constitute important and profitable factors for stand-alone photovoltaic water pumping system (PVPS) erections [1]. The supply of water for domestic usage, livestock watering and irrigation of the large palm oasis and local agriculture, remains the great challenge for the citizen and farmers, regarding at both high cost of electricity and theremote areas, where others are very far away from the national electric grid. Ghardaia region, in particular, is located in the mid northern part of this great south region, where, there is a great potential of both solar energy source and a huge underground water reserve. The yearly monthly daily average irradiance yield received on horizontal plan is about 6 kWh/m^2/day and mid static levels of water ground sources is varying between 10 m in (El-Golea 270 km south of Ghardaia) and 25 m in (M'Zab and Metlili valleys).

Since, the people of remote desert regions has no access to the national grid power and most of them are nomads, the others use the diesel motors which is associated with maintenance problems, high fuel supply cost and environmental pollution, the photovoltaic water pumping system (PVPS) seems to be more an appropriate solution for water supply to cover the need of inhabitants on domestic usage, especially for watering their animals.This is a way to avoid them from travelling long distances in seeking water, between regions. The consumption of fossil fuels also has an environmental impact, in particular the release of carbon dioxide (CO2) into the atmosphere. CO2 emissions can be greatly reduced through the application of renewable energy technologies, which are already cost competitivewith fossil fuels in many situations. Good examples include large-scale grid-connected wind turbines, solar water heating and off-grid stand-alone PV systems. However, an accurate sizing of such system may contribute in reducing the erection cost and provide an efficient use of such (PVPS) installation. Many off-grid Photovoltaic Pumping Systems (PVPS) had been studied and installed, accordingly. Study and characterization tests of complete PV

pumping systems had been carried out at our site, in Ghardaia and were the subjects of many international conferences and publications [2], [3], [4]. In this thesis, a simple but efficient direct coupling photovoltaic water pumping system (PVPS) is presented. It based upon Grundfos solar pump, having the following nominal electrical characteristics (DC 30V - 300V, I_{max} = 7A, P_{max}= 900 W), powered by (2 x 6) Isofoton PV module array, with nominal power (110w/24v) for each module. The mentioned sized PV pumping system has the purpose to meet the demand on water to irrigate a farm, located in Sebseb Valley, about 60 km south west of Ghardaia. Through three main chapters, an optimum photovoltaic pumping system (PVPS) design has been achieved. In chapter one and chapter two the p-n junction structure and the PV cell photovoltaic effect of PV cell are presented, respectively. However, in chapter three an optimum (PVPS)design and sizing has been studied, the chapter four provides a new mathematical approach for a maximum power optimization of the global system and in chapter five the Maximum power point tracking of the PV pumping system using Adaptive Neuron-Fuzzy Inference System (ANFIS) Prediction and Fuzzy Logic control (FLC) tracking has been investigated, through MATLAB simulation study upon the obtained data base of characterization results.

Chapter1: Semiconductors and P-N junction structure

1.1 Semiconductors

1.1.1...Definition

A semiconductor is a material with electrical conductivity intermediate in magnitude between that of a conductor and an insulator. Common semiconducting materials are crystalline solids, but amorphous and liquid semiconductors as hydrogenated amorphous silicon and mixtures of arsenic, selenium and tellurium are also known. Such compounds share with better known semiconductors intermediate conductivity and a rapid variation of conductivity with temperature, as well as occasional negative resistance [5]. Semiconductor materials are the foundation of modern electronics, including radio, computers, telephones, and many other devices. Such devices include transistors, digital and analog integrated circuits, many kinds of diodes including the light-emitting diode (LED), solar cells, the silicon controlled rectifier, and photo-diode. The semiconductor solar cells or photovoltaic panels directly convert light energy into electricity [6]. In a metallic conductor, current is carried by the flow of electrons. A pure semiconductor is often called an “intrinsic” semiconductor. The electronic properties and the conductivity of a semiconductor can be changed in a controlled manner by adding very small quantities of other elements, called “dopants”, to the intrinsic material. In crystalline silicon typically this is achieved by adding impurities of boron or phosphorus to the melt and then allowing it to solidify into the crystal. This process is called "doping" and the semiconductor is "extrinsic".

1.1.2…Energy band in solids

In solid materials, the energy bands each correspond to a large number of discrete quantum states of the electrons, and most of the states with low energy (closer to the nucleus) are full, up to a particular band called the valence band. Semiconductors and insulators are distinguished from metals because the valence band in any given metal is nearly filled with electrons under usual operating conditions, while very few

(semiconductor) or virtually none (insulator) of them are available in the conduction band, the band immediately above the valence band. In the semiconductors, electrons can be excited from the valence band to the conduction band depends on the band gap between the two bands. The size of this energy band gap serves as an arbitrary dividing line (roughly 4eV) between semiconductors and insulators. In the case of semiconductors, the gap is small, about 0.1 to 1 eV (the gap width in the Si is 1.12 eV and in Ge is 0.7eV and in the case of insulators, the gap is a forbidden region between highest filled band (valence band) and lowest empty or partly filled band (conduction band) is very wide, about 3 to 6 eV [7]. Conductors: valence band only partially filled, or (if it is filled), the next allowed empty band overlaps with it.

The different energy bands are divided into three following types:

a- Valence band: is the outermost (highest) electrical band filled with electrons ("filled": all states occupied) and insures the covalent liaison between the atoms of the network.
b- Conduction band: Is the next highest band to valence band (empty or partly filled).
c- Energy gap: energy difference between valence and conduction bands, called width of the forbidden band.

The different energy bands are illustrated in the figure 1.1

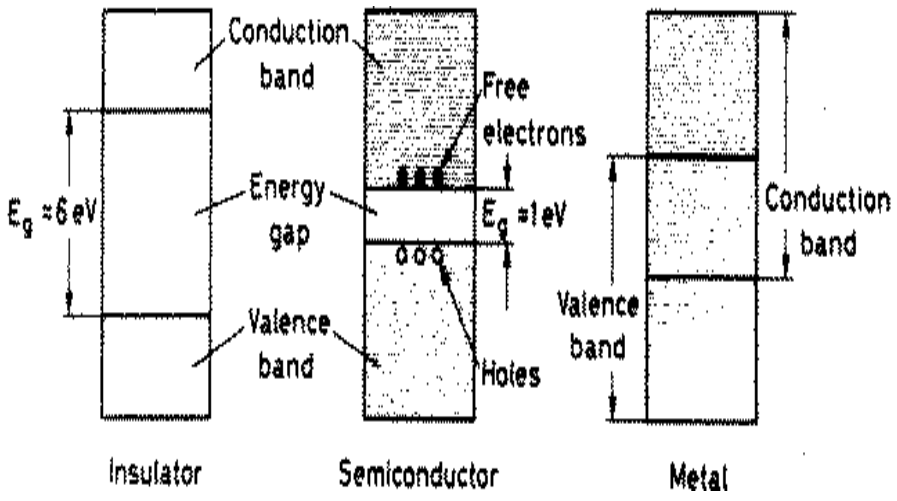

Figure 1.1 Different energy band structures

The energy band diagrams of semiconductors are rather complex. The detailed energy band diagram of a semiconductor is shown in Figure 1.2. The energy is plotted as a function of the wavenumber, k, along the main crystallographic direction in the crystal, since the band diagram depends on the direction in the crystal. The energy band diagrams contain multiple completely-filled and completely-empty bands. In addition, there are multiple partially-filled bands.

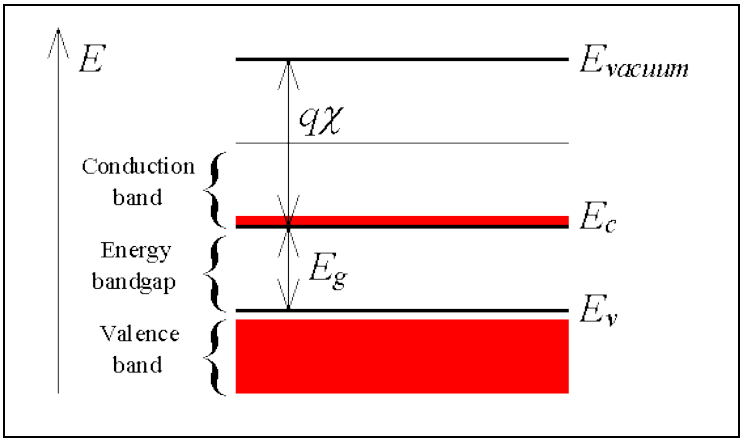

Figure 1.2 Energy band diagram in semiconductor

1.1.3…Electrical conductivity

According to their band structure, the solid materials are classified upon the electrical conductivityinto three following types: conductors, semiconductors and insulators:

a- Conductors: material capable of carrying electric current. material which has "mobile charge carriers" (e.g. electrons, ions,..) e.g. metals, liquids with ions (water, molten ionic compounds), plasma

b- Insulators: materials with no or very few free charge carriers; e.g. quartz, most covalent and ionic solids, plastics

c- Semiconductors: materials with conductivity between that of conductors and insulators; e.g. germanium Ge, silicon Si, GaAs, GaP, InP. Certain materials have zero resistivity at very low temperature called (superconductors).

In semiconductors, electrons in a completely filled band (valence band) cannot move, since all states occupied (Pauli principle); only way to move would be to "jump" into

next higher band (conduction band) needs energy. The figures 1.3 show the state of the two bands previous and post excited electrons.

In metals, electrons in partly filled band can move, since there are free states to move to, as shown in the figure 1.3.a.

Electrons excited to the conduction band also leave behind electron holes, unoccupied states in the valence band, as shown in the figure 1.3.b.

Both the conduction band electrons and the valence band holes contribute to electrical conductivity. The holes themselves don't move, but a neighboring electron can move to fill the hole, leaving a hole at the place it has just come from, and in this way the holes appear to move, and the holes behave as if they were actual positively charged particles

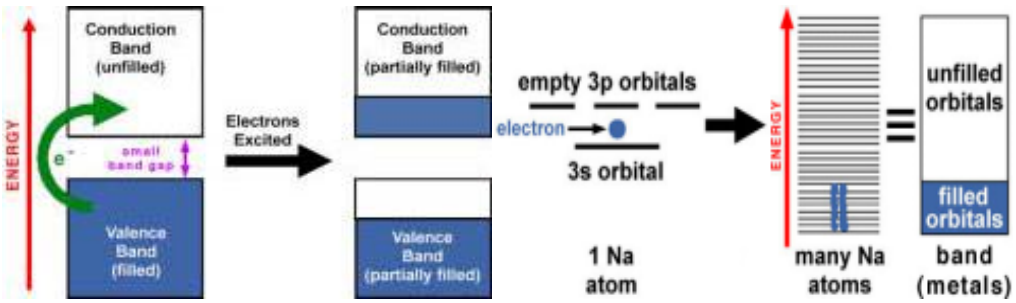

Previouspost previous post

(a) (b)

Figure 1.3 Previous and post excitation band states

1.1.4…Impact on electrical conductivity

Electrons having acquired an excess energy by thermal agitation or impact of photon can pass to the conduction band and to move through the network by successive jumps from one atom to another. Electrical conductivity increases with the number of electrons in the conduction band. The transfer of electrons from the valence to the conduction band obviously leaves empty seats in the valence band. These holes are actually positive charges by the deficit atoms in electrons.A hole may be occupied by the electron of a neighboring atom, resulting in final migration of the hole of an atom to the other. Thus partially depopulatedvalence band becomes conductive “hoping holes”.

At T = 0, there are no electrons in the conduction band, and the semiconductor does not conduct (lack of free charge carriers);

At T > 0, some fraction of electrons have sufficient thermal kinetic energy to overcome the gap and jump to the conduction band; fraction rises with temperature; e.g. at 20°C (293 K), Si has 0.9×10^{10} conduction electrons per cubic centimeter; at 50°C (323 K) there are 7.4×10^{10}.

When a free electron in the conduction band and the hole in the valence band meet on the same atom, the electron passes through the hole and the two charges carriers disappear simultaneously.

Figure 1.4 illustrates the migration of free electrons and holes in the Silicon (Si) atom following a thermal impact.

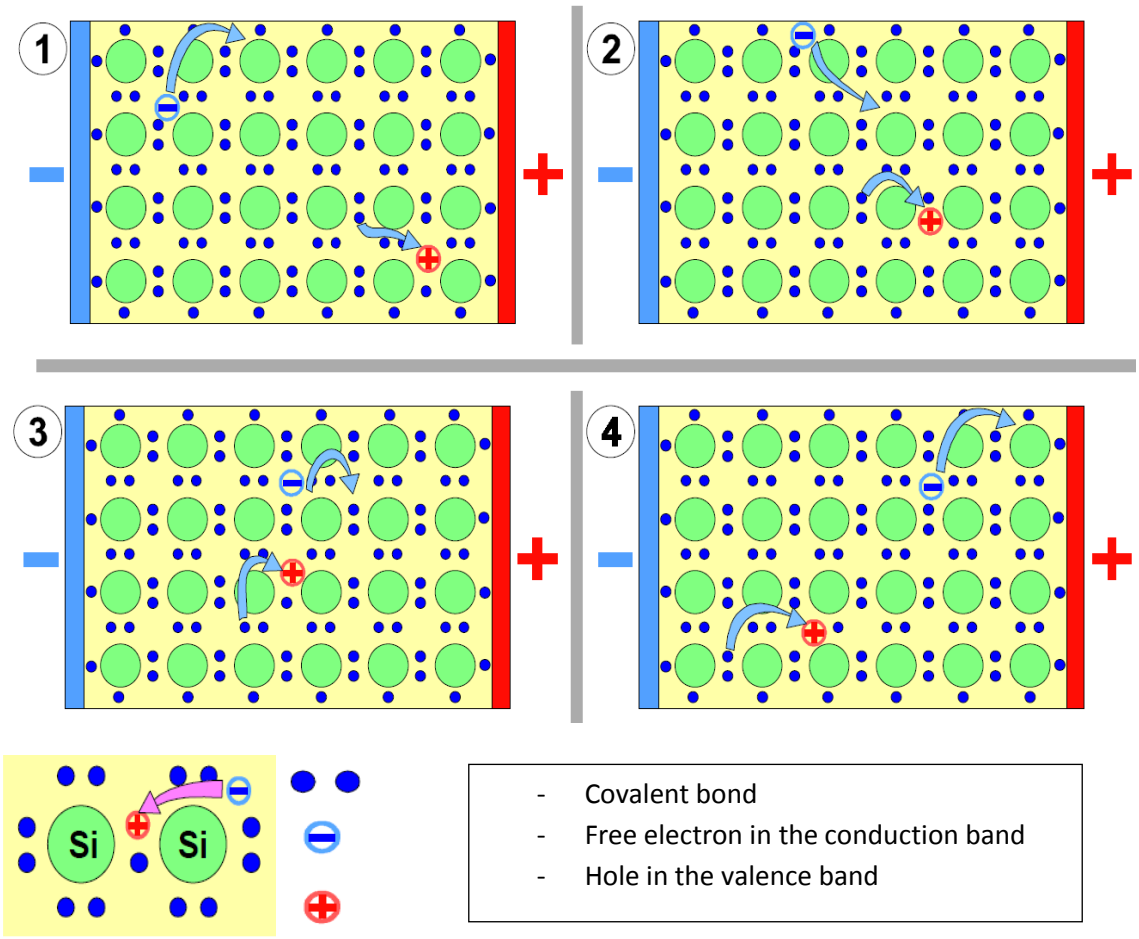

Figure 1.4 immigration of free electron and hole in Silicon atom under a thermal impact

1.1.5 Intrinsic and extrinsic semiconductors

Generally, the semiconductor is identified upon two main types: an intrinsic type also called an undoped semiconductor and extrinsic also called doped semiconductor.

a An intrinsic semiconductor

An intrinsic (undoped semiconductor) or i-type semiconductor is a pure semiconductor without any significant dopant species present. The number of charge carriers is therefore determined by the properties of the material itself instead of the amount of impurities. The electrical conductivity of intrinsic semiconductors can be due to crystal defects or to thermal excitation. In intrinsic semiconductors the number of excited electrons and the number of holes are equal: n = p.

bAn extrinsic semiconductor

An extrinsic (doped semiconductor); also called impure, is a semiconductor with small admixture of trivalent or pentavalent atoms. The property of semiconductors that makes them most useful for constructing electronic devices is that their conductivity may easily be modified by introducing impurities into their crystal lattice. The process of adding controlled impurities to a semiconductor is known as doping. The amount of impurity, or dopant, added to an intrinsic (pure) semiconductor varies its level of conductivity. Doped semiconductors are often referred to as extrinsic. By adding impurity to pure semiconductors, the electrical conductivity may be varied not only by the number of impurity atoms but also, by the type of impurity atom and the changes may be thousand folds and million folds.

1.1.6…n-type and p-type semiconductors

The doped semiconductors by adding trivalent or pentavalent atoms are classified by types called n-type or p-type semiconductors:

an-type semiconductor

n-type semiconductors are a type of extrinsic semiconductor where the dopant atoms called (donors) are capable of providing extra conduction electrons to the host material asphosphorus in silicon. This creates an excess of negative (n-type) electron charge carriers. As an example The addition of pentavalentimpurities such as antimony (Sb) dopant with 5 valence electrons to Silicon (Si), arsenic or phosphorous contributes free electrons, 4 electrons used for covalent bonds with surrounding Si atoms, one electron “left over ,greatly increasing the conductivity of the intrinsic semiconductor.

When the dopant donor donates extra electrons to the host, the product is called an n-type semiconductor. The process of doping is described as it introduces energy levels into band gap; those levels are filled with electrons and lie close to the conduction band so that even slight thermal agitation can release them into the conduction band[8].

The figure 1.5 illustrates n-type doping process presented as follows: (a) dopant phosphorus (Sb) atom in Silicon (Si), (b) migration of electrons from valence to conduction band, (c) electric conductivity of n-type semiconductor.

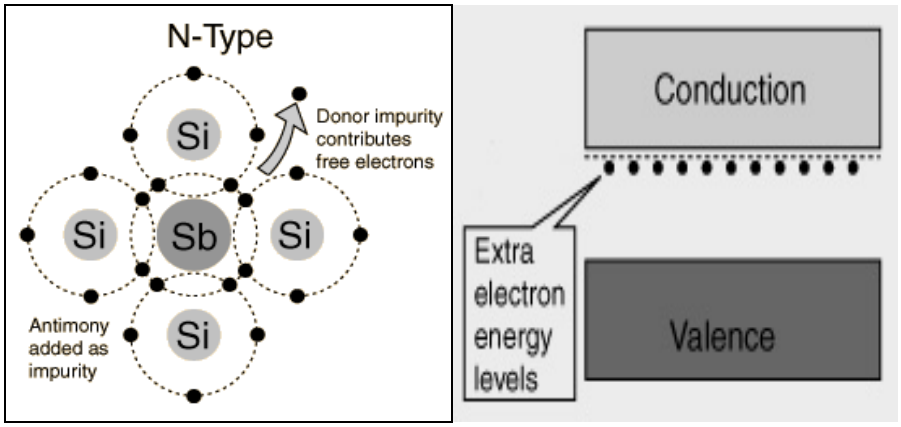

(a) (b)

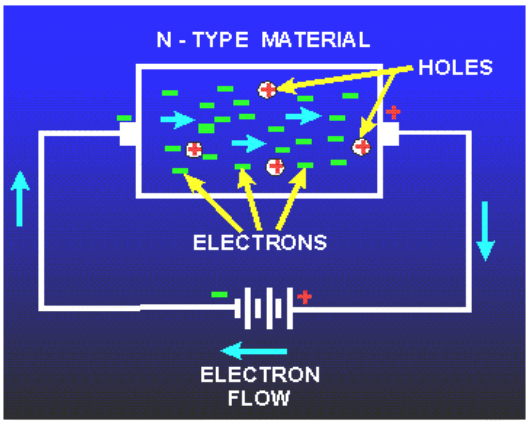

(c)

Figure 1.5 n-type doping procees (Phosphorus in Silicon)

b p-type semiconductor

A P-type semiconductor (P for Positive) is obtained by carrying out a process of doping, that is adding a certain type of atoms to the semiconductor in order to increase the number of free charge carriers (in this case positive). When the doping material is added, it takes away (accepts) weakly-bound outer electrons from the semiconductor

atoms. This type of doping agent is also known as an acceptor material and the vacancy left behind by the electron is known as a hole.

The purpose of P-type doping is to create an abundance of holes. In the case of silicon, a trivalent atom typically, such as boron is substituted into the crystal lattice. only 3 of the 4 covalent bonds filled vacancy in the fourth covalent bond. The result is that one electron is missing from one of the four covalent bonds normal for the silicon lattice. Thus the dopant atom can accept an electron from a neighboring atom's covalent bond to complete the fourth bond. Thus, the holes are the majority carriers, while electrons are the minority carriers in P-type materials.

The figure 1.6 illustrates p-type doping process presented as follows: (a) dopant boron(B) atom in Silicon(Si), (b) migration of holes from valence to conduction band, (c) electric conductivity of p-type semiconductor.

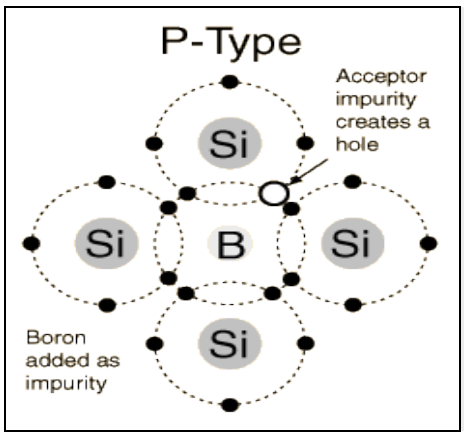

(a)

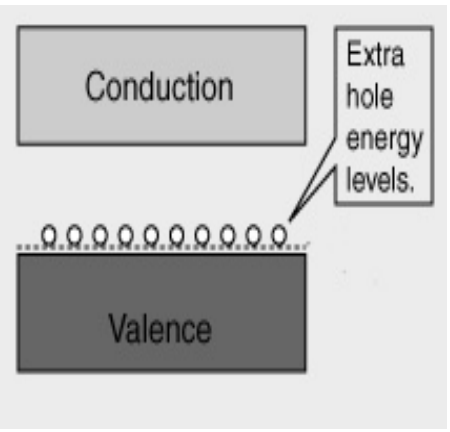

(b)

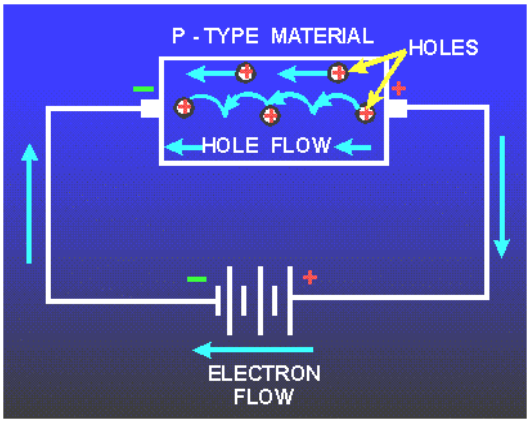

(c)

Figure 1.6 n-type doping procees (Boron in Silicon)

1.2 The p-n junction

1.2.1 The p-n junction structure

The p-n junctions are formed by joining n-type and p-type semiconductor materials, in which impurity changes abruptly from p-type to n-type. Since the n-type region has a high electron concentration and the p-type a high hole concentration, electrons diffuse from the n-type side to the p-type side. Similarly, holes flow by diffusion from the p-type side to the n-type side. If the electrons and holes were not charged, this diffusion process would continue until the concentration of electrons and holes on the two sides were the same, as happens if two gasses come into contact with each other. However, in a p-n junction, when the electrons and holes move to the other side of the junction, they leave behind exposed charges on dopant atom sites, which are fixed in the crystal lattice and are unable to move. On the n-type side, positive ion cores are exposed. On the p-type side, negative ion cores are exposed. An electric field Ê forms between the positive ion cores in the n-type material and negative ion cores in the p-type material (recombination of majority carriers). This region is called the depletion region since the electric field quickly sweeps free carriers out; hence the region is depleted of free carriers. A "built in" potential V due to Ê is formed at the junction.

The figure 1.7 shows p-n junction structure: (a) diagram of p-n junction formation and band structure, (b) electric field into the depletion zone.

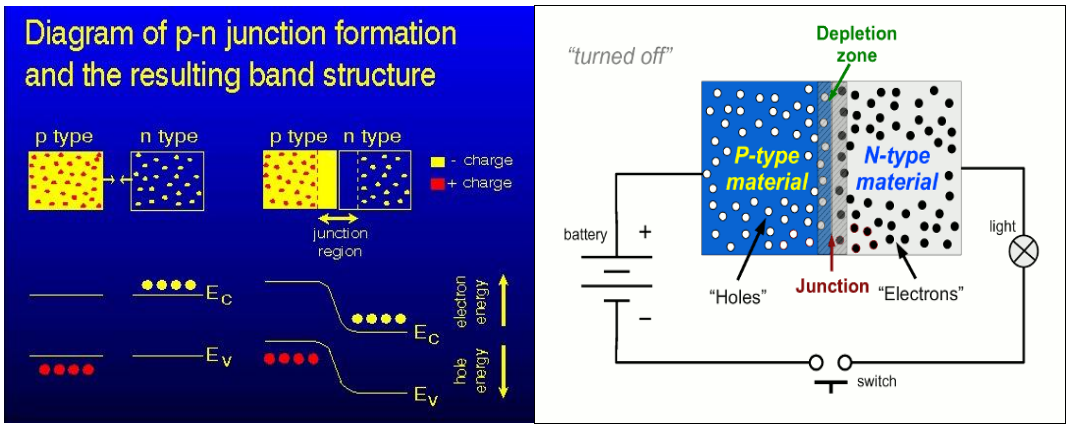

(a) (b)

Figure 1.7 p-n junction band structure and electrical field

1.2.2 The p-n junction under equilibrium conditions

Under equilibrium conditions, in the depletion region of a p-n junction, free of mobile charge carriers develops on either side of junction with fixed negative ions on p-side and fixed positive ions on n-side preventing further diffusion so that recombination between holes and electrons is inhibited. In this zone an electrostatic field is created.

The figure 1.8 the equilibrium between electrons and holes in the depletion zone

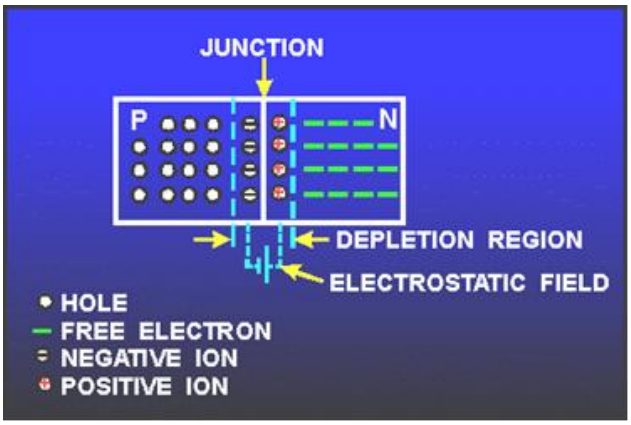

Figure 1.8 depletion region of the p-n junction under equilibrium conditions

1.3 Diode

1.3.1 Definition

Adiode is one of the simplest semiconductor devices. It is a p-n junction with voltage applied across it, called biased p-n junction, which has the characteristic of passing current in one direction only. However, unlike a resistor, a diode does not behave linearly with respect to the applied voltage as the diode has an exponential I-V relationship and therefore we cannot described its operation by simply using an equation such as Ohm's law. There are two types of diode p-n junction: “forward biased p-n junction”, when p-side more positive than n-side and “reverse biased p-n junction”, when n-side more positive than p-side. The two mentioned types are described in the following sections.

1.3.2…Forward biased p-njunction

If a suitable positive voltage (forward bias) is applied between the two ends of the PN junction,p-type charge carriers (positive holes) in p- side are pushed towards and across the p-n boundary.It can supply free electrons and holes with the extra energy they require to cross the junction as the width of the depletion layer around the PN junction is decreased.The direction of the electric field is from p-side towards n-side.

The figure 1.9 illustrate the different following stages of a forward biased diode

- p-type charge carriers (positive holes) in p side are pushed towards and across the p-n boundary (a)
- Direction of the electric field is from p-side towards n-side (b)
- n-type carriers (negative electrons) in n-side are pushed towards and across n-p boundary resulting the I-V characteristics of the forward biased diode, (c)
- Current flows across p-n boundary (d)

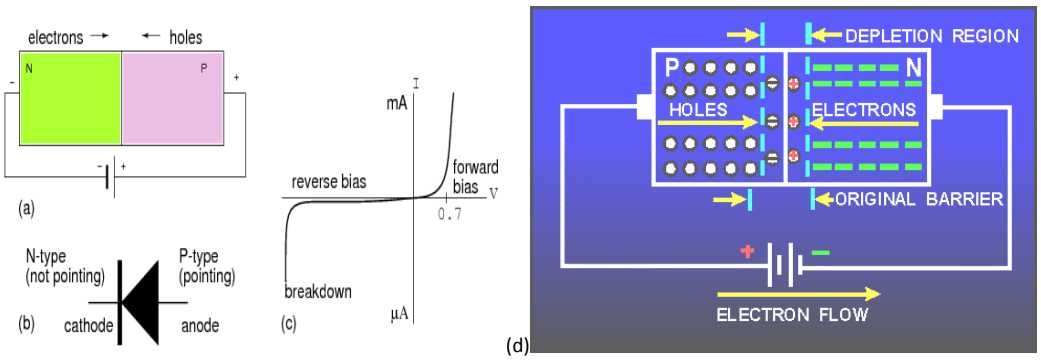

Figure 1.9forward biased diode structure and electrical characteristics

1.3.3 Reverse biased p-n junction

By applying a negative voltage (reverse bias) results in the free charges being pulled away from the junction resulting in the depletion layer width being increased. This has the effect of increasing or decreasing the effective resistance of the junction itself allowing or blocking current flow through the diode.Electric field direction is from n-side towards p-side.

The figure 1.10 illustrate the different following stages of a reverse biased diode

- Pushes charge carriers away from the p-n boundary, (a)
- Electric field direction is from n-side towards p-side (b)
- Electric characteristics of the diode –reverse bias (c)
- Depletion region widens, and no current flows, (d)

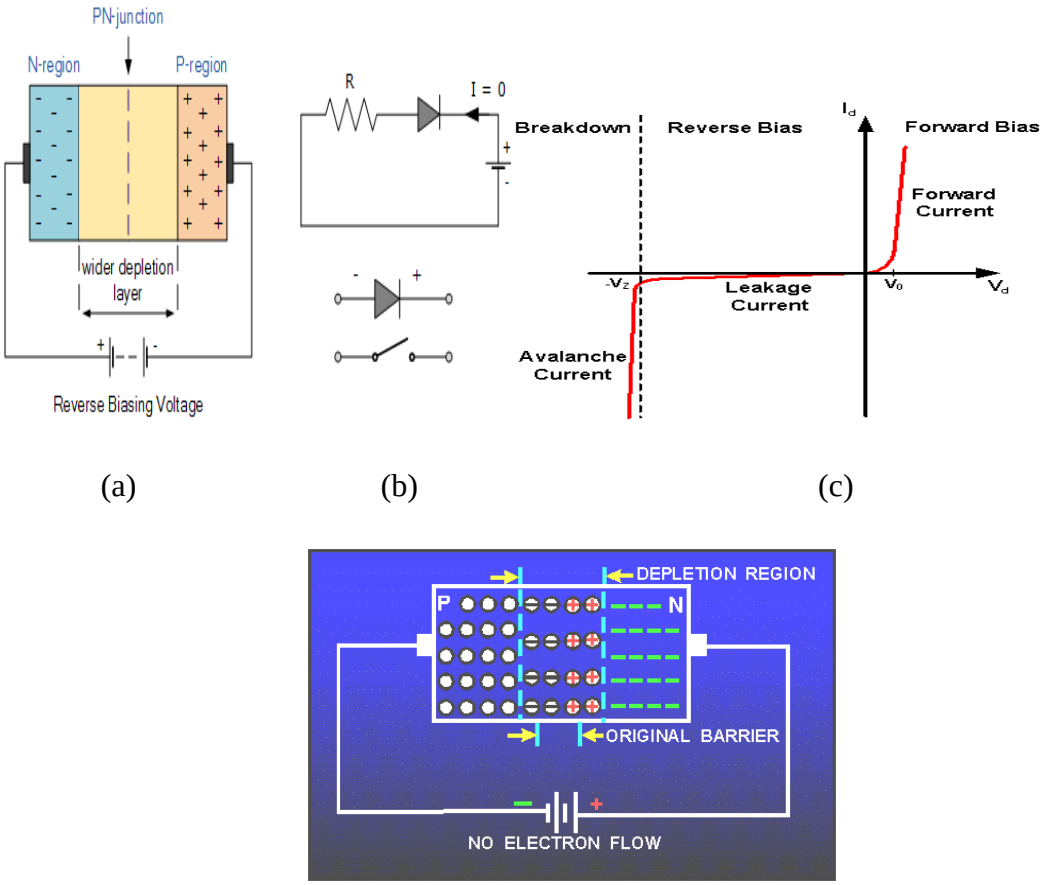

Figure 1.10reverse biased diode structure and electrical characteristics

Chapter 2: The photovoltaic effect in the solar cell

2.1 Photovoltaic cell effect

2.1.1 Photovoltaic conversion history

The Photovoltaic effect is the conversion of the energy of the light photons into electric energy [9]. The PV effect can occur in gasses, liquids and solids under maximum solar radiation between 0.35 and 3μm of wavelength. The history of the Photovoltaic (PV) dates back to 1839 when a French physicist, Edmund Becquerel, discovered the first photovoltaic effect when he illuminated a metal electrode in an electrolytic solution [10]. Four decades later British physicist, William Adams, with his student, Richard Day, discovered a photovoltaic material, selenium, and made solid cells with 1~2% efficiency which were soon widely adopted in the exposure meters of camera [11]. In 1905, Albert Einstein described the nature of light and the photoelectric effect on which photovoltaic technology is based, for which he later won a Nobel Prize in physics. In 1954 the first generation of semiconductor silicon-based PV cells was born, with efficiency of 6% [12], and adopted in space applications. In the 1960s, the space industry began to make the first serious use of the technology to provide power aboard spacecraft. Today, the production of PV cells is following an exponential growth curve since technological advancement of late 80s that has started to rapidly improve efficiency and reduce cost. This chapter discusses the fundamentals of PV cells and modeling of a PV cell using an equivalent electrical circuit.

2.1.2 Solar spectral radiation

a blackbodytheory

The sun is the source of insolation that gigantic, 1.4 million kilometer diameter, and thermonuclear furnace fusing hydrogen atoms into helium. The resulting loss of mass is converted into about 3.8 × 1020 MW of electromagnetic energy that radiates outward from the surface into space [13, 7]. Every object emits radiant energy in an amount that is a function of its temperature. The usual way to describe how much radiation an object emits is to compare it to a theoretical abstraction called a blackbody. A blackbody is

defined to be a perfect emitter as well as a perfect absorber. As a perfect emitter, it radiates more energy per unit of surface area than any real object at the same temperature. As a perfect absorber, it absorbs all radiation that impinges upon it; that is, none is reflected and none is transmitted through it. The wavelengths emitted by a blackbody depend on its temperature as described by Planck's law (2.1):

$$E_\lambda = \frac{3.74 \times 10^8}{\lambda^5 \left[\exp\left(14.400 / \lambda T\right) - 1\right]} \qquad (2.1)$$

Where,

E_λ : is the emissive power per unit area of a blackbody ($W/m^2 \mu m$),

T : is the absolute temperature of the body (K),

λ : is the wavelength (μm).

b Solar spectrum wavelengths

While the interior of the sun is estimated to have a temperature of around 15 million Kelvins, it emits radiant energy with spectral characteristics that well match those of a 5800 K blackbody [13, 7]. Just outside of the earth's atmosphere, the average radiant flux is about1.377 kW/m^2, which is the solar insolation. Also shown are the areas under the actual solar spectrum that corresponds to wavelengths within the ultraviolet UV (5%), visible (43%), and infrared IR (53%) portions of the spectrum. The visibleSpectrum, which lies between the UV and IR, ranges from 0.38 μm (violet) to 0.78 μm (red). The solar spectrum behavior outside atmosphere and at sea level plots as well as well as the solar energy distribution is shown in the figures 2.1.a and 2.1.b.

The different energy wavelengths of the spectrum are:

Ultraviolet UV	$0.20 < \lambda < 0.38$ μm
Visible	$0.38 < \lambda < 0.78$ μm
Infrared IR	$0.78 < \lambda < 10$ μm

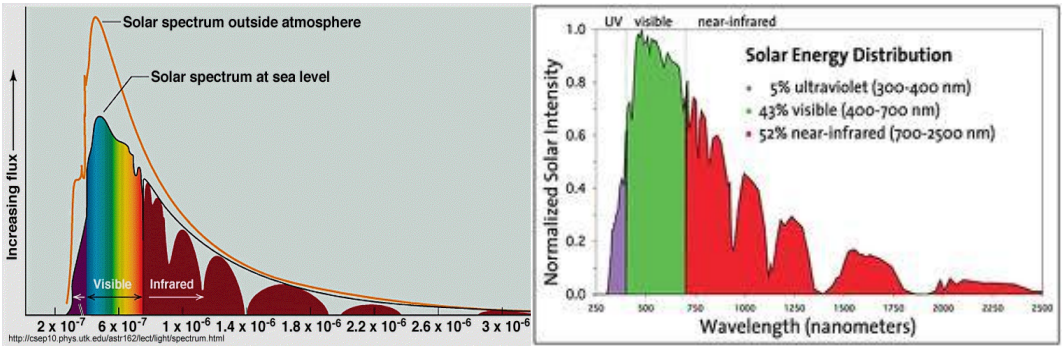

(a) Solarspectrumoutsideatmosphere (b) Extraterrestrial solar Spectrum different wavelengths

Figure 2.1 solar spectral structure outside atmosphere and wavelenght distribution

The energy content of the photon is related to its wavelength, presented by the equation 2.2.There is a maximum cut-off wavelength necessary to excite one valence e-. For a silicon photovoltaic cell, photons with wavelength greater than 1.11 μm have energy hν less than the 1.12-eV band-gap energy needed to excite an electron.

$$E = h\upsilon \quad (2.2), \text{ with } C = \lambda\upsilon$$

Where,

C is the speed of light (3×10^8 m/s), υ is the frequency (hertz), λ is the wavelength (m), and where, E is the energy of a photon (J) and h is Planck's constant (6.626×10^{-34} J-s).

c Air Mass (AM)

When the solar radiation makes its way toward the earth's surface, some of it is absorbed and scatter light rays by various particles in the atmosphere, giving the terrestrial spectrum an irregular shape[14]. The terrestrial spectrum also depends on how much atmosphere the radiation has to pass through to reach the surface. The length of the path h2 taken by the sun's rays as they pass through the atmosphere, divided by the minimum possible path length h1, which occurs when the sun is directly overhead, is called the air mass ratio, m. As shown in figure 2.2, under the simple assumption of a flat earth the air mass ratio can be expressed by the following equation (2.3):

Air Mass ratio: $$m = \frac{h_2}{h_1} = \frac{1}{\sin\beta} \qquad (2.3)$$

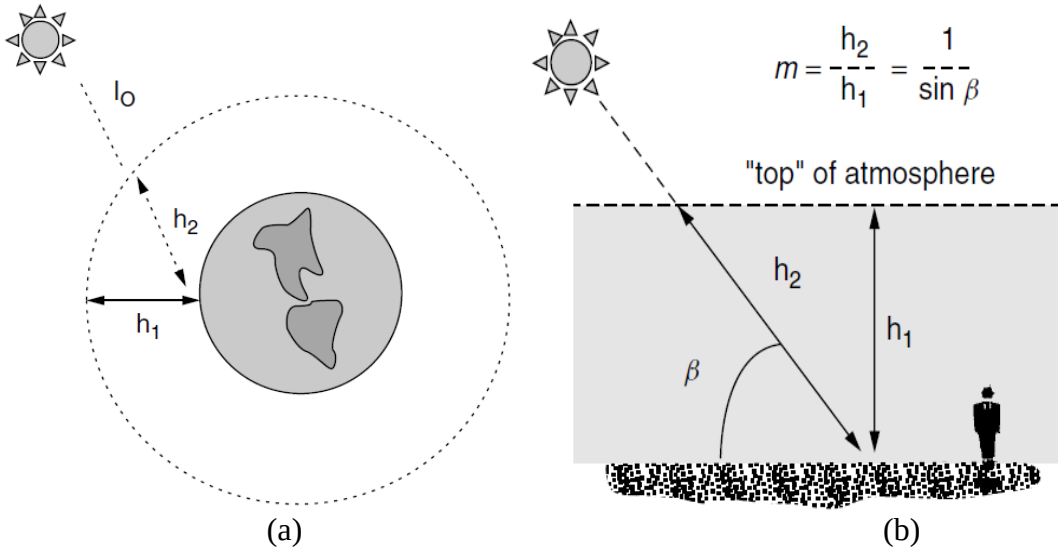

Figure 2.2:(a) The air mass ratio m is a measure of the amount of atmosphere the sun's raysmust pass through to reach the earth's surface.

(b) For the sun directly overhead, m = 1, Solar spectrum for extraterrestrial (m = 0),

Where,

h_1 = path length through the atmosphere with the sun directly overhead,

h_2 = path length through the atmosphere to reach a spot on the surface,

β = the altitude angle of the sun.

Thus, an air mass ratio of 1 designated "AM1" means that the sun is directly overhead. By convention, AM0 means no atmosphere; that is, it is the extraterrestrial solar spectrum. Often, an air mass ratio of 1.5 is assumed for an average solar spectrum at the earth's surface. With AM1.5, 2% of the incoming solar energy is in the UV portion of the spectrum, 54% is in the visible, and 44% is in the infrared. The impact of the atmosphere on incoming solar radiation for various air mass ratios is shown in the previous figure 2.1. As sunlight passes through more atmospheres, less energy arrives at the earth's surface and the spectrum shifts some toward longer wavelengths.

2.1.3 Solar declination

a solar position

The sun rises in the east and sets in the west and reaches its highest point sometime in the middle of the day. In many situations, it is quite useful to be able to predict exactly where in the sky the sun will be at any time, at any location on any day of the year. In

the context of photovoltaic, we can, for example, use knowledge of solar angles to help pick the best tilt angle for our modules to expose them to the greatest insolation.[13,7] On June 21st (the summer solstice), the sun reaches its highest point, and a ray drawn at that time from the center of the sun to the center of the earth makes an angle of 23.45◦ with the earth's equator. On that day, the sun is directly over the Tropic of Cancer at latitude 23.45◦. At the two equinoxes (the 21st September and 21st March), the sun is directly over the equator. On December 21st (winter solstice), the sun is 23.45◦ below the equator, which defines the latitude known as the Tropic of Capricorn. As shown in figure2.3, the angle formed between the plane of the equator and a line drawn from the center of the sun to the center of the earth is called the solar declination (δ). It varies between the extremes of ± 23.45◦, and a simple sinusoidal relationship that assumes a 365-day year and which puts the spring equinox on day n = 81 provides a very good approximation, according to the following equation (2.4):

$$\delta = 23.45 \sin [360/365 (n - 81)] \quad (2.4)$$

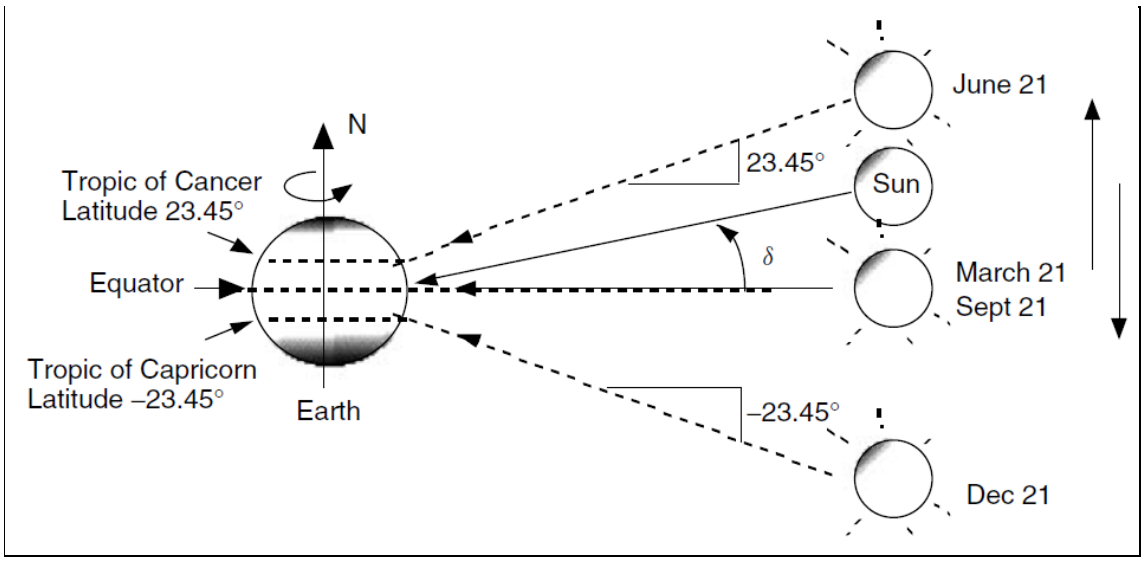

Figure 2.3An alternative view with a fixed earth and a sun that moves up and down. The angle between the sun and the equator is called the solar declination δ.

The angles of the Sun's declination and latitudes of the sub solar points throughout the year Seasons of the Northern Hemisphere are shown in the following figure 2.4

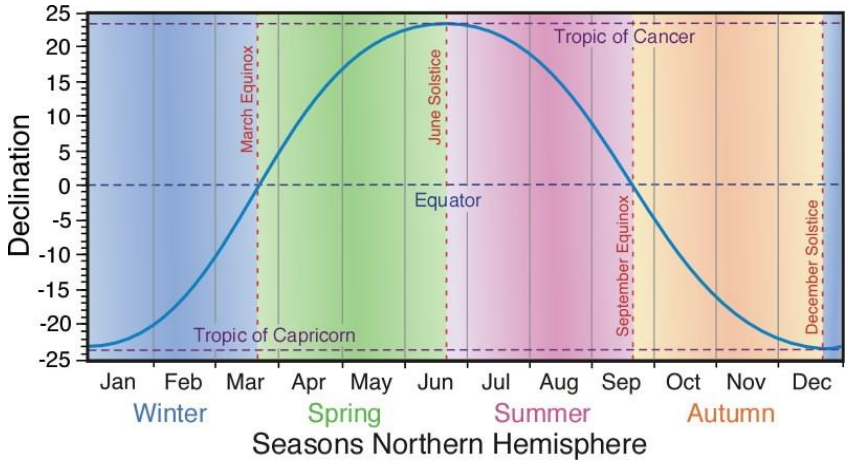

Figure2.4:Angles of the Sun's declination and latitudes curve for Northern Hemisphere.

Computed values of solar declination on the twenty-first day of each month are given in Table 2.1.

Month	Jan	Feb	Mar	Apr	May	Jun	Jul	Aug	Sep	Oct	Nov	Dec
δ (°)	-20.1	-11.2	+0.0	+11.6	+20.1	+23.4	+20.4	+11.8	+0.0	-11.8	-20.4	-23.4

Table 2.1:Solar declination angles of the 2st day of each month

b Tilt angle

It is the optimum inclination for an optimum PV modules erection. Figure 2.5 shows a south-facing collector on the earth's surface that is tilted at an angle equal to the local latitude, L. As can be seen, with this tilt angle the collector is parallel to the axis of the earth. During an equinox, at solar noon, when the sun is directly over the local meridian (line of longitude), the sun's rays will strike the collector at the best possible angle; that is, they are perpendicular to the collector face[13],[14]. At other times of the year; the sun is a little high or a little low for normal incidence, but on the average it would seem to be a good tilt angle. Solar noon is an important reference point for almost all solar calculations. In the Northern Hemisphere, at latitudes above the Tropic of Cancer, solar noon occurs when the sun is due south of the observer. South of the Tropic of Capricorn, in Ghardaia for example, the optimum position of a collector or PV array is facing full south with tilt angle equals to the latitude of site (32°).

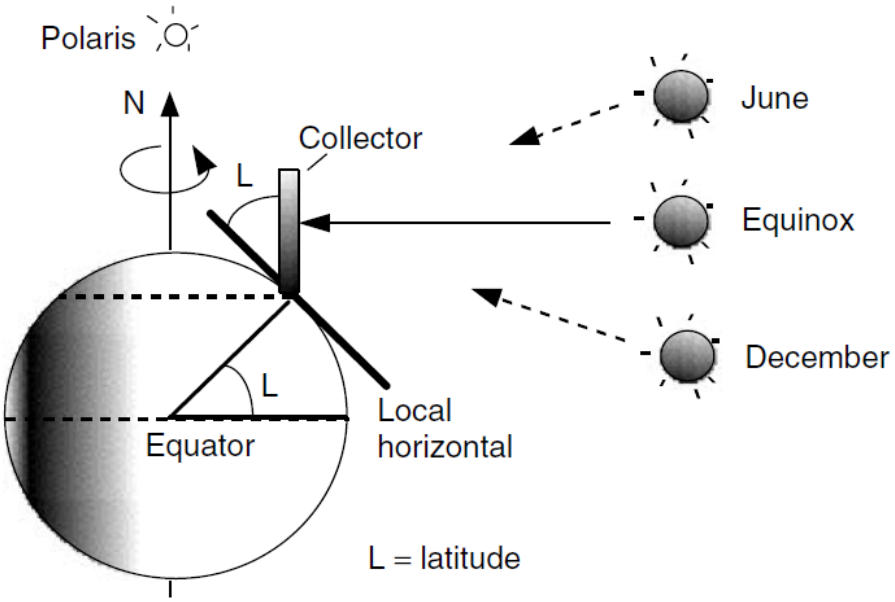

Figure *2.5*A south-facing collector tilted to an angle equal to its latitude is perpendicularto the sun's rays at solar noon during the equinoxes

2.1.4 Photovoltaic cell junction structure

The Photovoltaic (PV) cell or solar cell is made of the same kinds of semiconductor materials, such as silicon, used in the microelectronics industry. A solar cell is essential a P-N junction with a large surface area [15].The depletion region as explained previously with the diode is the area around the P-N junction where the electrons from the N-type silicon, have diffused into the holes of the P-type material. The N-type material is keep thin to allow light to pass through to the P-N junction.

The PV cell P-N junction structure and a silicon PV cell are presented in the following figures 2.6.a and 2.6.b.

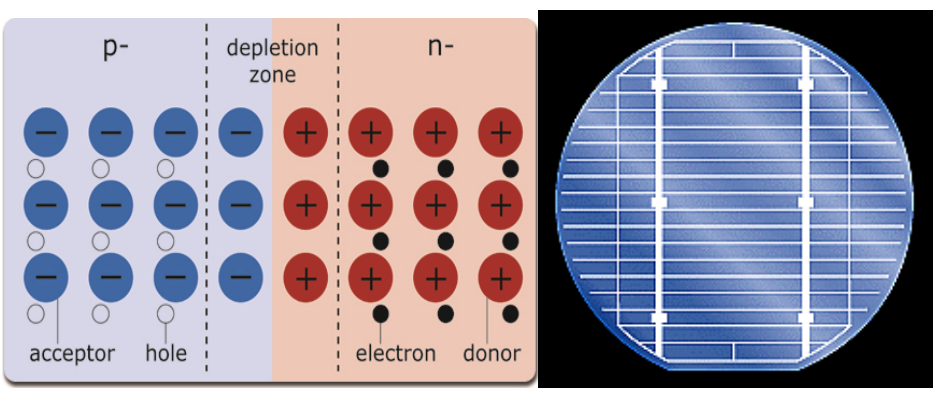

(a) (b)

Figure 2.6: PV cell structure

2.1.5 Photovoltaic cell junction conduction

For solar cells, a thin semiconductor wafer is specially treated to form an electric field, positive on one side and negative on the other (on its top and bottom), as shown in the figure 2.7.a. When light energy strikes the solar cell, electrons flow out of the n-side into the connecting wire, through the load, and back to the p-side where they recombine with holes in the P-N junction. If electrical conductors are attached to the positive and negative sides, forming an electrical circuit, the electrons can be captured in the form of an electric current. This electricity can then be used to power a load, such as shown in the figure 2.7.b.

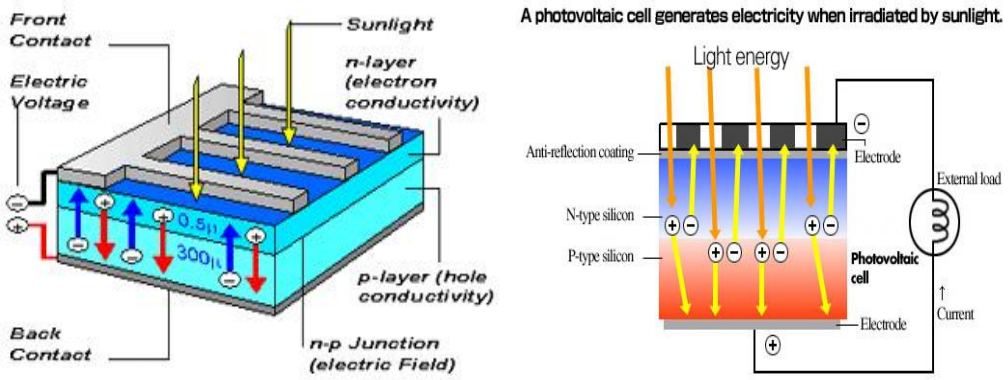

➢ (b)

Figure 2.7 generation of electricity by the PV cell

2.1.6 Different PV cell technologies;

- ➢ Mono-Crystalline silicon cells: High thickness because they have low absorption coefficient and to reduce transmission losses and high efficiency (15%)
- ➢ Poly-crystalline silicon:
- ▪ Thin film cells: thickness of 10 to 50 mm.
- ▪ Amorphoussiliconcells.
- ▪ GaAscells.
- ▪ TeCdcells.
- ▪ CIS cells.

2.2 Electrical Characteristics of the PV cell

2.2.1The Simplest PV cell Model

aIdeal solar cell equivalent circuit

The ideal model of a PV cell consists of an ideal current source connected in parallel with a rectifying diode [16]. The current source represents the current generated by photons (often denoted as I_{ph} or I_L), and its output is constant under constant temperature and constant incident radiation of light. The ideal model equivalent solar cell circuit is represented in the figure 2.8 and the corresponding I-V characteristic is described by the Shockley solar cell equation 2.6.

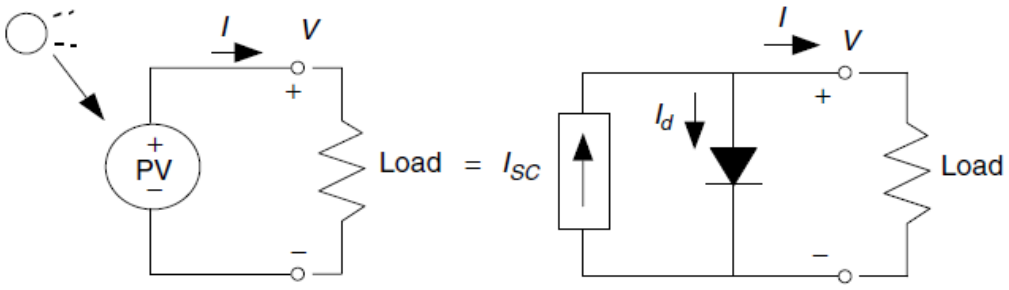

Figure 2.8: A simple equivalent circuit for a photovoltaic cell consistsof a currentsource driven by sunlight in parallel with a real diode.

There are two key parameters frequently used to characterize a PV cell. Shorting together the terminals of the cell, as shown in Figure 2-9 (a), the photon generated current will follow out of the cell as a short circuit current (Isc). Thus, Iph = Isc. As shown in Figure 2-9 (b), when there is no connection to the PV cell (open-circuit), the photon generated current is shunted internally by the intrinsic p-n junction diode. This gives the open circuit voltage (Voc). The PV module or cell manufacturers usually provide the values of these parameters in their datasheets.

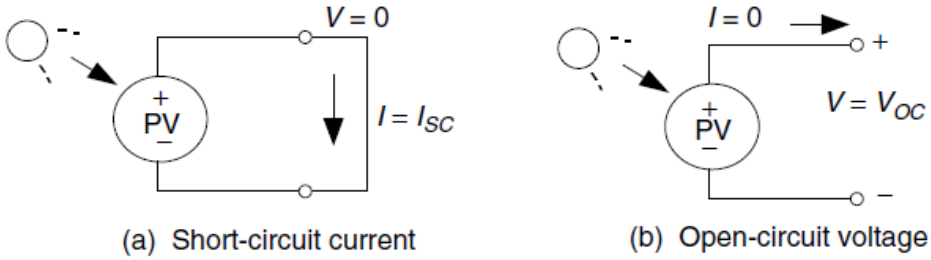

Figure 2.9: Short-circuit current I_{SC} and the open-circuit voltage V_{OC}

b Ideal solar cell I-V characteristics

The output current (I) from the PV cell is found by applying the Kirchhoff's Current Law (KCL) on the equivalent circuit shown in Figure 2-9.a

$$I = I_{sc} - I_d \quad (2.5)$$

Where,
Isc is the short-circuit current that is equal to the photon generated current,
Id is the current shunted through the intrinsic diode.

The diode current *Id* is given by the Shockley's diode equation:

$$I_d = I_0(\exp(q\mathrm{V_d} / K_B T) - 1) \quad (2.6)$$

Where,
q is the electron charge (1.602×10-19 C),
V_d is the voltage across the diode (V),
K_B is the Boltzmann's constant (1.381×10-23 J/K),
T is the junction temperature in Kelvin (K).
Io is the reverse saturation current of diode (A), serving as a reminder that a solar cell in the dark is simply a semiconductor current

Replacing *Id* of the equation (2.5) by the equation (2.6) gives the current-voltage relationship of the PV cell, represented by the equation 2.7

$$I = I_{sc} - I_0(\exp(qV / K_B T) - 1) \quad (2.7)$$

Where,
V is the voltage across the PV cell, and *I* is the output current from the cell.The reverse saturation current of diode (*Io*) is constant under the constant temperature and found by setting the open-circuit condition as shown in Figure 2-9.b.
Using the equation (2.7), let $I = 0$ (no output current) and solve for *Io*.

$$0 = I_{sc} - I_0(\exp(qV_{oc}/K_BT) - 1) \quad (2.8)$$

$$I_{sc} = I_0(\exp(qV_{oc}/K_BT) - 1) \quad (2.9)$$

$$I_0 = \frac{I_{sc}}{(\exp(qV_{oc}/K_BT) - 1)} \quad (2.10)$$

When the leads from the PV cell are left open, I = 0 and we can solve (2.9) for the open-circuit voltage V_{OC}:

$$V_{oc} = \frac{KT}{q} Ln\left(\frac{I_{sc}}{I_0} + 1\right) \quad (2.11)$$

And at 25◦C, (2.9) and (2.11) become

$$I = I_{sc} - I_0(\exp(38.9V) - 1) \quad (2.12)$$

And

$$V_{oc} = 0.0257 Ln\left(\frac{I_{sc}}{I_0} + 1\right) \quad (2.13)$$

To a very good approximation, the photon generated current, which is equal to *Isc*, is directly proportional to the irradiance, the intensity of illumination, to PV cell [17]. Thus, if the value, *Isc*, is known from the datasheet, under the standard test condition, *Eo*=1000W/m^2 at T_{cell} =25°Cthe air mass (*AM*) = 1.5, then the photon generated current at any other irradiance, *E* (W/m^2), is given by the equation 2.14

$$I_{sc}I_E = I_E\left(\frac{E}{E_0}\right)I_{sc}I_{E_0} \quad (2.14)$$

The figure 2-10 shows that current and voltage relationship of the PV cell (often called as an *I-V* curve).The PV cell output is both limited by the PV cell current and the PV cell voltage, and it can only produce a power with any combinations of current and

voltage on the *I-V* curve. It also shows that the cell current is proportional to the irradiance.

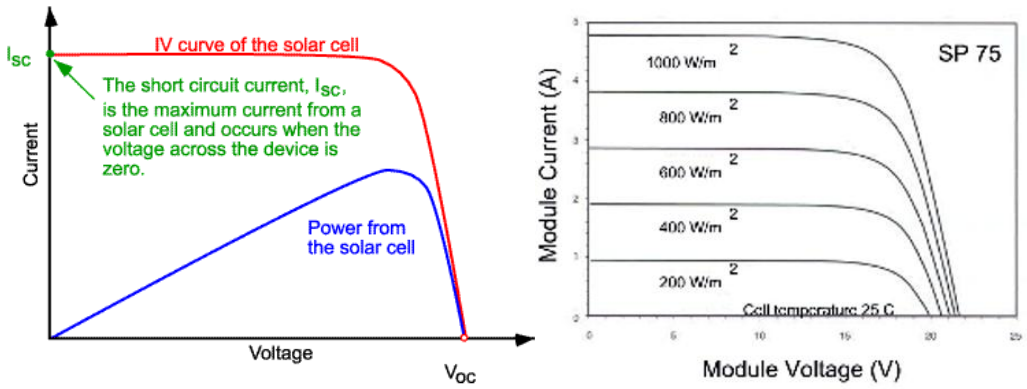

a.I-V characteristics and power b. I-V characteristics under different solar intensity

Figure 2.10 PV cell I-V characteristics

2.2.2 The More accurate PV cell Model

aAccurate solar cell equivalent circuit

In a practical PV cell, there is a series of resistance in a current path through the semiconductor material, the metal grid, contacts, and current collecting bus [18].

a) SeriesResistance

   (R_s) Series resistance its effect becomes very conspicuous in a PV module that consists of many series-connected cells and the value of resistance is multiplied by the number of cells.

b) ParallelResistance

   (R_p) This is also called shunt resistance. It is a loss associated with a small leakage of current through a resistive path in parallel with the intrinsic device [18].

c) Recombination

   Recombination in the depletion region of PV cells provides non-ohmic current paths in parallel with the intrinsic PV cell [18] [19]. This can be represented by the second diode (*D2*) in the equivalent circuit, as shown in the figure 2.11

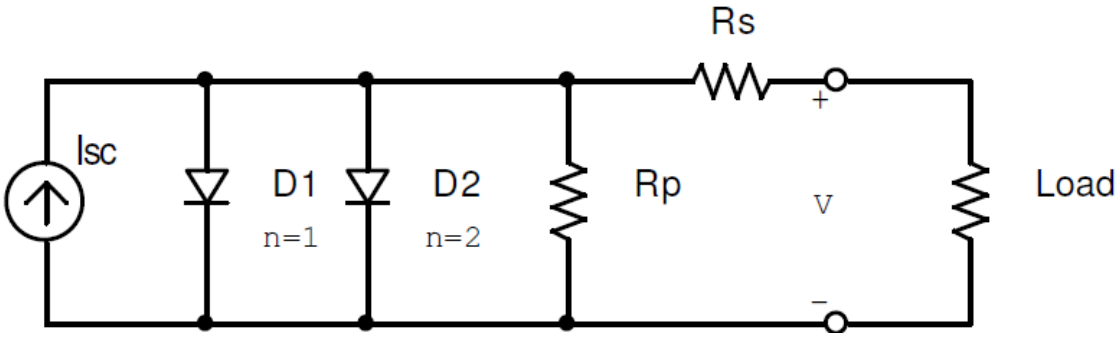

Figure 2-11: More accurate equivalent circuit of PV cell

b Accurate solar cell I-V characteristics

To analyze figure 2.11, start with the simple equivalent circuit (2.8), and then from the current-voltagerelationship of the PV cell, the equation 2.7, the impact of RS is added, then we obtain new relationship presented by the following equation

$$V_d = V + I \cdot R_s \qquad (2.15)$$

Summarizing these effects by including series and parallel resistances, the current-voltage relationship of PV cell is written as:

$$I = I_{sc} - I_{0_1}\left[\exp q\left(\frac{V + I \cdot R_s}{K_B T}\right) - 1\right] - I_{0_2}\left[\exp q\left(\frac{V + I \cdot R_s}{2K_B T}\right) - 1\right] - \left(\frac{V + I \cdot R_s}{R_p}\right) \quad (2.16)$$

It is possible to combine the first diode (*D1*) and the second diode (*D2*) and rewrite the equation (2.8) in the following form.

$$I = I_{sc} - I_0\left[\exp q\left(\frac{V + I \cdot R_s}{nK_B T}\right) - 1\right] - \left(\frac{V + I \cdot R_s}{R_p}\right) \qquad (2.17)$$

Where,

n: is known as the "ideality factor" (takes the value between one and two) [19].

I and V are the output current and voltage of the PV cell,

I_{ph}: photo-current,

I_{01} and I_{02}: are the reverse saturation current of the diodes,

Rs and Rp: serial and parallel resistances,

T: is the junction temperature in Kelvin (K).

q: is the electron charge (1.602×10^{-19} C),

k_B: is the Boltzmann's constant (1.381×10^{-23} J/K),

2.2.3 Photovoltaic Module

The photovoltaic module is formed of some solar cells, which is combined in series and parallel in the aim to provide the required output voltage and current under normal conditions [13]. Protecting for water, dash, humidity and heat, the solar cells are placed in the encapsulation, which has single or double flat glasses. Through the flat glass, the light possible radiates the surface of the solar cell. The solar cell functions to convert the photon energy to the electric energy. The electric energy resulted by the solar cell is direct current (dc) electric. Performance of the solar cell or photovoltaic module depends also on the efficiency. Maximum efficiency of the photovoltaic is approximate 15% for mono-crystal silicon and around 12% for poly-crystal silicon. Because the efficiency is relative low, to get the huge power capacity of the solar generator, many photovoltaic modules are required. The performance of the module can be identified with some methods, but one of the methods knows the model of the solar cell. The PV module is known by its type and its nominal electrical I-V characteristics at STC (Standard Test Condition).

2.2.4 Photovoltaic Generator

aPhotovoltaic field

The photovoltaic field or photovoltaic generator (PVG) or solar-generator is composed of some combination of series and parallel PV modules and known by its nominal output power. The voltage output of the solar-generator depends on the photovoltaic modules connected in series. The current output of the PV generator depends on the photovoltaic modules connected in parallel, which means the PV modules can be wired in series to increase voltage, and in parallel to increase current.

bPV Modules in Series

For modules in series, the I–V curves are simply added along the voltage axis. That is, at any given current, which flows through each of the modules, the total voltage is just the sum of the individual module voltages as is suggested in figure 2.12.a

In an ideal case when numbers (n) of the identical photovoltaic module are connected in series, the open-circuit voltage equals to n^{th} the voltage of one individual module, the output voltage is given by the equation 2.18

$$V_{oc} = \sum_{1}^{n} V_n = V_1 + V_2 + V_3 + ... + V_n \qquad I \geq 0 \qquad (2.18)$$

$$\text{Where, } V_{oc} == nV_{oc1} = nV_{oc2} = nV_{oc3} = ... = nV_{ocn} \qquad I=0$$

The ideal I-V characteristic of n=3 identical PV modules in series by the simulation model is presented in the figure 2.12.b.

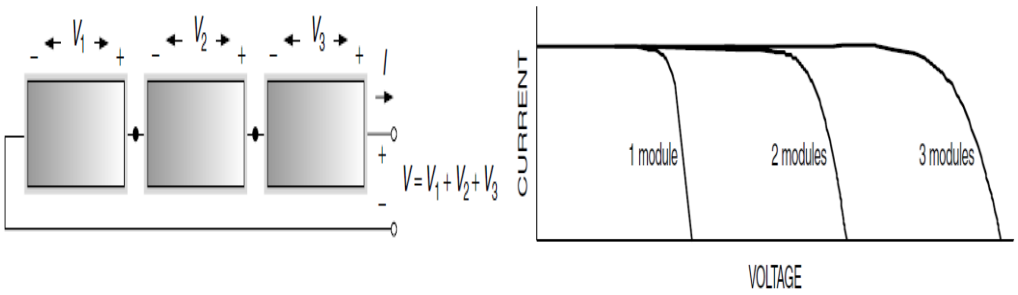

Figure 2.12: PV modules connected in series and their I-V characteristics

c PV Modules in parallels

For modules connected in parallel as shown in the figure 2.13, the same voltage is across each module and the total current is the sum of the currents. That is, at any given voltage, the I-V curve of the parallel combination is just the sum of the individual module currents at that voltage.

The numbers (n) of the identical module are jointed in parallel. The resulting voltage (V_{SG}) is the same for each module and the resulting current (I_{SG}) is the sum of the respective currents I_1 until I_n of the module:

For modules in parallel, at any given voltage the resulting current is given by the equation 2.19

$$I_{sc} = \sum_{1}^{n} I_n = I_1 + I_2 + I_3 + ... + I_n \qquad (2.19),$$

Where, $V_{oc} == V_1 = V_2 = V_3 = ... = V_n$

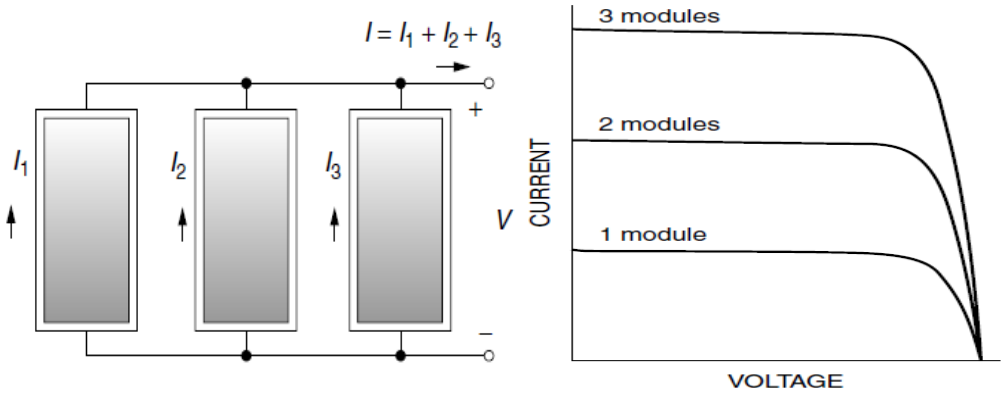

Figure 2.13: PV modules connected in parallel and their I-Vcharacteristics

d PV Modules in series and parallels

The solar-generator of the photovoltaic system with the big capacity is usually consist of a combination of series and parallel modules for which the total I-V curve is the sum of the individual module I-V curves. The integrated assembly of the photovoltaic modules together with support structure (foundation, tracking, box junction, cable and other components) is defined as the photovoltaic array. There are two ways to imagine wiring a series/parallel combination of modules: The series modules may be wired as strings, and the strings wired in parallel, or the parallel modules may be wired together first and those units combined in series. Although, the I-V curves for arrays are the same.by default, the PV array is composed by the combination (PXS) or (SXP) ,where P is the number of strings or PV module rows in parallel and S is the number of PV modules in series.

The figure 2.14a shows a PV array of two parallel strings of three series modules each (2X3).

The figure 2.14bshows a PV array of three strings in series of two parallel modules in each (3X2).

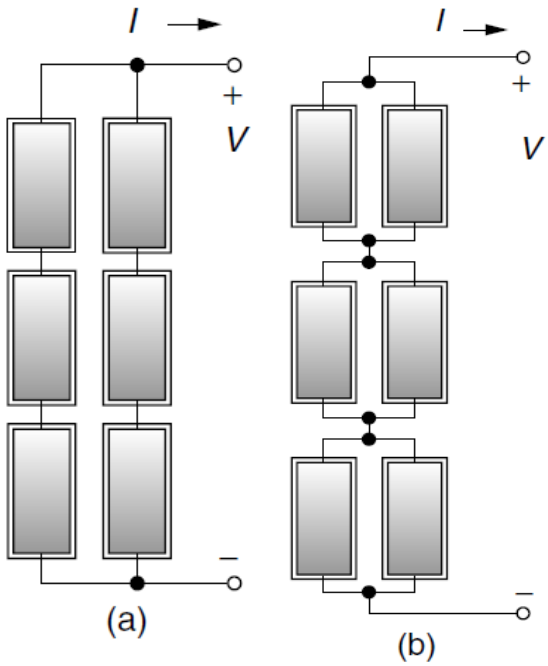

Figure 2.14: PV modules connected in series/parallel

The current and voltage outputs of the solar-generator in the photovoltaic array are given by the following equations: equation 2.20.a shows the voltage output and equation 2.20.b shows the current output.

$$V_{out} = \sum_{1}^{n} V_n = V_1 + V_2 + V_3 + ... + V_n \quad (2.20.a)$$

$$I_{out} = \sum_{1}^{m} I_m = I_1 + I_2 + I_3 + ... + I_m \quad (2.20.b)$$

The power of the solar-generator (Pout) is written in the Equation 2.21:

$$P_{out} = \sum_{1}^{n} V_n \sum_{1}^{m} I_m = (V_1 + V_2 + V_3 + ... + V_n)(I_1 + I_2 + I_3 + ... + I_m) \quad (2.21)$$

2.2.5Impact of temperature and insolation on I-V curves

a- Impact of outdoor conditions on STC values

Any PV module is known by its I-V characteristics at STC (Standard Test Conditions) and its SOC (Standard Operating Conditions) given by the Manufacturers.As cell temperature increases, the open-circuit voltage decreases substantially while the short-circuit current increases only slightly. Therefore, the PV cell performs better on cold, clear days than hot ones. For crystalline silicon cells, V_{OC}drops by about 0.37% for each degree Celsius increase in temperature and I_{SC}increases by approximately 0.05%. The net result when cells heat up is the maximum power slides slightly upward and toward the left with a decrease in maximum power available of about 0.5%/◦C. Given this significant shift in performance as cell temperature changes, it should be quite apparent that temperature needs to be included in any estimate of module performance.

Standard Test Conditions (STC)

- Solar Irradiance: 1 kW/m2.
- Air mass: AM 1.5.
- Cell temperature: 25 ºC.

b- Nominal Operating Cell Temperature (NOCT)

Cells vary in temperature not only because ambient temperatures change, but also because insolation on the cells changes. Since only a small fraction of the insolation hitting a module is converted to electricity and carried away, most of that incident energy is absorbed and converted to heat. To help system designer's account for changes in cell performance with temperature, manufacturers often provide an indicator called the NOCT, which stands for Nominal Operating Cell Temperature. The NOCT is cell temperature in a module when ambient is 20◦C, solar irradiation is 0.8 kW/m^2, and wind speed is 1 m/s. To account for other ambient conditions, the following expression may be used, equation 2.22,

$$\mathrm{T}_{cell} = \mathrm{T}_{amb} + \left[\frac{NOCT - 20^{\circ}}{0.8}\right] E \quad (2.22)$$

Where,

T_{cell} is cell temperature (◦C), T_{amb} is ambient temperature, and S is solar insolation (kW/m^2).

Standard Operating Conditions (SOC)

- Solar Irradiance: 0.8 kW/m^2.
- Wind speed: 1 m/s.
- Ambient temperature: 20 ºC.

Except the Sun intensity and Temperature effect there other factors influencing electrical design of the solar array:**.**

- Sun angle.
- Shadow effect.
- Effect of climate.
- Electrical load matching.
- Sun tracking.

2.2.6Performances ofsolar Generator

a The maximum power point

The maximum power point (MPP) is a vertex point between the current line and the voltage line at the I-V curve with the widest area, at which the product of current and voltage reaches its maximum. The voltage and current at the MPP are the coordinates of the operating point (operating voltage V_m and current I_m). There is a unique MPP at the *I-V* curve produced at each solar intensity hit (Irradiance), at which the module operates with the maximum efficiency and produces the maximum output power (P_{max}). It is possible to visualize the location of the MPP by fitting the largest possible rectangle inside of the *I-V* curve, and its area equal to the output power which is a product of voltage and current, as it is illustrated in the figure 2.15a.

The output power of a photovoltaic generator is the product of the output current delivered to the electricload and the voltage across the PV module junction, and then it is represented by the following equation 2.23:

$$P_m = V_m * I_m \quad (2.23)$$

The figure2.15a shows the Maximum Power Point (MPP) produced by an I-V characteristic curve at a hit of solar radiation.

The graph of the figure 2.15b illustrates the Maximum Power delivered by 2x2 Isofoton (110/24) PV modules.

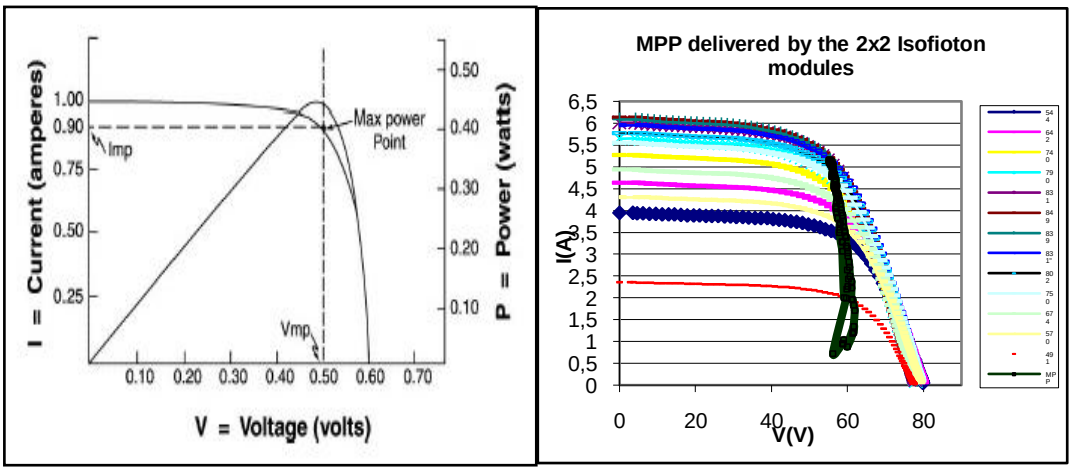

(a) (b)

Figure 2.15: the MPP on I-V curve and the MPP line delivered by a (2X2) PV array

b Fill Factor (FF)

The performance of solar cell or a PV module or a PV array is characterized by the quality of its (I, V) sharpness curve, which consists of the rate power, that the PV array can provide from its total power capacity rate production to feed such load, under outdoor conditions. This rate is called the *Fill Factor* (FF) and is defined as the ratio between the maximum power point (MPP= P_{max}) and the (I_{sc}*V_{oc}) product. The fill factor has no units and can also be approximated by an empirical relationship presented by the relation 2.24. It can be visualized as the ratio of two rectangular areas, as is plotted inthe figure 2.16.

$$FF = \frac{V_m * I_m}{Voc * Isc} \quad (2.24)$$

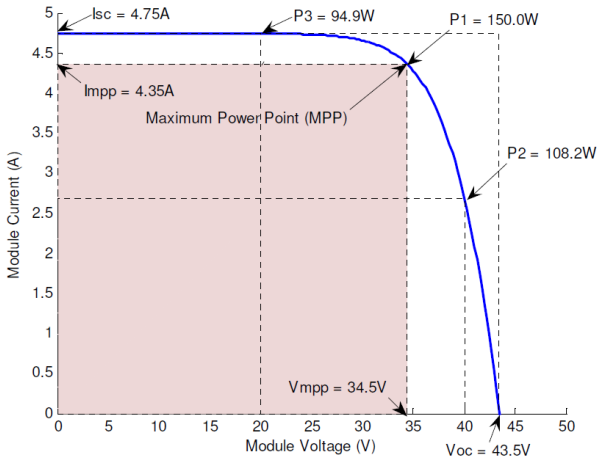

Figure 2.16: Maximum power Point Area

c Power Conversion Efficiency

The power conversion efficiency of a PV array or PV generator is defined as the ratio between the solar cell output power and the solar power hitting the solar cell total surface. In the case of a PV Generator, this efficiency is obtainedby the comparison between energy output of PV generator (V_m*I_m) and solarincident ray on its total PV cell surfaces. The input power equals the irradiance E(W/m^2) multiplied by the cell areaA_{pv},and then it is calculated by the formula2.25.

$$\eta_{PV} = \frac{V_m \cdot I_m}{E \cdot A_{PV}} \quad (2.25)$$

Where,

V_m and I_m are the maximum voltage and maximum current of the PV generator output

E solar incident ray on the PV generator surface

A_{pv} Total PV generator area

Chapter3: Study and sizing of a photovoltaic pumping system (PVPS)

3.1 Sizing of a PV pumping design

3.1.1 Purpose of the project

The Photovoltaic Water Pumping Systems (PVPS) constitute a potential option to drawdown water in the remote desert areas for domestic usage, irrigation and livestock watering. The abundance of both solar irradiance and the ground water sources, in Ghardaia region are suitable to profit of this new technology.Through a sizing studyof a stand-alone PV pumping system an optimal installation design has been occurred in the purpose to be eventually erected on real farm in Sebseb region, about 60 km south west of Ghardaia. The mentioned PVPS installation is designed and studiesto supply an average daily quantity of water reaches the 30 m^3, drawn from the borehole of the farm with Manometric Total Head (TMH = 25m). Upon technical data of both the well and the water consumption, a PV pumping design has been obtained.The (PVPS) consists of a submersible Grundfos DC pump with nominal electrical characteristic(DC maximum voltage V_{max}= 30V - 300V, maximum current I_{max} = 7A, maximum power P_{max}= 900 W), PV powered by (2 x 6) Isofoton PV module array with nominal electrical characteristics (Open circuit voltage V_{oc} = 40V, Short circuit current Isc=3.5A, maximum power P_{max}= 110W) each.

In general the sizing of any PV pumping system should pass through the following steps.

- Characteristics of the site
- Technical data of the well
- Estimation of the daily water need.
- Estimation of the required energy
- Photovoltaic field peak power

3.1.2 Characteristics of the site

a Water and solar sources

Ghardaia province is located in the central gate of the great Algerian Sahara. The capital town is about 600 km far from Algiers. Rocky land in West-southern part and sandy in the eastern part.Ghardaïa's ancient water distribution system was devised by the Mozabites, keeping in view the ephemeral flows of its oueds (rivers). Realizing the preciousness of this natural resource, the Mozabites developed a unique hydraulic system of underground tunnels to harvest rainwater and divert it to the oases. They have an equitable water distribution to all gardens and also maintain good flood protection measures. The water supply is accessed in a number of ways through an incredible irrigation system that distributes water from many wells. Well drilling occurs to a depth ranging from 20 m to 150 m. The water static level of wells and boreholes varies between 20 m and 50 m in Metlili and Sebseb valleys and less than 10m in Menia basin, south of Ghardaïa.TheAlbian fossil groundwater reserves are estimated at 1.5 trillion m3. The region is classified as arid and semi-arid area and has a great solar radiation potential with an estimated daily annual average yield ranges from 6kW/m²/day until 7kW/m²/day, received on tilted PV surface at optimum angles. The minimum average temperature level recorded in January, the coldest month is about 10.7 °C; however, July is the hottest month with an average temperature level is about 34°C.The monthly annual solar radiation histogram received on horizontal and tilted surfaces by radio-metric sun-tracker at Ghardaia site is shown in the figure 3.1.

The insolation is measured in sun-hours,

(1 sun-hour = 1 kwh/m^2 /day)

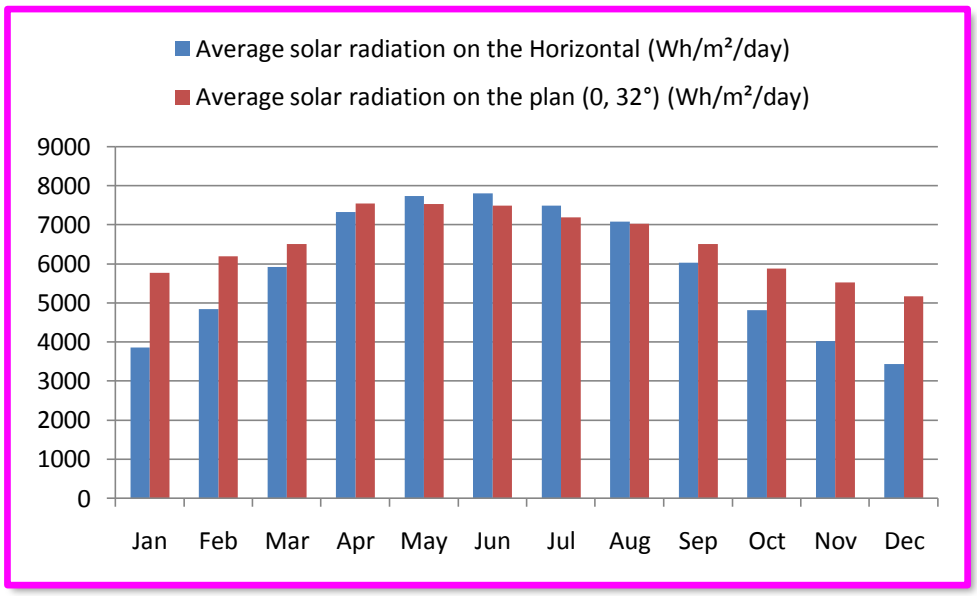

Figure 3.1 Yearly solar irradiance on horizontal & tilted plan recorded in Ghardaia

The yearly monthly Max, Min and average temperatures recorded in Ghardaia is illustrated in the figure 3.2.

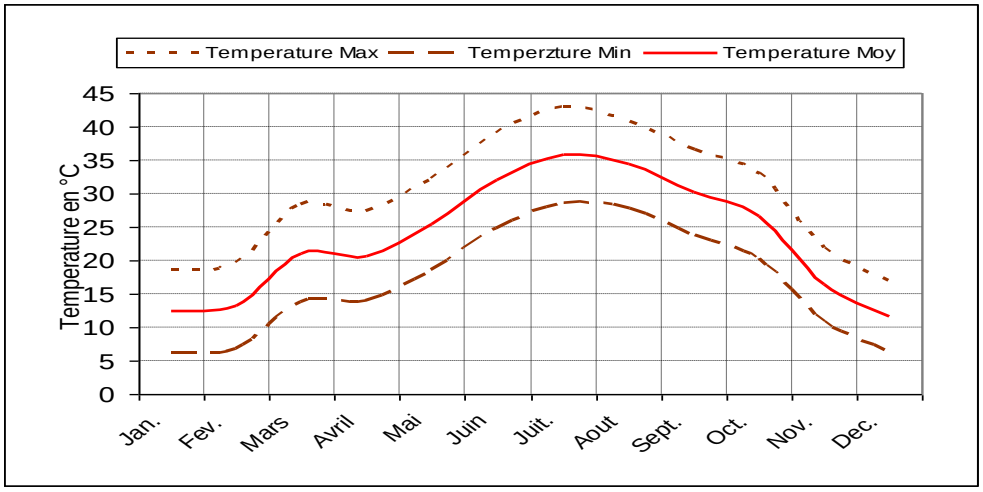

Figure 3.2. Annual monthly temperatures

b Location and meteorological characteristics of Ghardaia

Location: about 600 Km south of Algiers

Latitude: 32° 36’ N

Longitude: 3° 81’E

Elevation above the sea level: 450 m

Specification: Classified as arid and semi-arid area.
Sunny days: around 80% per year.
Daylight hours: range from 5 until 10 hours.
Summer Ambient Temperature: 26 °C to 42 °C
Yearly irradiance: from 5kWh until 8kWh per day (On horizontal PV surface)
Agriculture: Palm trees, Livestock, local vegetables.

3.1.3 Technical data of the well

Maximum monthly daily average cumulative water demand: $30m^3$ /day
Diameter of the borehole (diameter of the well): 1.80m
Static head: SH=16m
Dynamic head: DH =20m
Elevation of the tank from the ground: TH=2m
Hydraulic load losses estimated at 10%
Total Manometric Head TMH= 25 m
Distance between the well and the tank: 200m
Diameter of the water conduction pipe: 50/60
Capacity of the tank: $200m^3$

The Total Manometric Head is calculated by the following relation;
$TMH = Hg + L_h$
Hg: Geometric Height between the dynamic level and the pipe outlet.
L_h: Losses of the hydraulic load caused by the water friction on the piping wall, these losses are in function of the piping distance (D), their diameter (dp) and of the pump flow rate.
Upon the above technical data of the borehole, the Total Manometric Head is obtained as follows:
$TMH = Hg + L_h = D_H + T_H + (10\%Hg)$
$THM = 20+2+(22 \times 0.1) = 24.2$ m
Then, the TMH is estimated at 25m

3.1.4 Estimation of the water need

a- Influence factors on water estimation

It is more complex to estimate the water requirements for an irrigation application, and thus is beyond the scope of this work. The kind of crop, meteorological factors (temperature and humidity, wind speed and cloud cover), method of irrigation (prevent any water losses) and the variation of insolation throughout the seasons of the year are the principal factors to be considered. The water in the well does not always stay at the same level throughout the year. To be sure the well will produce enough water year round; measurements should be made during the driest month of the year, when the water level in the well and the recharge rate are usually the lowest.

Three different parameters needs on should be considered to determine the quantity of water to be pumped by such PV-powered water pumping system:

- Water for drinking and cooking
- Water for livestock
- Water for crop irrigation

b- Estimation of the farm water demand

During hot seasons, the farm demand on water doesn't exceed the nominal capacitywhich is 30 m^3/day.It will be approximately the maximum system's requirement during 7 sun-hours daily.

There is no energy storage (no batteries). The farm has a storage consists of a ground storage tank of 200 m^3 capacity. It is enough to satisfy the farm need in water and the surplus quantity is used to substitute any deficit in water demand during the cloudy days when there is no much insolation level to provide the starting current for the motor pump, or when the system is stand by for further maintenance. The figure 3.3 shows the variation of the yearly monthly daily estimated volumes of water to be provided by the expected PV pumping system.

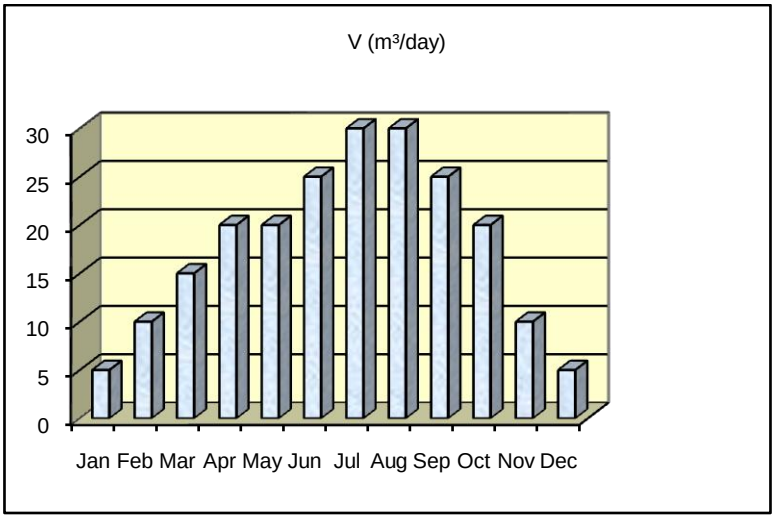

Figure 3.3: Monthly daily average of required water volumes

3.1.5 Estimation of the required energy

a. The daily required hydraulic energy in (Wh/day):

The daily required hydraulic energy is the total hydraulic energy should be achieved by the Motor-pump to extract a daily flow rate volume of water Q_d (m3/day) from a given head TMH (m) (Total Manometric Head). The Motor-pump hydraulic energy is calculated by the equation 3.1

$$E_h = C_h x Q_d x \text{ TMH} \qquad (3.1)$$

Where,

E_h: hydraulic energy to be achieved by the pump in Watt-hour per day (Wh/day)

C_h: Hydraulic constant is dimensionless

Q_d: Daily flow rate or the daily required volume of water in cubic meter per day (m^3/day)

TMH: Total Mano-metric Head (Difference of water pressure between the pump inlet and the pipe outlet) in meter (m).

By mean of water density (ρ= 1000 Kg/m2) and the Gravitation(g= 9.81 m/s^2), the hydraulic constant is calculated as follows;

$C_h = g \cdot \rho = [9.81 (m/s^2) \times 10^3 (Kg/m^3)] / 3600 (s/h)$, and then it becomes;

$C_h = 2.725 (Kg.s.h/m^2)$.

Thus, the daily required hydraulic powerfinal relationship is presented as follows;

$$E_h = 2.725 \times Q_d \times TMH \qquad (3.2)$$

In our case study the maximum average daily required volume of water has been estimated of about $Q_d = 30\ m^3$. This quantityshould be pumped from the well with Total ManometricheightTMH = 25 m. Thus, the predicted maximum daily hydraulic energy required by the couple Motor-pump is calculated by mean of the equation 3.2, and, then it becomes:

$$E_h = 2043.75 \text{ Wh/day}$$

b. The daily required electric energy in (Wh/day)

The daily required electric energy is the total electric energy demanded by the couple Motor-pump to drawdown the daily quantity of needed water.Assuming the overall efficiency of the couple pump- electric motor is $\eta_p = 45\%$ which yields a demanded input electric power calculated by the equation 3.3:

$$Ee = \frac{C_h \times Q_d \times TMH}{\eta_p} \qquad (3.3)$$

Where;

E_e : is the maximum daily required electric energy in Watt-hour per day (Wh/day)

C_h: Hydraulic constant dimensionless, $C_h = 2.725$

Q_d :The maximum daily flowrate of water in Cubic meter per (m^3/day)

TMH: Total Manometric Head in meter (m)

η_p: The couple Motor-pump efficiency in (%)

In our case study, the daily required electric energy is estimated as follows;

$$E_e = (2.725 \times 30 \times 25)/45\%$$

$$E_e = 4541.66 \text{ Wh}$$

3.1.6 Estimation of the required total peak power

a. The Photovoltaic field nominal Peak power in (W)

The sizing (Dimensioning) of a Photovoltaic Pumping System (PVPS) consists of determining the nominal photovoltaic peak power necessary to feed such system. Based on the data base of the yearly monthly daily average of the solar radiation (insolation) and the monthly daily average of daylight hours, the nominal Peak Power of the predictive photovoltaic field necessary to feed a PV Pumping System (PVPS) to drawdown a maximum daily volume of water froma fixed TMH is calculated by the following model presented by the equation (3.4);

$$P_{peak} = \frac{E_e}{\left[Dl_h\left(1 - Losses\right)\right]} \qquad (3.4)$$

Where,

P_{peak} : The nominal Peak Power of the photovoltaic field in Watt (W)

E_e: Electric energy required in (Wh/day)

Dl_h : Number of daylight hours of the weakly insolated month

According to the averages of solar radiation (table 3.1), recorded by the Radio-metric SUN-Tracker installed in our site at Ghardaia, during the years 2005, 2006 and 2007, December is the month of the cold season, where the maximum irradiance received on tilted PV panel with tilt angle equal to the latitude of the site (32°) is the most weak (5180 kWh/m2/day). It is also the month, where the number of daylight hours (insolation per day) is the most less, and then is estimated of about (*Dl*=5 sun-hours). So for a full south facing PV panel with tilt angle equal to the latitude of the site (L=32°), the average of insolation-hours reaches is about 7 sun-hours. The losses caused by dust and temperature are estimated of about (losses = 20%).

Accordingly, the Nominal Peak Power (NPP) of the photovoltaic PV array able to provide an electric energy of about (E_e = 4541.66 Wh) to feed such PV pumping system is calculated by the equation (3.4) and the obtained result is as below:

$$P_{peak} = \frac{E_e}{\left[Dl_h\left(1 - Losses\right)\right]}$$

P_{peak} = 4541.66 /[5 x (1 –20%)]

P_{peak} = 1135.416 Watt, it can be estimated at 1200 Watt

The table 3.1 below shows the averages of solar radiation on horizontal and tilt surface

as well as the daylight-hours, recorded by the radio metric sun-tracker, installed at our site in Ghardaia;

Month	Average solar radiation on the Horizontal (Wh/m²/day)	Average solar radiation on the plan (0, 32°) (Wh/m²/day)	Daylight hours (Hours)
Jan	3871	5778	5,778
Feb	4842	6196	6,196
Mar	5926	6513	6,513
Apr	7339	7554	7,554
May	7745	7532	7,532
Jun	7812	7493	7,493
Jul	7503	7200	7,2
Aug	7090	7033	7,033
Sep	6036	6513	6,513
Oct	4824	5892	5,892
Nov	4026	5534	5,534
Dec	3437	**5180**	**5,18**

Table 3.1: Monthly daily averages of solar radiations and daylight-hours recorded at Ghardaia

b. Configuration of the Photovoltaic field

The configuration of the PV array is composed of Isofoton (110/24) PV modules, erected outside the PV pumping laboratory. The selection of the PV generator configuration is carried out in manner that it can fulfill the required nominal peak power, previously calculated and it is necessary that the I-V characteristics of the pump set match those of the PV array. The maximum required power by the pump, the maximum current and voltage are the main electric characteristics, which should be involved in the PV generator configuration. In our case, the PV array configuration should match the electric characteristics of the selected DC Grundfos pump (DC V_m = 30 - 300V, $_{Isc}$ = 7A, P_m= 900 W), which is available in our PV pumping laboratory.With reference to the nominal electric characteristics of the Isofoton PV module,the estimated number on the mentioned PV module required by the PV pumping system is determined by mean of themodel presented by the equation 3.5. The following table resumes the I-V characteristics required by the pump and the I-V characteristics provided by the PV generator configuration. of the pump is a DC Grundfos model pump with the electric characteristics(DC V_m = 30 - 300V, I_{sc} = 7A, P_m= 900 W).The mentioned Grundfos type

is also available in our PV pumping laboratory.With PV modules of Isofoton (110W/24V) type, the estimated number matching to the demand of the PV pumping system is obtained by mean of the following model:

Number of PV modules = P_{peak} of Photovoltaic field/P_{peak} of the module

Number of PV modules = 1200W/110W =10.909, estimated at 12 PV modules.

The selected PV generator configuration consists of two parallel PV arrays of 6 IsofotonPV modules each,

An example of such PV generator configuration based on Isofoton PV module type is shown in the table 3.2;

	Electric energy E_e(Wh)	Daylight hours Dl (S-hours)	Losses (%)	Peak power P (W)	Nominal Voltage V (V)	Nominal Current I (A)	PV array Configuration
First string	(4541.66)/2	5	20%	1200/2	40 x 6	3.5	6 modules in series
Second string	(4541.66)/2	5	20%	1200/2	40 x 6	3.5	6 modules in series
Total PV array design	(4541.66)	5	20%	1200	40 x 6	7	(2 x 6)

Table 3.2 PV array configuration based upon Isofoton (110/24) PV module type

3.2 Characterization tests

3.2.1 Purpose of the characterization

The characterization is the main step in each PV pumping system sizing, since the electric characteristics of both the PV module and the Motor-pump couple were given in STC (Standard Test conditions) which are (Solar Irradiance: 1 kW/m2, Air mass: AM 1.5, PV cell junction temperature: 25 ºC). The characterization work consists on series of tests carried out under the outdoor conditions of the local site, for the aim to investigate the performances of the different parts of the PV pumping system.

During the 2005 and 2006, complete PV water pumping test bench has been installed at our URAER (Applied Research Unit for Renewable Energies)/ Ghardaïa to carry out the characterization tests on both DC and AC water pumps. The characterization of the

PV module or PV arrays were performed with a completePVPM2540C (Peak Power Measuring Device for PV-Modules).The obtained results will constitutes a data base to be used in such required study of PV pumping systems. The two main facilities and the method of test are described in the following section.

3.2.2 Material and Method

a. Synoptic of the Photovoltaic Module Test Bench

The Photovoltaic test facility is composed of a main device PVPM2540C (Peak Power Measuring Device for PV-modules) of type PVPM2540C, which enable the measurement of the I-V curve of photovoltaic modules, a combined sensor of Phox sensor model, for measuring the irradiance and the PV cell temperature and a support frame to hold the PV module during test The figure 3.4 shows the synoptic of the photovoltaic module test bench.

The Connecting Peripheral Devices are described as follows;

- **PVPM2540C:** The PVPM is a mobile measuring device with integrated battery supply and battery charger in a durable metal housing. The device has its own industrial miniature PC and a high-contrast LCD display and thus its function is independent of other devices. However if desired a PC can be attached for data transfer and further analysis of the measured values over a standard interface. The PVPM is operated comfortably over few keys and an onscreen menu. The functions are defined self-describing and the user is always led by the program.

- Phox sensor with Pt1000: Phox sensor with Pt1000 temperature sensor is a combined sensor for measuring the irradiance and the PV cell temperature. The PVPM expects this temperature to be nearly the same as that of the measured module. This will be true with sufficient precision if the reference cell and the PV module were exposed to the sunlight for same period of time (at least 5 minutes).Very important is a sufficient irradiance to the module and precise alignment of the reference cell towards the module. Often the easiest way is to clip the combined sensor directly to the side or top of the measured module.

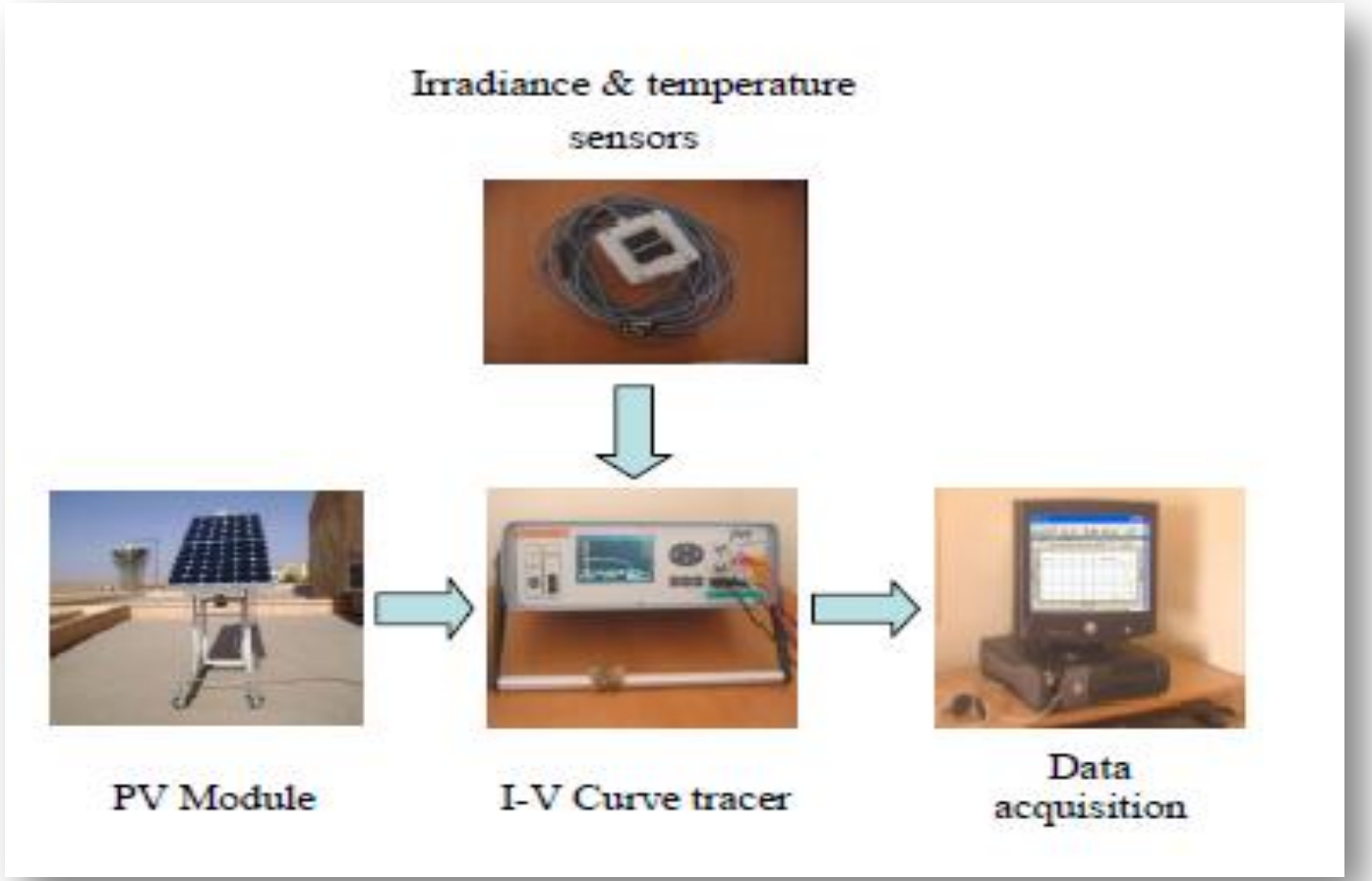

Figure 3.4: Synoptic of the PV module test bench

- Support frame: is a steel support frame to hold the PV module exposed to the sun during the test operation. The PV module subject to test is placed on this frame, in a place with enough exposure to the solar radiation (no shadow), at an optimal tilt angle close to the local latitude.

- PC: The device internally stores the data of more than 100 measurements, only. For more number of scans it is necessary to add an external PC connected to the PVPM. The results of the test should be stored at the end of the measurement to be treated later.

bMethod of PV module test

- Mounting the PV module subject to test on the support frame or connecting the PV array configuration directly to the PVPM2540.

- Characterization tests were carried out at outdoor conditions of the local site.

- The scans of measurements were taken from thesunrise until the sunset within a scan period of at most 5minutes.

- The I-V curve characteristics are shown on the PVPM2540 miniature high-contrast LCD display.

- The data transfer is performed via a PC.

c Synoptic of the Photovoltaic Water Pumping Test Bench

The synoptic of the stationary PV water pumping facility installed at URAER/Ghardaïa is shown in the figure 3.5. It consists of a complete test bench assembled by the following parts:

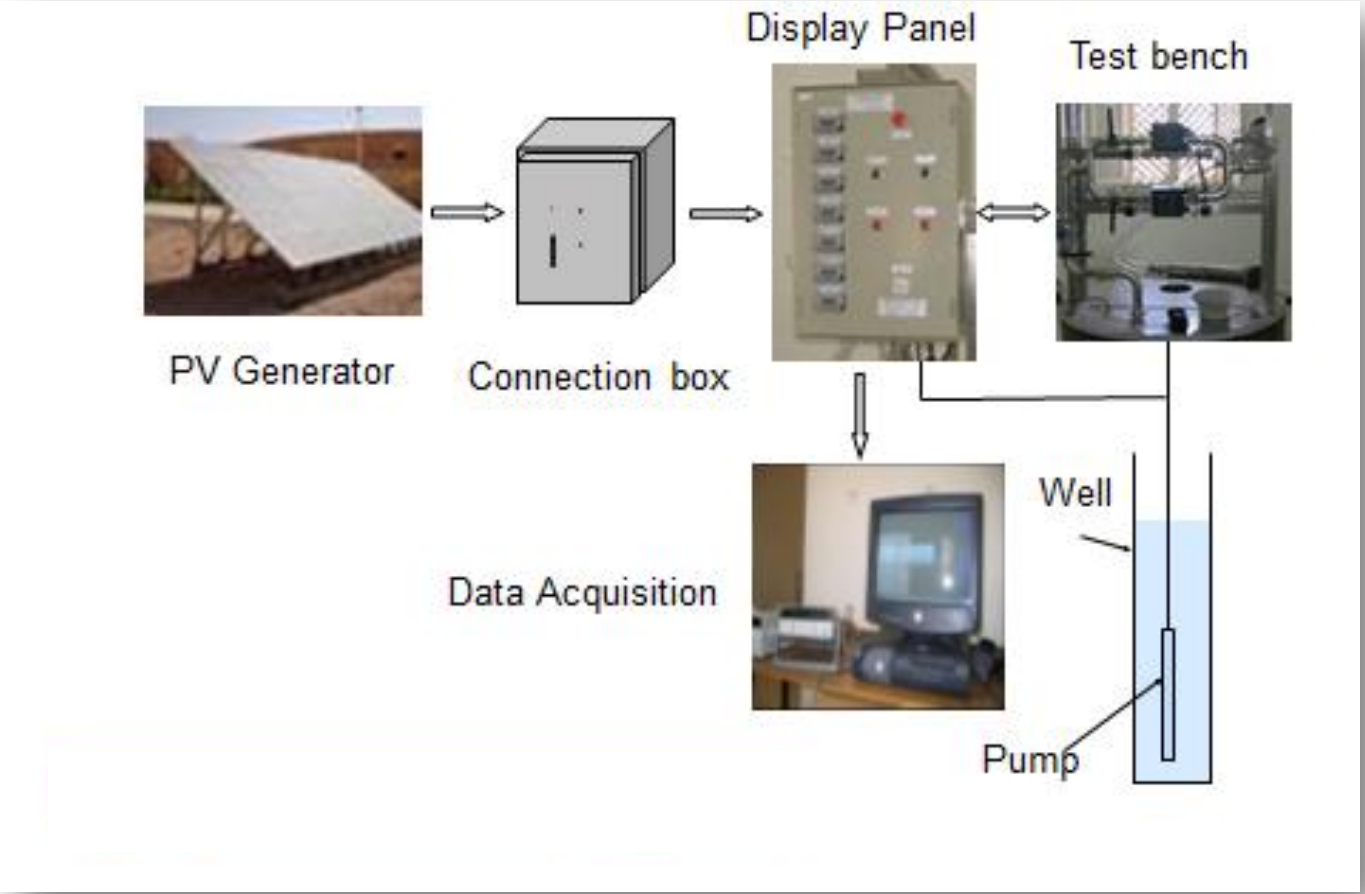

Figure 3.5: Synoptic of the PV pumping test bench

❖ **Inside the lab:**

- Stainless steel tank (artificial well), type Acerinox 1.4301 2B / 034DC7, completed by hydraulic system which involve two flow meters, two pressure sensors and control valve to adjust the water pressure.
- MPPT (300W) for low power
- DC/AC inverter for three phase pumps.
- Electrical panel display which displays the following parameters:
  - Current I(A)
  - Voltage V(V)
  - Temperature (°C)
  - Irradiance (W/m2)
  - Pressure P1: simulated well head ranges from 0 to 160m.
  - Pressure P2: simulated well head ranges from 0 to 10m.
  - Pressure P3: static level of the tank (artificial well) ranges from 0 to 2.50m.
- Connexion box to select the different configuration (DC pump, DC/AC pump via the inverter and DC pump via MPPT).
- Data logger - Agilent 34970A connected to PC

❖ **Outside the lab:**

- PV generator composed of 26 Isofoton(110W/24) PV module type , implemented about 40m away from the lab, south facing, tilted with an inclination angle close to the latitude of the local site (32°).
- Earth installation.

dMethod of PV pump test

- Mounting of the pump in the artificial well (Stainless steel tank of 2m)of the test bench,previously filled of water(Stainless steel tank of 2m).
- Pumping in closed loop.
- Control the fixed pressure: Due to the unpredictable irradiance, the pressure control valve must be adapted continuously according to the actual irradiance to keep the fixed water pressure which corresponding to the fixed head (the friction is negligible).
- Flow rate and the cumulative water volume are measured with flow-meter.
- The results are shown on the display panel and recorded on PC via Data Logger, simultaneously.

3.2.3 Characterization of the PV Generator

a Description of the measurement

The PVPM automatically measures the I-V-characteristic of the PV array at a capacitive load. From the measured data it calculates the effective solar cell characteristic, P_{peak} (Peak power) and Rs (Shunt resistance). After the measurement the data are stored automatically in a non-volatile storage and so are available also later in the office. The following results are displayed, as illustrated in the figure

Permanent values:

- Peak Power P_{peak}
- Internal Series Resistance Rs
- Internal Parallel Resistance Rp
- Current values, depending on irradiation and temperature:

V_{max} , I_{max} , P_{max} , V_{oc} , I_{sc} , FF, T_{cell} , E_{eff}

The I-V characteristic can also be shown directly on the LCD display of the PVPM as illustrated in the figure3.6, which show the evolution of the characteristics during a clear sky day.

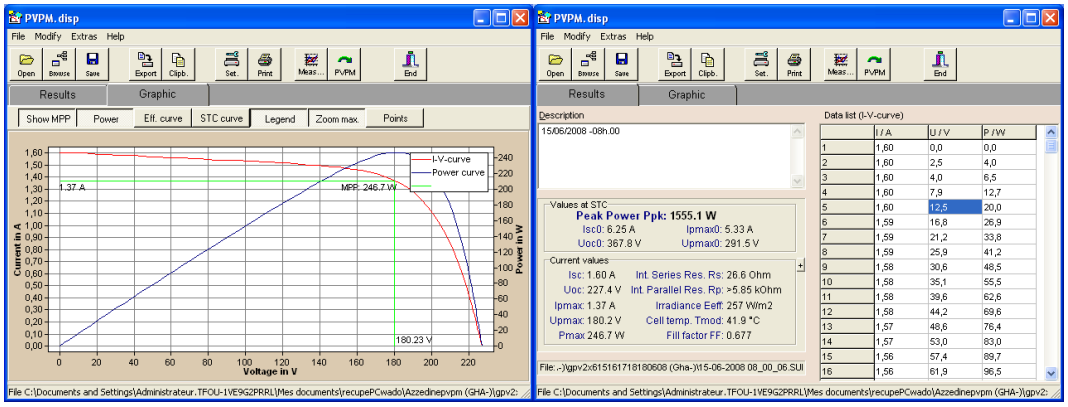

(a) At time: 8h:00

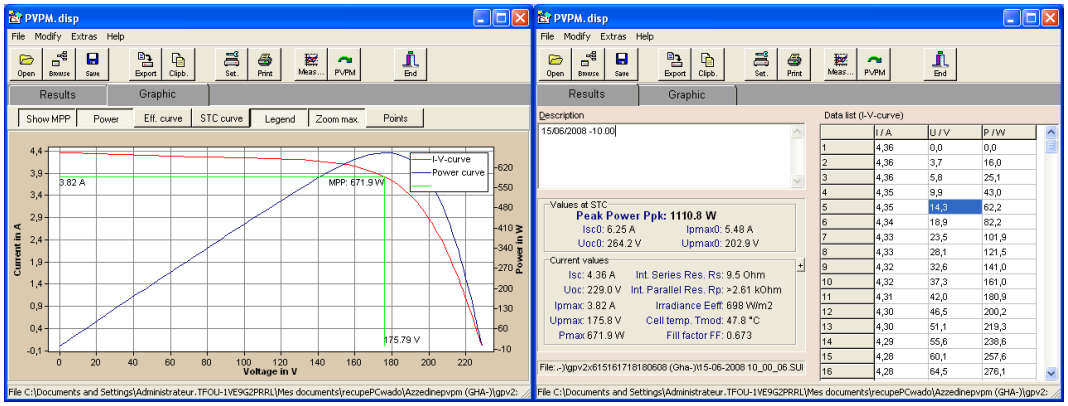

(b) At time: 10h:00

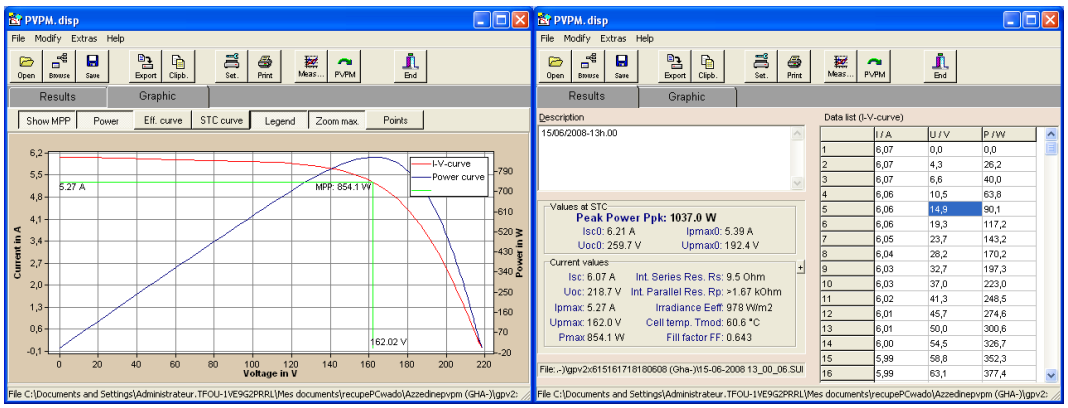

(c) At time: 13h:00

Figure 3.6: Different I-V characteristics of the PV generator (2x6) displayed by the PVPM LCD

b Results and Discussion

The characterization tests have been undertaken on one PV Isofoton module, separately,and then several tests were carried out on the PV array (2 x 6) configuration. Through the treatment of the recorded results, the experimental Fill factor (FF) and Efficiency (η_{pv}) have been obtained, for each configuration.

Nominal I-V characteristics and the performances of the PV array configuration achieved following the characterization tests are shown in the table 3.3.

PV array design	Nominal I-V characteristics			Total PV cell area	Fill Factor	PV arrayefficiency
Modules PVG (P x S)	I_{sc} (A)	V_{oc} (V)	P_{peak} (W)	A_{pv} (m²)	FF (%)	η_{pv} (%)
PVG1 (1x1)	3.5	40	110	0.72	72	12
PVG (2 x 6)	7.0	240	1320	8.64	75	12.75

Table 3.3 Nominal I-V characteristics and experimental performances of the PV array

As it is mentioned in the previous chapter.2, the performances of each PV array is characterized by the quality of its (I,V) sharpness curve, which consists of the rate power that the PV array configuration can provide from its total power capacity rate production to feed such load (pump).The achieved performance values following the characterization of the PV array configuration (2X6) are: FF = 75% and η_{pv} = 12.75%.
Since the PV Isofoton module is mono-crystal cell and its efficiency is around 15% at Standard Test Conditions (STC), the obtained experimental efficiency means that the Mono-crystal Isofoton (110/24) PV modules are very adapted to deliver a significant amount of energy under the outdoor conditions of the local site.

The PV array I-V characteristics curves recorded on clear day are at different insolation levels are illustrated in the figure3.7.

- PV generator I-V curve at E= 215 W/m^{2}and T_{cell} =34.6 °C
- PV generator I-V curve at E= 413 W/m^{2}and T_{cell} =45 °C
- PV generator I-V curve at E= 602 W/m^{2}and T_{cell} =49.5 °C
- PV generator I-V curve at E= 978 W/m^{2}and T_{cell} =51.9 °C

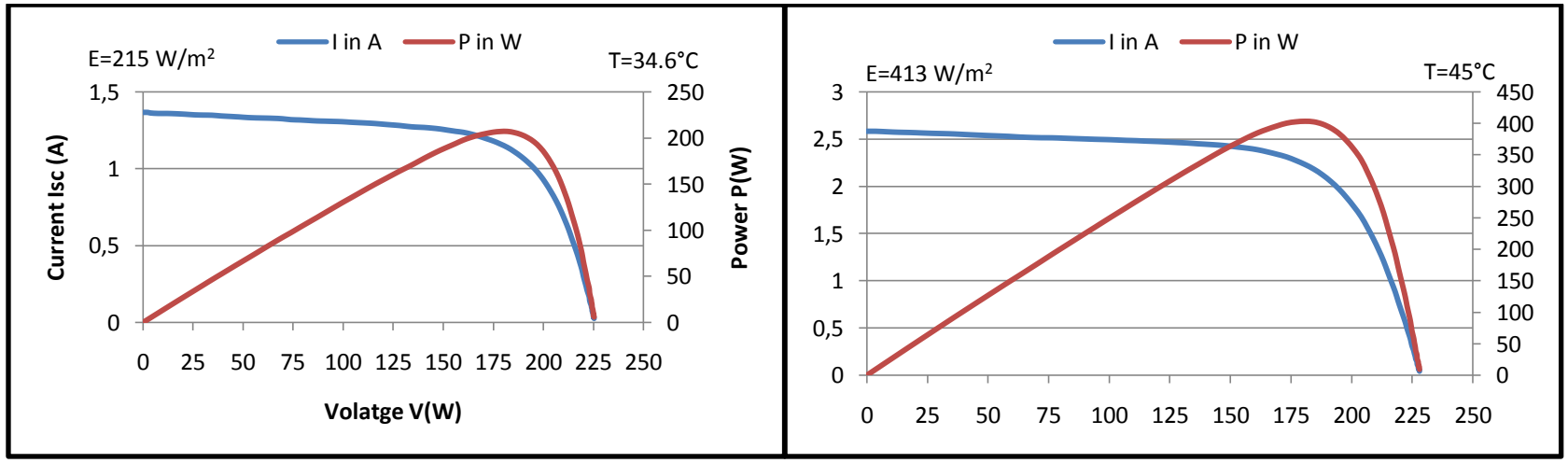

(a) (b)

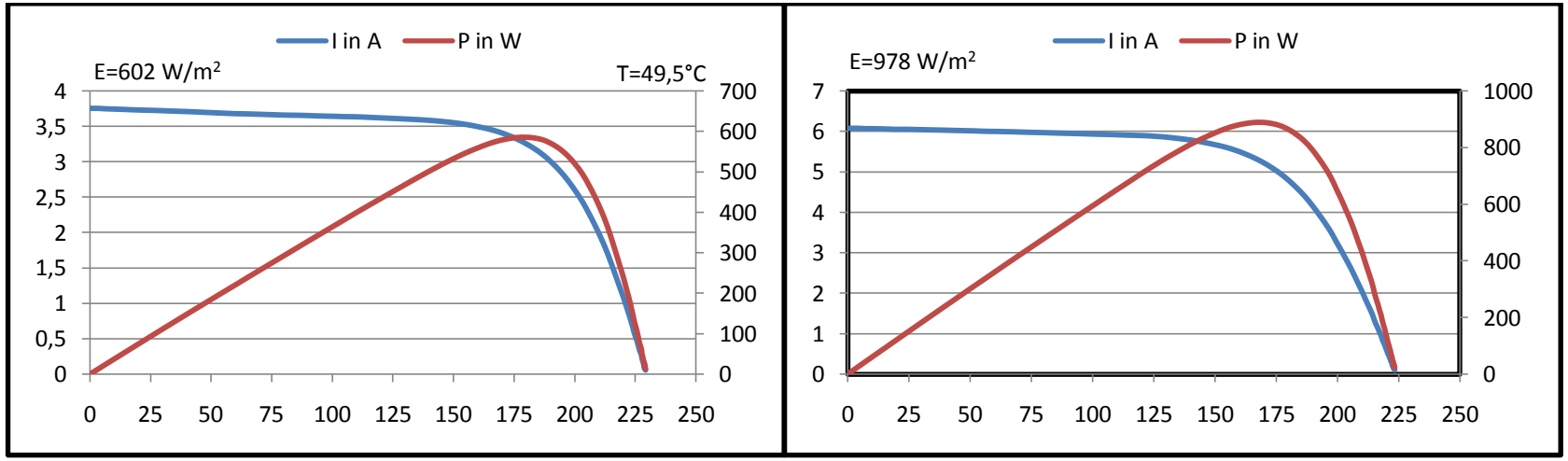

(c)Figure 3.7: I-V curves of PV generator (2x6) characterization at different insolation's (d)

The variation of PV generator I-V and P-V curves recorded at different solar radiations on clear sky day are presented in the figure 3.8 (a & b), below.

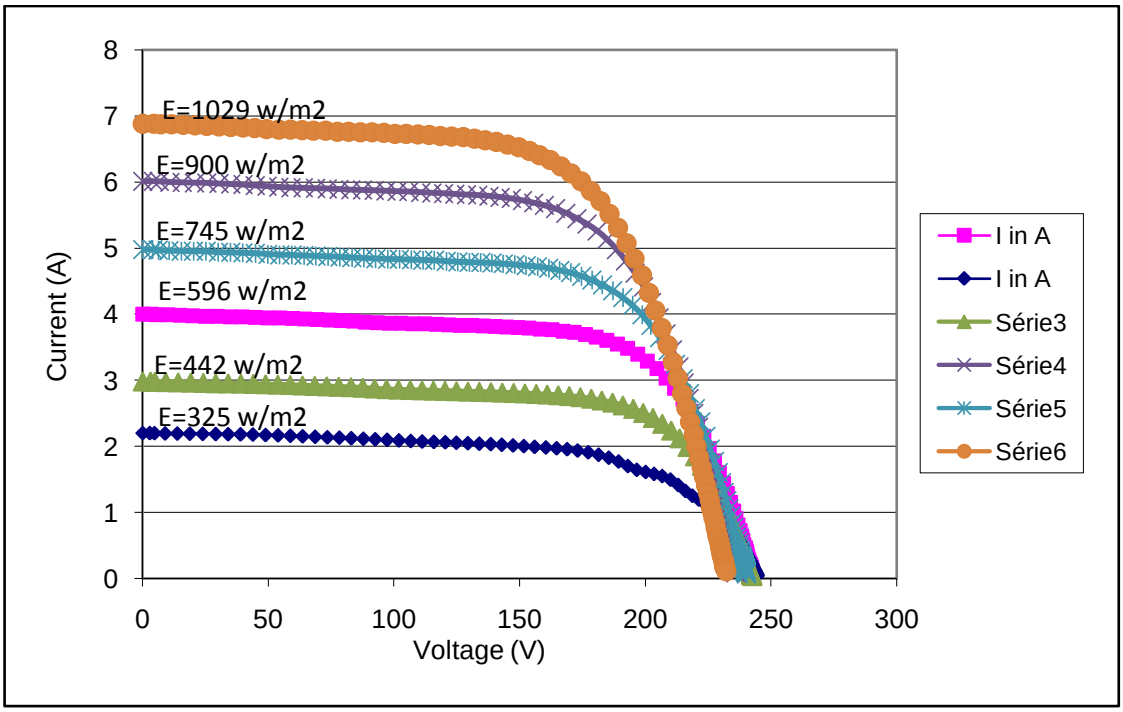

(a) I-V curves at different solar radiations

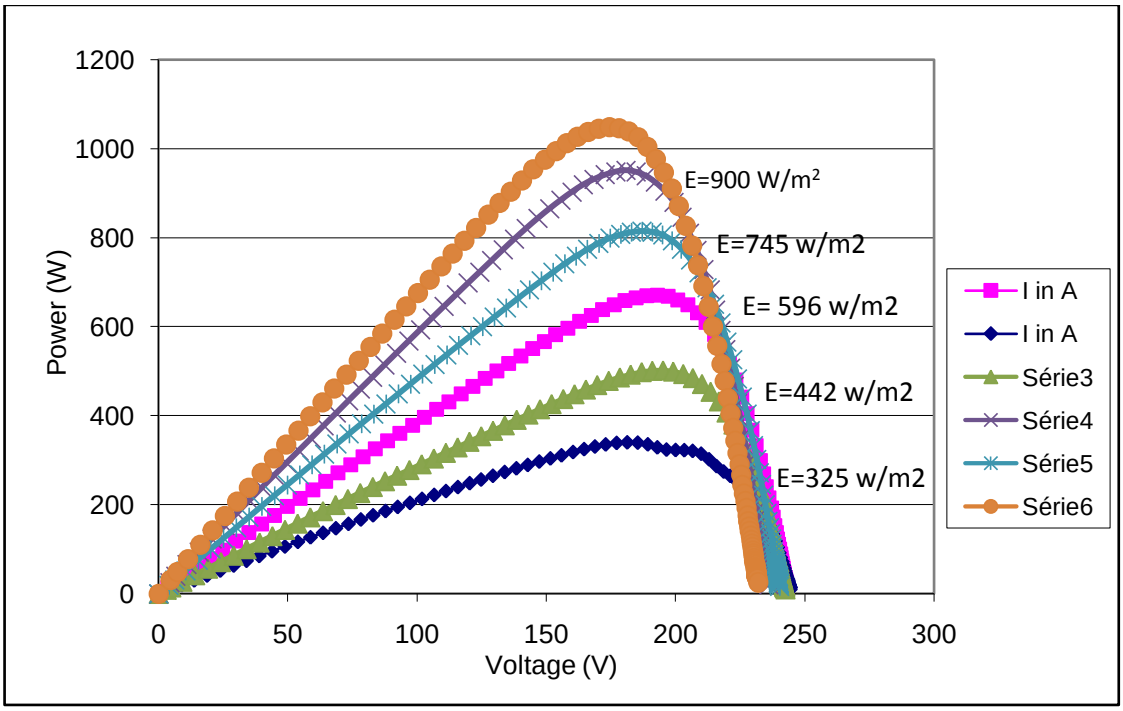

(b) Corresponding P-V curves at the same solar radiations

Figure 3.8; the PV Generator I-V and P-V curves at same solar radiations

3.2.4 Characterization of DC Grundfos pump

a Description of the measurement

PV powered by the selected PV generator configuration, which consists of two parallel strings with 6 Isofoton (110W/24V) PV modules connected in series, each. The DC Grundfos pump has been put into tests, under the outdoor conditions of the site.The pump is tested for different Total Manometric Heads (TMH) ranging from 10m until 40m, during straight eight (8) hours of pumping, in selected clear sky days. All data of the instantaneous output power P(W), hourly discharge of the water (flow rate Q (m3/h)), the current I(A), voltage V(V) and the solar radiation intensity E(W/m²) were stored in data logger - Agilent 34970A-.

The obtained data have been treated, then the study included different parameters affecting the pump performances as, the required electrical energy, the hydraulic energy provided by the pump, the incident energy received on the PV array, then the pump efficiency and the overall efficiency of the system have been calculated, for each head.

b Results and Discussion

The daily electric energy required by the pump is obtained by integrating [7] the power P (W) demanded by the pump over a 7 hours of straight pumping, is given by the equation 3.5

$$E_{em} = \int_{day} P.dt \quad (3.5)$$

The daily hydraulic energy provided by the pump is calculated by the formulae.3.6:

$$E_{hm} = C_h * H * \int_{day} Q.dt \quad (3.6)$$

The incident energy received on the PV array area during 7 daylight hours is given by the formulae. 3.7:

$$E_{im} = A_{pv} * \int_{day} E.dt \quad (3.7)$$

The pump efficiency is obtained by the comparison of the hydraulic energy provided by the pump and the electric energy coming from the PV array, and it is given by the formulae. 3.8:

$$\eta_p = \frac{E_h}{E_e} \quad (3.8)$$

The characterization test results of the Grundfos DC pump (0.9 kW), PV powered by the PV Generator (2x6) at different TMH are concluded in the following table 3.4,

TMH	Daily Cumulative Water	Daily pumping Duration	Flow rate	PV array configuration
(m)	(m^3/day)	(Hours)	(m^3/h)	Isofoton module 110W/24V (Parallel x Serial)
10	55.35	7	7.887	2 x 6
15	50.12	7	7.051	2 x 6
20	42.25	7	6.205	2 x 6
25	36.02	7	5.116	2 x 6
30	28.63	7	4.100	2 x 6
35	21.23	7	3.015	2 x 6
40	15.25	7	2.203	2 x 6

Table 3.4: Daily cumulative water and average flowrates at different TMH

The solar radiation E(W/m^2) and power P(W) of the pump recorded on clear sky day are plotted in the figure 3.9,

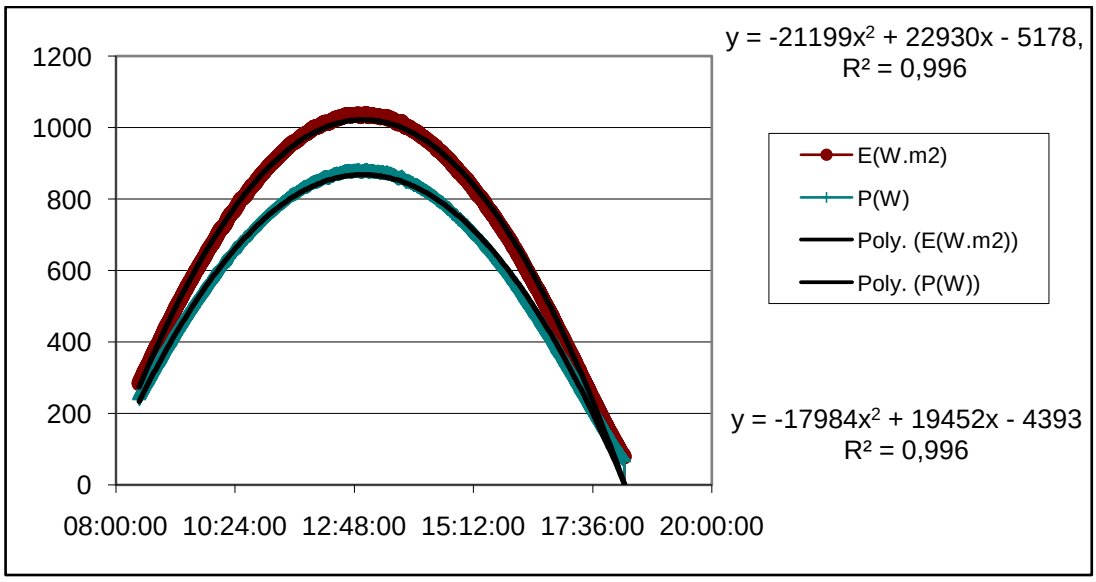

Figure 3.9: Insolation and power provided by the pump at TMH = 25 m

The overall efficiency provided by the Motor-pump set (DC Grundfos 0.9 kW) to drawdown the needed daily volume of water at TMH = 25 m is presented in the following figure 3.10,

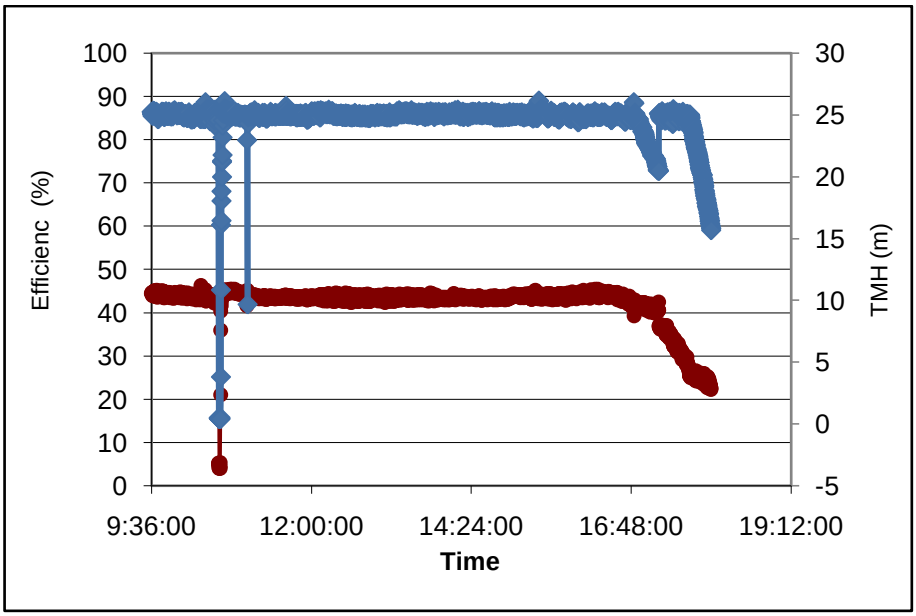

Figure 3.10: Overall efficiency provided by the pump at TMH = 25 m

The results obtained fromthe Characterization tests of the Grundfos pump at the required Total Manometric Head (TMH) fit well with the calculated results

3.2.5 Conclusion of the sizing study

The task of sizing a PV-system consists of finding the better trade-off between cost and reliability.The results obtained upon the characterization tests on the different parts of the PV pumping selected design averred a succefull efficiency of the whole system to satisfy the need of the farm on the required daily average water volume, throughout the year. The dimensioning of the PV pumping system is based in general on the water compensation.The surplus of the pumped volume of water during sunny days is used to compensate the deficit during the low insolation days or when the system is in case of damage. However a tank with great capacity is required for a maximum accumulation of water quantity.

Chapter4: New Mathematical model for an optimum energy exploitation of a standalone photovoltaic pumping system (PVPS)

4.1 Problematic

Through the sizing of the mentioned direct coupling photovoltaic pumping system (PVPS), which will eventually be erected on a real well of the Sebseb region to supply a farm with the monthly daily required quantity of water, a mismatch has been averred between the power supplied by the PV array and the power required by the pump set.As it is mentioned in the chapter3, the dimensioning study of such system is based on the cumulative water volume. In such direct coupling PV water pumping system (No storage battery) is based on the storage of water instead of the storage of energy. The PV generator is configured in manner to provide the maximum energy to cover the maximum need of the load. However, the demand of the load is not linear because the demand on water is not constant. Through the plots of bothyearly monthly daily average energy provided by the PV Generator and the required energy by the pump of the obtained PV water pumping system design, the mismatch is apparent in the Demand/Supply curves, as it is illustrated in the figure 4.1.

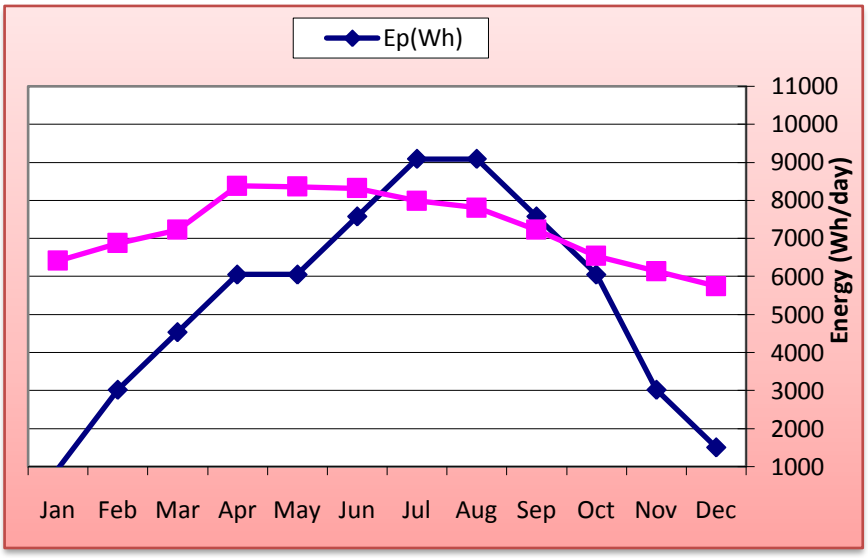

Figure 4.1: The plots showing the mismatch between the Demand/Supply energy

4.2New mathematical model idea

4.2.1 Idea of the new approach

The idea to obtain a new mathematical approach has risen following the investigation of the Demand/supply energy plots where a mismatch has been averred between the load (pump) and the PV generator following a stand-alone PV water pumping sizing. The concept to be reach is to exploit the surplus energy produced by the PV generator in the same PV water pumping system. The idea has been occurred and proved through an oral presentation, in the 5thInternational Conference on Sustainable Energy and Environment Protection (SEEP2012) held in Dublin, Ireland, during 5th – 8th June 2012. In the following sections, a summarization of this model is presented [20].

4.2.2 Purpose of the new approach

The purpose of the new mathematical model is to obtain an estimated model to be used as mathematical toolsto reach an optimum exploitation of the Photovoltaic (PV) array output energy, by ensuring linearity between the required and provided energy. The developed mathematical approach is based on the control of the mean monthly daily pumped volume of water according to the mean monthly daily energy produced by the PV array. For a maximum exploitation of the PV array output energy, the predicted quantity of water must be adequately used. In irrigation, some kinds of crops are suggested to be added during the months of surplus output PV array power and others are omitted during months of deficit.

4.2.3Mathematical Model steps

In the aim to exploit the maximum energy provided by the PV generator in a standalone PV water pumping system (PVPS), the energy consumed by the pumpmust be equal or slightly lower than the energy produced by the PV Generator [21], [22]. This condition is fulfilled through the equation 4.1.

$$Ep \leq Epv \quad (4.1)$$

Where,

E_p is the energy consumed by the pump

E_{pv} The energy produced by the PV generator

Based on the equation (3.4) previously mentioned in chapter 3, the energy consumed by the pump and the energy provided by the PV generator are presented by the following equations (4.2) and (4.3):

$$Ep = (Ch * V * H)/(ŋp * Kl) \quad (4.2)$$

$$Epv = ŋpv * Ei * Apv \quad (4.3)$$

Where, K_l is the overall losses, and then bysubstituting the equations (4.2) and (4.3) into the equation (4.1), the last becomes as follows:

$$(Ch * V * H)/(ŋp * Kl) \leq ŋpv * Ei * Apv$$

Thus, the following model which controls the water volume according to the irradiance is issued and presented by the following model (4.4):

$$V \leq [(ŋpv * ŋp * Apv * Kl)/(Ch * H)] * Ei \quad (4.4)$$

Taking into consideration that the efficiency averages of the PV array and the pump are constant under different circumstances, the mathematical model (4.4) is concluded and presented by the following equation (4.5):

$$V = K * Ei \quad (4.5)$$

Where, K is constant;

$$K = [(ŋpv * ŋp * Apv * Kl)/(Ch * H)]$$

4.2.4Application of the new model on local site irradiance data

By mean of the concluded model, the constant K is calculated, and then the monthly daily average volumes of water have been obtained according to the yearly monthly daily average solar radiations previously recorded. The figure.4.2 involves the maximum monthly average volumes of water that the PV water pumping set can provide at maximum energy exploitation. The curves of the figure.4.3 show the linearity between the water volumes and irradiance falling on the PV Generator, previously designed.

The figure.4.4 shows the difference between the volumes of water (V (m^3/day), recorded previously upon the demand of the farm owner in the previous sizing design of the PV water pumping system (PVPS) and the new current calculated volumes V_1(m3/day) by mean of the new mathematical model, that the system is able to provide. The figure 4.5, averred the good approach between the energy produced by the PV array and the energy consumed by the pump. The previous results (figure 4.1) averred that only less than 60% of the produced energy by the PV array is consumed during some months, however the new results show an optimum PV array output energy vary between 90% and 95% is consumed by the pump set.

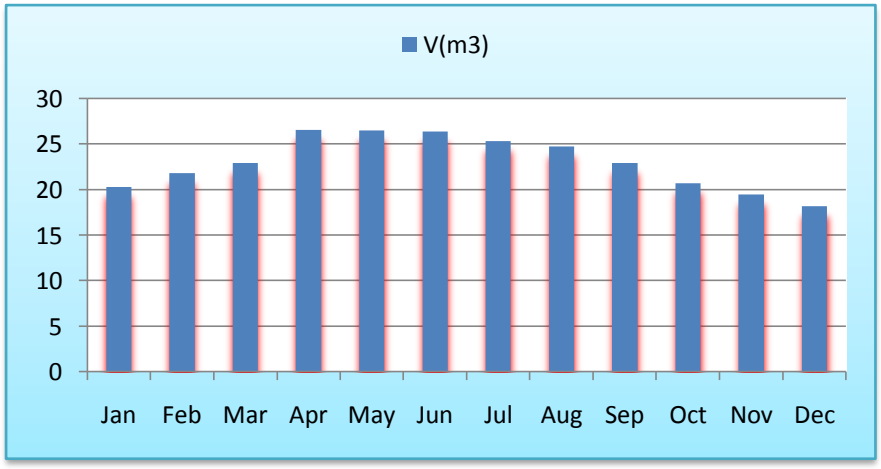

Figure 4.2:New calculated monthly daily average volume of water

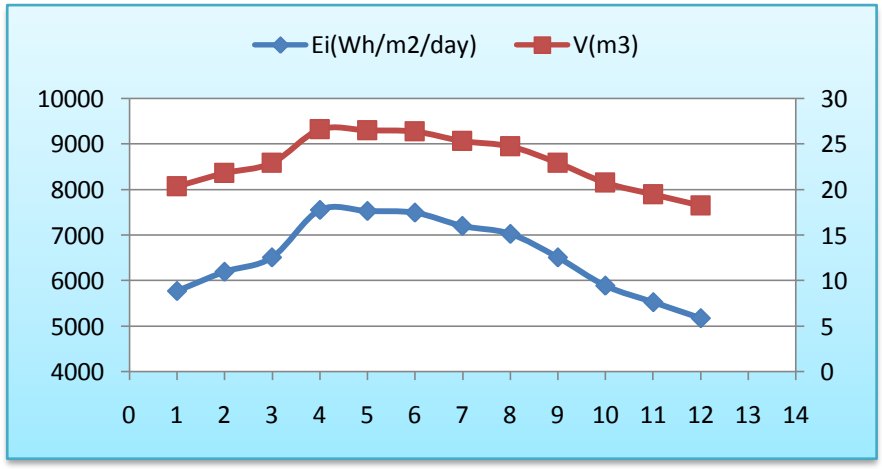

Figure 4.3: Demand/Supply energy to provide the volumes V(m^3)

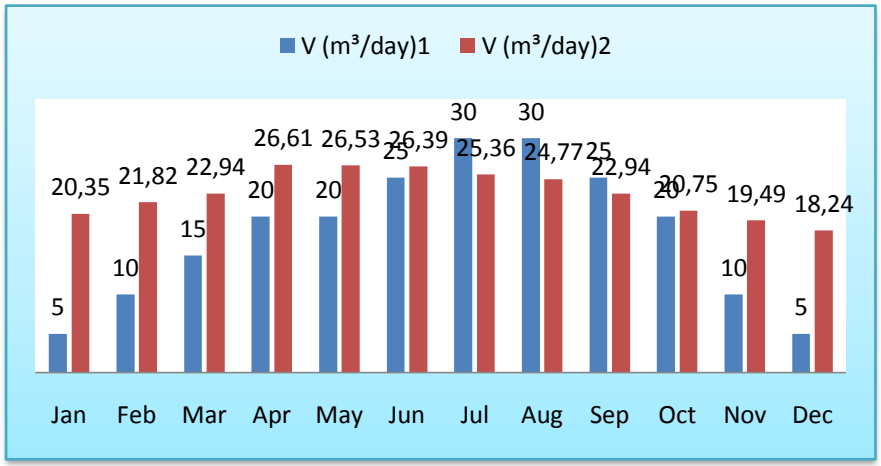

Figure 4.4: the previous demanded and the new estimated water volume averages

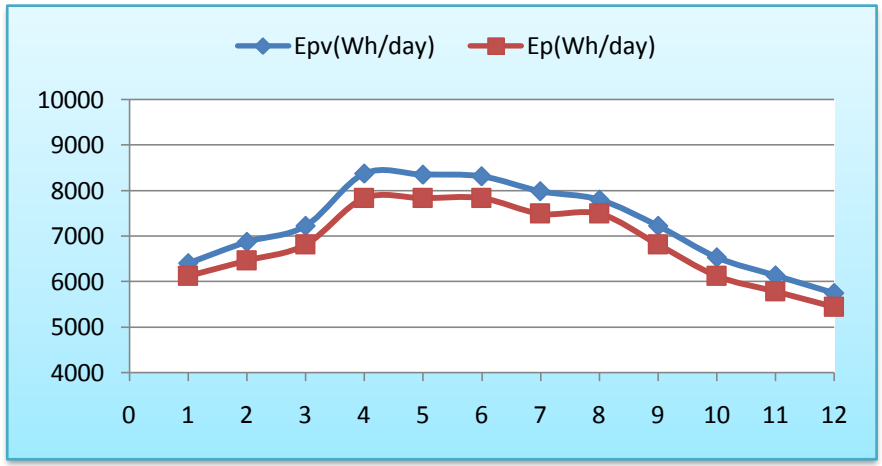

Figure 4.5: The plots of the new demand/supply energy of the PVPS

4.3Conclusion

A suitable mathematical model for the exploitation of the maximum optimal energy produced by the PV generator in a stand-alone PV water pumping system has been developed. The validation of the model was performed with the known results obtained through the characterization tests of the different parts of the designed PV water pumping system. By mean of this new mathematical model, a new estimation of the water monthly daily volume averages have been calculated and then the curves of the energy provided by the PV generator and the energy consumed by the pump set have been plotted. The obtained curves of demand and supply energies are approachable.

The objective of this work is to profit from the maximum PV water pumping efficiency, since the PV module efficiency is affectedby degradation outdoor parameters as temperature anddust and the pump by muddy water. The care to use the water in irrigation or livestock watering led focusing on a deep study to predict the needed kind of crops and the number and type of animals to be fed by water throughout the seasons. The developed model needs to be confirmed through other real PV water pumping system data of different regions.

Chapter5: Maximum Power point Tracking using ANFIS prediction and Fuzzy Logic Control FLC

5.1 Purpose of tracking

In general, the cost of electricity from the solar array system is more expensivecompared to electricity from the utility grid [23], [24]. For that reason, it is necessary to study carefully the efficiency of the entire solar system to design an efficient system to cover the load demands with lower cost. In the previous chapters, we have seen that the PV array converts solar energy to electric energy. In its V–P characteristic curve, there is a maximum point commonly called the maximum power point (MPP), at which the module operates with maximum efficiency and produces the maximum power output P_{max}.In order to obtain an operating point close to this MPP, a controlled DC/DC converter is usually employed to interface the energy flow from the solar module to the load. The main task of MPP seeking and DC/DC converter operation is provided by a control unit (MPPT Controller), where one of the known MPP tracking algorithms is usually implemented. This continuously checks the output (current and voltage) of the PV module.

5.2Solar Tracking System

5.2.1Solar Tracking Techniques

The solar tracking system is a device for orienting a solar panel or concentrating a solar reflector or lens towards the sun. PV arrays and concentrators, especially in solar cell applications, require a high degree of accuracy to ensure that the concentrated sunlight is directed precisely to the powered device. There are two ways to track the maximum power of any PV generator: The mechanical tracking, which called Solar tracking system and the electrical tracking, called the Maximum power point tracking (MPPT). The mechanical tracking is a system that “physically moves” the modules to make them point more directly at the sun. The electrical tracking of the PV array or the Maximum Power Point Tracking (MPPT) is a fully electronic system thatvaries the electrical operating point of the modules so that the modules are able to deliver the maximum energy. This soft technique is carried out on optimal fixedPV arrays. In our case study, an electrical tracking method or the tracking of the maximum operating point is carried

out on the mentioned PV generator composed by (2X6) Isofoton (110/24) PV modules, subject to the PV water pumping system design, previously sized and characterized.

5.2.2 MPPT in Direct Stand-alone Photovoltaic Pumping System

It is difficult to supply electrical energy to small applications in remote areas from the utility grid or from small generators. Stand-alone photovoltaic (PV) systems are the best solutions in many small electrical energy demand applications such as communication systems, water pumping and low power appliances in rural area [25], [26].

When a PV module is directly coupled to a load, the PV module's operating point will be at the intersection of its I–V curve and the load line which is the I-V relationship of load. For example in Figure 5-1, a resistive load has a straight line with a slope of 1/Rload as shown in Figure 5-2. In other words, the impedance of load dictates the operating condition of the PV module. In general, this operating point is seldom at the PV module's MPP, thus it is not producing the maximum power. A study shows that a direct-coupled system utilizes a mere 31% of the PV capacity [27]. A PV array is usually oversized to compensate for a low power yield during winter months. This mismatching between a PV module and a load requires further over-sizing of the PV array and thus increases the overall system cost. To mitigate this problem, a maximum power point tracker (MPPT) can be used to maintain the PV module's operating point at the MPP. MPPTs can extract more than 97% of the PV power when properly optimized [28].

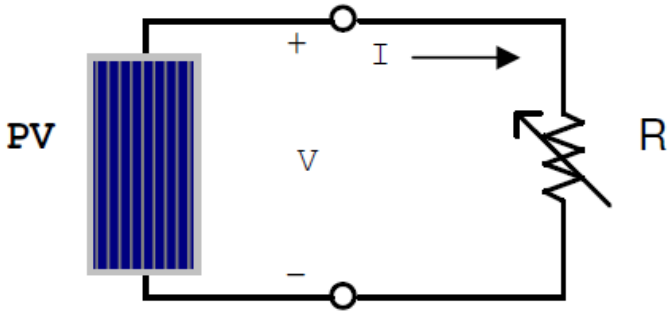

Figure 5.1:PV module is directly connected to a variable resistive load.

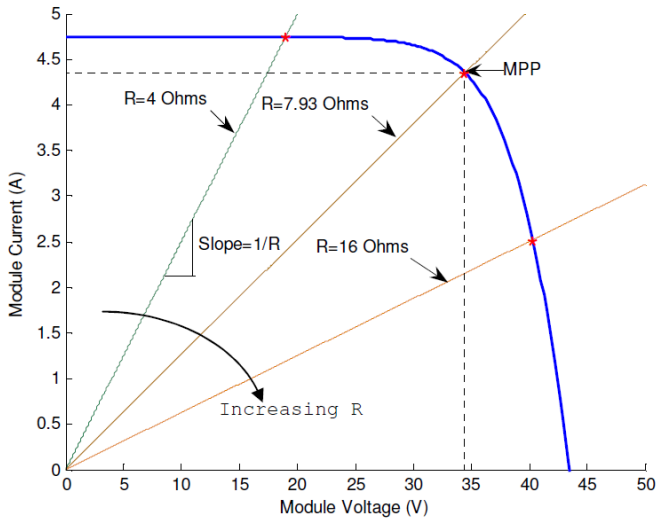

Figure 5.2: I–V curves of BP SX 150S PV moduleand various resistive loadssimulated with the MATLAB model at STC (E=1 KW/m2, T= 25 °C) [5].

5.2.3 Mechanism of Load Matching

a- The PV array I-V characteristics load matching

As mentioned already through the dimensioning study of our PV pumping system, the simple type of PV water pumping system uses a direct coupled PV motor-pump setup. This configuration has a severe disadvantage in efficiency because of a mismatched operating point, as shown in Figure 5-3 and in the figure 5.4. For this example, the water pumping system would not start operating until irradiance reaches at 400W*/m2*. Once it starts to run, it requires as little as 200W*/m2* of irradiance to maintain the minimum operation. This means that the system cannot utilize a fair amount of morning insolation just because there is insufficient starting torque. Also, when the motor is operated under the locked condition for a long time, it may result in shortening of the life of the motor due to input electrical energy converted to heat rather than to mechanical output, Different studies had been run in our laboratory to overcome the mismatching between the PV generator and the load (pump). Different PV array configurations had been put into test to select the optimal architecture which produces the maximum rating energy. The subject has been evaluated in the International Conference on Sustainable Energy and Environment Protection-SEEP2010-, held in Bari, Italy within the period 28th June– 1stJuly 2010. Accepted and published in the journal “Energy”, volume 39- March 2012, [29].

The figure 5.3 shows the PV array I-V characteristics with varying irradiance and a DC motor I-V curve;

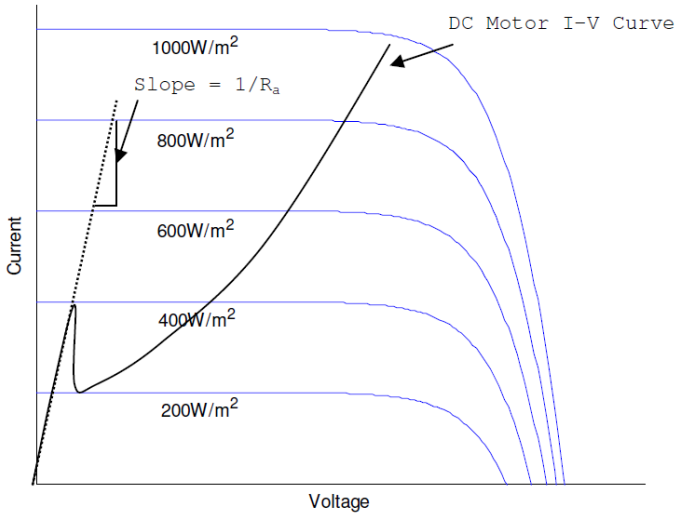

Figure 5-3: PV I-V curves with varying irradiance and a DC motor I-V curve.

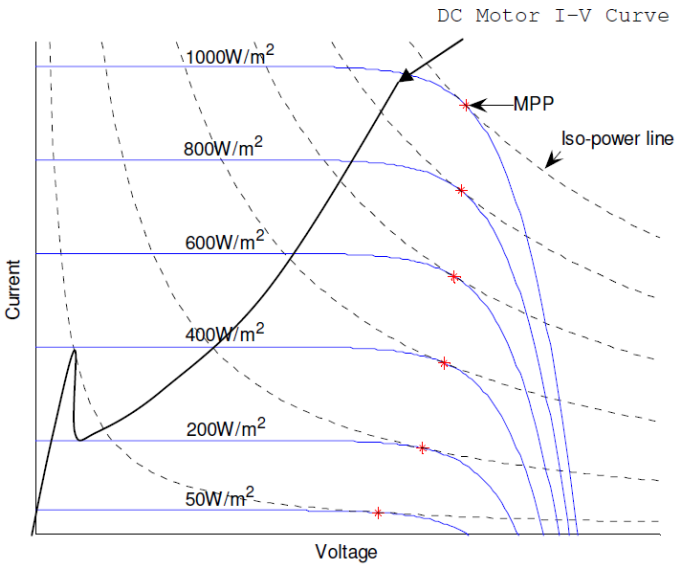

Figure 5-4: PV I-V curves with iso-power lines(dotted) and a DC motor I-V curve

There is a MPPT specifically called a linear current booster (LCB) that is designed to overcome the above mentioned problem in water pumping systems. The MPPT maintains the input voltage and current of LCB at the MPP of PV module. The power produced at the MPP is relatively low-current and high-voltage which is opposite of those required by the pump motor. The LCB shifts this relationship around and converts into high-current and low-voltage power which satisfies the pump motor characteristics. The tracing of the iso-power (constant power) line from the MPP reveals that the LCB

could start the pump motor with as little as 50W/*m2* of irradiance (assuming the LCB can convert the power without loss).

b- Maximum Power Point Tracking Modeling

There are many external and internal influences which have an effect on the efficiency of the PV panel. The maximum power point (MPP) of a PV system depends on cell temperature and solar irradiation, so, it is necessary to continually track the MPP of the solar array [25] to match the load. Therefore, the tracking control of MPP is a complicated problem. Many tracking control model have been proposed to overcome this problem. It is generally considered that a positive sign indicates power being delivered to the load and a negative sign indicates power being consumed by the solar cells. Taking into account the sign definitions in Figure 5.5, the power at any point of the characteristic is expressed by the below equation 5.1

$$P = V \cdot \left(I_L - I_0 \left[\exp\left({qV}/{\mathrm{K_B T}} \right) - 1 \right] \right), \quad \text{with } I_L \approx I_{SC} \qquad (5.1)$$

The final concluded model is presented by the following expression;

$$P = V \cdot \left(I_L - I_0 \left[\exp\left({V}/{V_T} \right) - 1 \right] \right), \quad \text{with } V_T = {\mathrm{K_B T}}/{q}$$

The P-V curve of different sign is presented in the plot of the figure 5.5 and the different power sign is presented in the table 5.1;

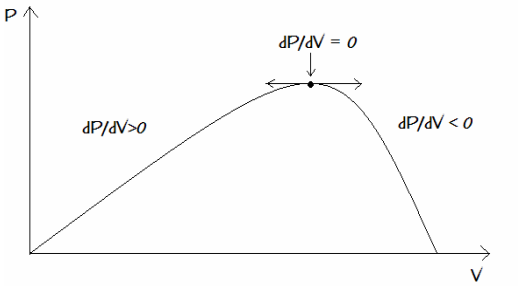

Figure 5.5: P-V curve different signs

dP/dV> 0_ PV module output voltage increases
dP/dV = 0_PV module output voltage is kept
dP/dV< 0_PV module output voltage decreases

Table 5.1 output voltage different signs

It is clear that the value of the power at the short circuit point is zero, because the voltage iszero, and also the power is zero at the open circuit point where the current is zero. There is apositive power generated by the solar cell between these two points. It also happens thatthere is a maximum of the power generated by a solar cell somewhere

in between. Thishappens at a point called the maximum power point (MPP) with the coordinates V = V_m andI =I_m. A relationship between V_m and I_m can be derived, taking into account that at themaximum power point the derivative of the power is zero, which presented by the following equation 5.2

$$\frac{dP}{dV} = 0 = I_L - I_0\left[\exp\left(V_m / V_T\right) - 1\right] - \left(V_m / V_T\right) I_0 \exp\left(V_m / V_T\right) \qquad (5.2)$$

Hence, the coordinates of the maximum power output (MPP) of the solar generator are expressed by the following: maximum current is expressed by equation 5.3.a and the maximum voltage is expressed by the equation 5.3.b

$$I_m = I_L - I_0(\exp(V_m / V_T) - 1) \qquad (5.3.a)$$

$$V_m = V_{oc} - V_T Ln(1 + V_m / V_T) \qquad (5.3.b)$$

5.3 The Proposed PV water pumping System

5.3.1 Synoptic of the proposed system

The proposed system put into test is the obtained PV water pumping system design asdirect coupling stand-alone typewithout backup batteries. As shown in Figure 5.6, the system consists of the following parts:

- A PV generator composed of (2X6) Isofoton (110/24) PV modules.
- An Adaptive Neuron Fuzzy Inference based System (ANFIS).
- A Fuzzy Logic Controller (FLC).
- A Cuk Converter.
- A Grundfos DC submersible pump

The system including the subsystems will be simulated to verify the functionalities.

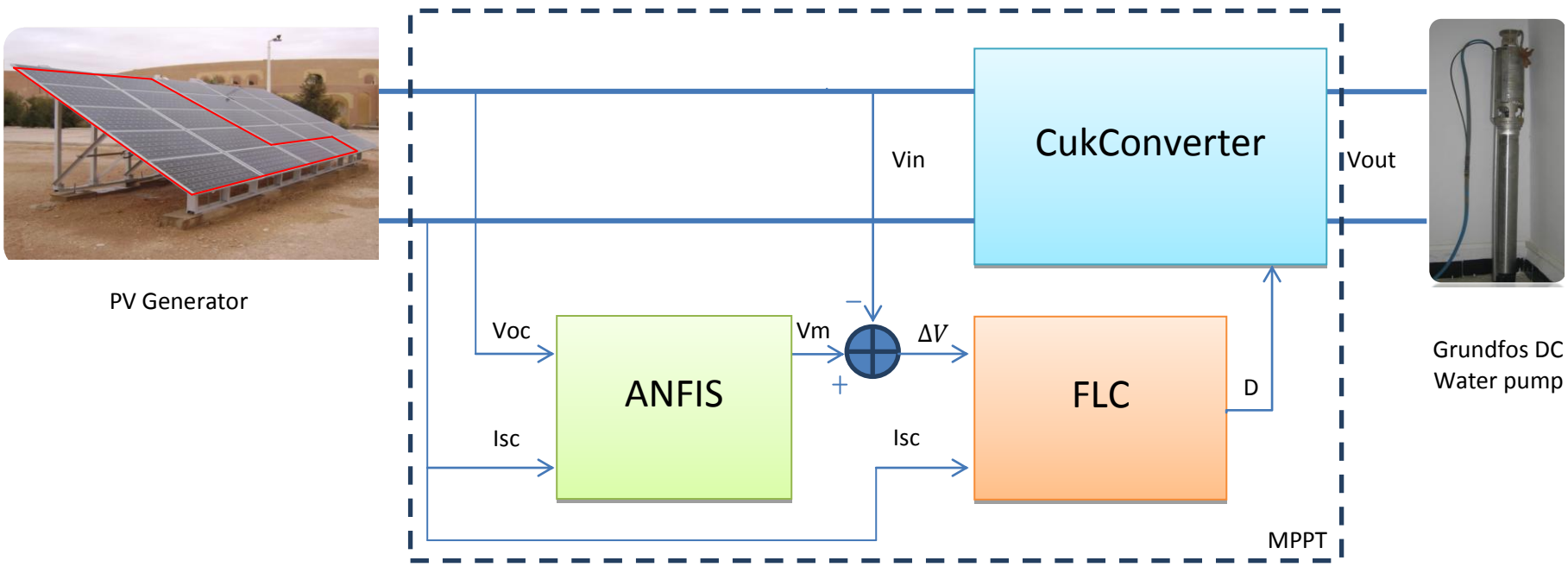

Figure 5.6:Block diagram of the proposed PV water pumping system.

In this chapter, linear correlation is proposed to analyze the experimental data to select the appropriate PV parameters that can recognize the MPP location. Short circuit current (Isc) and open circuit voltage (Voc) are selected as inputs factors instead of environmental influences. Thischapter demonstrates how these simple factors are necessary to locate an accurate MPP under wide changes in environmental conditions. The statistical analysis is used to classify the data in appropriate fuzzy memberships. The proposed maximum power point tracking (MPPT) model depends on an Adaptive Neuron-Fuzzy Inference System (ANFIS) which is designed as a combination of the Sugeno fuzzy model and neural network(ANFIS) of five layers with four fuzzy rules is used to acquire a high precision of locating the maximum voltage V_{max} with few adaptation epochs. The fuzzy logic controller (FLC) utilizes the ANFIS output voltage to track the MPP. The MPPT controller is designed to acquire high efficiency with low fluctuation.

Accordingly, in this paper Iscand Voc are used as inputs to the ANFIS PV panels instead of solarirradiation and cell junction temperature. The reasonfor this substitution is the difficulty of cell junctiontemperature measuring. In addition the simplicity of Iscmeasurement solves the problem of solar irradiance externalsensor. In addition at different load; voltage, currentand power represent the output parameters of PV panels.When the load is directly coupled to the PV panel, thisleads to a certain mismatch between the actual and theoptimum operation voltage (V_{max}) of the solar generatorwhich lessens the generated power from PV panels, the mismatch can be defeated by introducing a matching DC/DC converter.

5.3.2DC/DC converter between the load and PV generator

In order to extract maximum power from a PV module, a maximum-power-point tracker (MPPT), which is a DC/DC converter associated with the control unit, is usually connected between the photovoltaic module and the load.The DC-DC converter or DC chopper protects the condition of the voltage output in thePhotovoltaic system. In addition to regulating the voltage output, the DC-DC converter Functions as the maximum power point (MPP) tracker. Because the radiation intensity changes, the current and voltage output of the solar-generator always fluctuate and the MPP of the solar-generator also moves. With the MPP tracker, the power output of the solar-

generator is near optimum. The dc chopper can be used as switching mode regulator to convert a DC voltage normally unregulated, to a regulated dc voltage output. The regulation is normally achieved by pulse-width modulation (PWM) at a fixed frequency and the switching device is commonly a power IGBT or MOSFET.

5.3.3Buck-boost converter (Cuk converter)

Buck-Boost converter is used to step up/step down thevoltage of PV system. To control the DC-DC converterwe should control the duty cycle (D) of converter MOSFETtransistor [30]. The duty cycle represents the ratio oftime open of electronic switch using a square wave signalto open this switch. The relation between input andoutput voltage of Buck-Boost converter can be calculatedfrom the equation (5.4);

$$\frac{V_o}{V_{in}} = \frac{D}{1-D} \quad (5.4)$$

Where;

V_o is a load voltage on a converter output terminal.

V_{in} is a PV operating voltage on converter input terminal.

D is the duty cycle of electronic switch.

Its relationship to the duty cycle (D) is:

- If 0 < D < 0.5 the output is smaller than the input.
- If D = 0.5 the output is the same as the input.
- If 0.5 < D < 1 the output is larger than the input.

Refer to equation 5.4 the rate of change of duty cycle in term of V_{in} can expressed by the derivative of the DC/DC converter duty cycle D versus the PV voltage on converter input terminal V_{in} and then it is represented by the equation 5.5;

$$\frac{\partial D}{\partial V_{in}} = \frac{-Vo}{(Vo+Vin)^2} \quad (5.5)$$

Solar irradiance varies quickly with time, which means that the maximum power point also moves to another curve quickly. Therefore, the MPPT controller should also be capable of reaching the MPP as quickly as possible in order to reduce the output power oscillations and the system power loss.

5.4 Maximum Power Point Tracking Algorithms

5.4.1Role of MPP tracking algorithms

In order to increase the power conversion efficiency of PV solar cells, PV system should be operated optimally. The state of the art techniques to track the maximum available output power of PV systems are called the Maximum Power Point Tracking (MPPT). It is an essential task in a PV control system because it maximizes the power output of the PV system for a given set of conditions, and therefore maximizes the array efficiency. As it is explained in the previous section, the MPPT algorithm tells a MPPT controllerhow to move the operating voltage. Then, it is a MPPT controller's task to bring the voltage to a desired level and maintain it.

5.4.2The MMP tracking techniques

Many efficient techniques have been developed and proposed to locate and track the maximum power point (MPP) of PV cells. The most recent used tracking techniques are: the Perturb and Observe (P&O) methods [31], the constant voltage method, the short-current pulse method. Recently the Intelligent controlling methods are widely used; they consist of the Artificial Neural Network (ANN) method [32].The fuzzy logic Control (FLC) method [33]., and Adaptive fuzzy logic control (AFLC) [34]. The Fuzzy Logic Controller (FLC) based method performs well under varying climate conditions (cell temperature and irradiance) [35]. In this context, effort has been concentrated on the development of software as a yet simple and cost effective solution [36]. The difficulties that face these methods are the rapid changes in solar radiation and the variety in cell temperature which affects the MPP setting. ((The drawbacks of these methods come from its high cost, difficulty, complexity, and non-stability [33])). External sensors are used in many approaches to measure solar irradiation and ambient temperature to estimate the MPP as a function of data measured.In addition, the popular algorithms such as P&O and incremental conductance continue oscillation around the

optimum operating point which causes power losses [36]. Moreover, theseAlgorithms may not give good results to the fast dynamic response [37] and also it is very difficult to get an analytical expression in determining the optimum operating voltage for different solar cell technologies under changing weather conditions. In order to solve this problem and to improve the stability of the MPPT controller, a novel MPPT algorithm based on ANN and fuzzy logic controller schemes using polar information on PV systems is proposed. The proposed method uses the advantages of neural networks to predict the MPP voltage in time as a reference voltage for fuzzy logic controller. This paper is inspired from the ANN methods which were developed in the previous works [38]. The benefits of using ANN are that there are no requirements for knowledge on internal system parameters, less computationaleffort and provide a compact solution for multivariable problems.

5.5 Maximum Power Point tracking (MPPT) using ANFIS Prediction

5.5.1 Description of the method

The main purpose of such controlling techniques is the way of adjustment the duty cycle of the shunt MOSFET transistor of maximum power point tracking (MPPT) converter. The MPPT converter is used to maintain the PV array's operating point at the MPP. MPPT controller does this by controlling the PV array's voltage or power independently of the load [25]. The fuzzy controller introduced in [31] uses dP/dI and its variations (dP/dI), as the inputs and computes MPPT converter duty cycle. The adaptive fuzzy tracker of maximum power point considers variation of duty cycle, but it uses (dP/dV) and (dP/dI) to adapt duty cycle of the DC-DC converter [33]. The previous type of search is called on-line search algorithm which does not need reference MPP parameters. Therefore, it does not require measure of temperature and solar irradiation [33], [39]. Fast and stable MPP tracking under a high environment changes need reference MPP parameters. A solar radiation is used in [34] and [25] to obtain a reference power and voltage. The maximum power point voltage (V_{max}) is obtained as a reference voltage in [40] as a function of open circuit voltage (V_{oc}). A neural network was also used to estimate the MPP in[36], [37] using solar irradiation. The paper presents a method based on Adaptive Neuron-Fuzzy Inference System (ANFIS) to

estimate the MPP using the data collected from several experiments performed in different environmental conditions. This paper utilizes statistical analysis methods to analyze the data of experiment that has been collected through the characterization tests in outdoor conditions of the local site in Ghardaia. The statistical analysis will confirm the necessity of using both V_{oc} and short circuit current (I_{sc}) as input data for ANFIS to estimate maximum power point voltage(V_{max}). The data will be used to test the ANFIS output with deduced appropriate rules.

5.5.2 Adaptive Neuro-Fuzzy Inference System (ANFIS) architecture

a- Introduction of ANFIS

Adaptive Neuro-Fuzzy Inference System (ANFIS)[41] proposed by Jang (1993) is a multi-layer feed-forward neural network that combines ANN and fuzzy logic. It eliminates the basic problem in fuzzy system design, which defines the membership functions and designs fuzzy rules, by effectivelyusing the learning capability of ANN for automatic fuzzy rule generation and parameter optimization (Nayak et al., 2004). Moreover, ANFIS not only maintains the mapping ability of ANNs but also possesses the advantages of fuzzy if-then rules for describing the local behavior of such mapping and solving the highly non-linear control problem robustly. ANFIS has been widely studied and successfully applied to hydrology and water resources, such as Chang (2006). The figure 5.7 illustrates the synoptic of the Fuzzy Inference System (FIS);

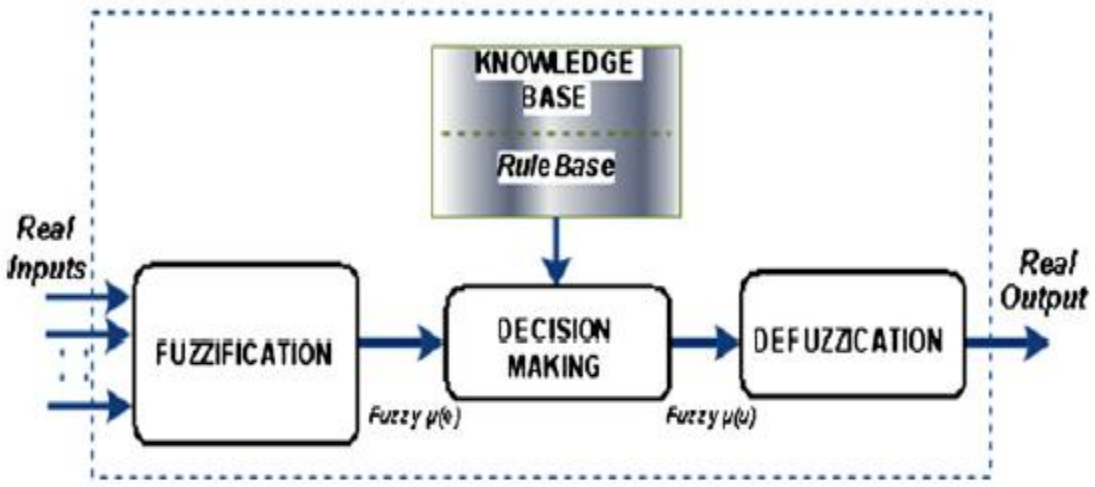

Figure 5.7 Fuzzy Inference System design

b- Description of ANFIS structure

The basic structure of a FIS consists of three conceptual components: a rule base, which contains a selection of fuzzy rules; a database, which defines the membership functions (MF) used in the fuzzy rules and a reasoning mechanism, which performs the inference procedure upon the rules to derive an output as shown in the figure 5.8.Neural network models are data based whereas fuzzy logic models are based on expert knowledge.

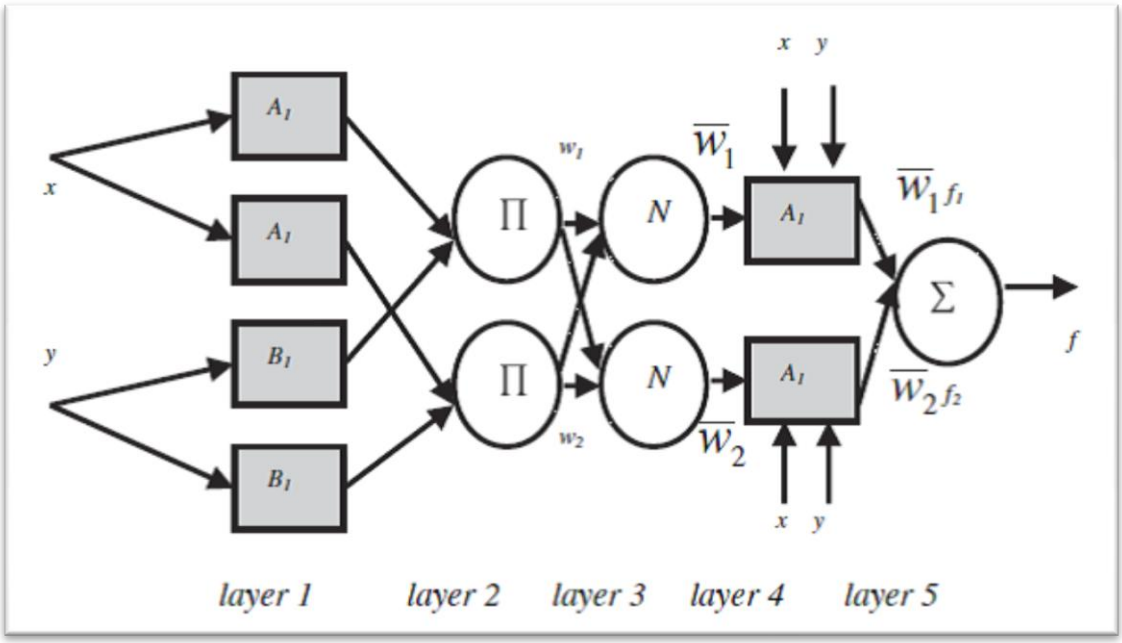

Figure 5.8: Architecture of an ANFIS equivalent to a first-order Sugeno fuzzy model with two inputs and two rules.

Generally, the architecture of ANFIS consists of five layers. The first layer consists of input nodes where each node corresponds to a linguistic label with a membership function (MF). In this study, a bell-shaped MF and a Gaussian MFs are used. The output of the first layer specifies the degree where the given input satisfies the MF. The second layer consists of rule nodes and the output of each node represents the firing strength of a rule. The node generates its output by multiplying all incoming signals involved in the rule. Therefore, the outputs of this layer are the products of the corresponding degrees fromLayer 1. The third layer consists of average nodes that compute the ratio of each rule's firing strength to the sum of all rules' firing strength. The fourth layer consists of consequent nodes. The function of consequent nodes is to compute the contribution of each rule towards the total output. The fifth layer consists

of output nodes. This layer includes a stable single node that sums up values of all signals to calculate thefinal output.

- Layer 1: consists of adaptive nodes that generate membership grades of linguistic labels based upon premise signals, using any appropriate parameterized membership function such as the generalized bell function:

$$O_1 = \mu_{Ai}(x) = \frac{1}{1 + \left|\frac{x - c_i}{a_i}\right|^{2b_i}}$$

Where output O1, i is the output of the i^{th} node in the first layer, x isthe input to node i, Ai is a linguistic label ("small," "large," etc.) fromfuzzy set A = (A1, A2, B1, B2,) associated with the node, and {ai, bi, ci} is the premise parameter set used to adjust the shape of themembership function.

- Layer2: In this layer the nodes are fixed nodes designated Π, which represent the firing strength of each rule. The output of each node is the fuzzy AND (product or MIN) of all the input signals:

$$O_{2i} = w_i = \mu A_i(x)\mu B_i(y) \quad i = 1, 2$$

- Layer 3: The output of the layer3 is the normalized firing strengths. Each node is a fixed rule labeled N. The output of the i^{th} node is the ratioof the i^{th} rule's firing strength to the sum of all the rules firingstrengths:

$$O_{3,i} = \overline{w}_i = \frac{w_i}{w_1 + w_2} \quad i = 1, 2$$

- layer 4 :The adaptive nodes in the layer4 calculate the rule outputs based upon consequent parameters using the function:

$$O_{4,i} = \overline{w}_i f_i = \overline{w}_i(p_i x + q_i y + r_i)$$

Where,

W_i is a normalized firing strength from layer 3, and (p_i, q_i, r_i) is the consequent parameter set of the node.

- layer 5: The single node in layer.5, labeled P, calculates the overall ANFIS output from the sum of the node inputs:

$$O_{4,i} = \sum_i \overline{w}_i f_i = \frac{\sum_i w_i f_i}{\sum_i w_i}$$

c- Training the ANFIS

The adaptive network based fuzzy inferencesystem (ANFIS). The system is an adaptive network functionallyequivalent to a first-order Sugeno fuzzy inference system. TheANFIS uses a hybrid-learning rule combining back-propagation,gradient-descent and a least-squares algorithm to identify andoptimize the Sugeno system's signals. The equivalent ANFIS architectureof a first-order Sugeno fuzzy model with two rules is shownin Figure 5.8. The model has five layers and every node in a given layerhas a similar function. The fuzzy IF-THEN rule set, in which theoutputs are linear combinations of their inputs, is:

$$\text{Rule 1} : \textit{if } x \textit{ is } A_1 \textit{ and } y \textit{ is } B_1 \textit{ then } f_1 = p_1x + q_1x + r_1$$
$$\text{Rule 2} : \textit{if } x \textit{ is } A_2 \textit{ and } y \textit{ is } B_2 \textit{ then } f_2 = p_2x + q_2x + r_2$$

Training the ANFIS is a two-pass process over a number of epochs. During each epoch, the node outputs are calculated up to layer 4. At layer 5, the consequent parameters are calculated using a least-squares regression method. The output of the ANFIS is calculated and the errors are propagated back through the layers in order to determine the premise parameter (layer 1) updates.

d- Input/output ANFIS parameters

Solar irradiation, ambient temperature and wind speedare the main environmental factors that affect PV systems.I_{sc}, V_{oc}, V_{max} and MPP current (I_{max}) are themain characteristics that specify the PV panels [42][43][44]. I-V curve characteristics and celljunction temperature of PV panels is adjusted due to anychanges in environmental conditions.MPP changes due to irradiance level and cell junctiontemperature. Ambient temperature with current flows inPV cell increase the cell junction temperature. The temperatureof cell junction is the main factor that reducesthe maximum power output of PV panel.

e - Proposed ANFIS through MATLAB simulation

To generate a Sugeno-type fuzzy inference system (FIS)structure Genfis1(Generate an FIS structure from datawithout data clustering) is used in Matlab toolbox to producean FIS structure for an yearly experiment data of the PV generator (2 X 6) based on different proposed Gauss and Generalized bell membershipfunctions. The ANFIS model programmed in MATLABis used to predict V_{max} using I_{sc} as a first input of ANFISmodel and V_{oc} as a second input. According to eitherreach to error criterion or the number off epochs settingin ANFIS function the input MFs parameters and outputlinear MFs of a Sugeno-type FIS structure is modified toreach best MFs that clustering input output data withminimum root mean square error(RMSE).

- The figure 5.9 (a, b and c) illustrate the ANFIS V_{max} output RMSE of the whole data base. The RMSE plots show that the RMSE of ANFIS ouputs vary between 2 and 5.5 for an interval epochs between 50 and 150.

- Six models with a small number of rules (3x4) and minimum of epochs (between 50 and 150) achieved minimum RMSE, using Bell-shaped MFs as shown in the figure 5.10. The Bell shaped GBMF(3,4) has achieved the best RMSE (3.02), as it is plotted in red color.

- Six models with small number of rules (4x3) and minimum of epochs (between 50 and 150) achieved minimum RMSE, using Gaussian MFsas shown in the figure 5.11. The Gaussian GMF(4x3)has achieved the best RMSE(2.89), as it is plotted in red color.

- The Figure 5.12illustrates the ANFIS V_{max} outputs versus the experimental V_{max} outputs. The curve shows a very good linearity. Ingeneral, the ANFIS outputs changes after 100 epochs applying different groups of inputs Gauss MFs or Bell-shaped MFs. The number of rules have been generated depends on the number of MFs, which is the product number of input1 (current I_{sc})time MFs and the input2 (open circuit voltage V_{oc}) time MFs. Hence optimizing with minimum numbers of rules is very important in control system designed. Minimum error setting is associated with the system precision requirements.

- Through the mentioned tested models, the two selected V_{max} RMSE obtained by GBMF (3x4) and GMF (4x3)inputs have been plotted in the figure 5.13. The best selected RMSE is that obtained by mean of GMF(4x3) input.

- The figure 5.14 (a, b, c and d) illustrate the ANFIS V_{amx} output RMSE of combined (training,testing and checking) data base achieved through the GMF (4x3).

- The plots of the figure 5.15 (a, b, c and d) illustrate the ANFIS V_{max} output achieved by mean of GMF (4x3) inputs versus the Experimental V_{max} .The obtained curves show an optimal linearity.

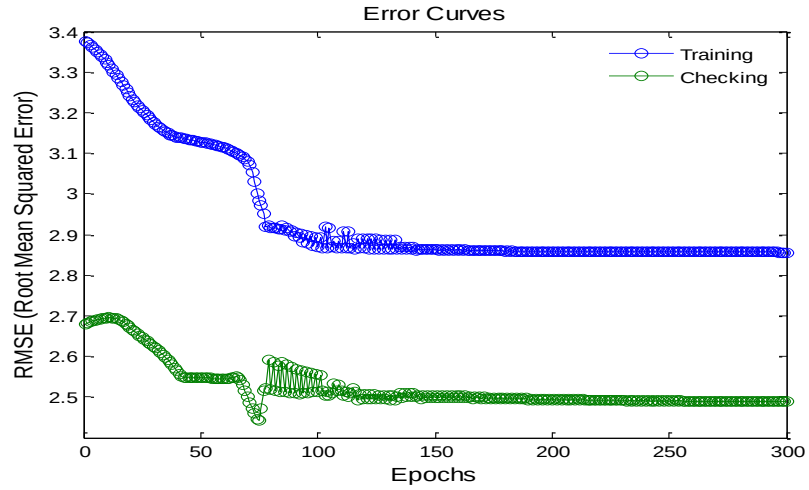

Figure 5.9.a: ANFIS V_{max} output RMSE (Training & checking the whole data base)

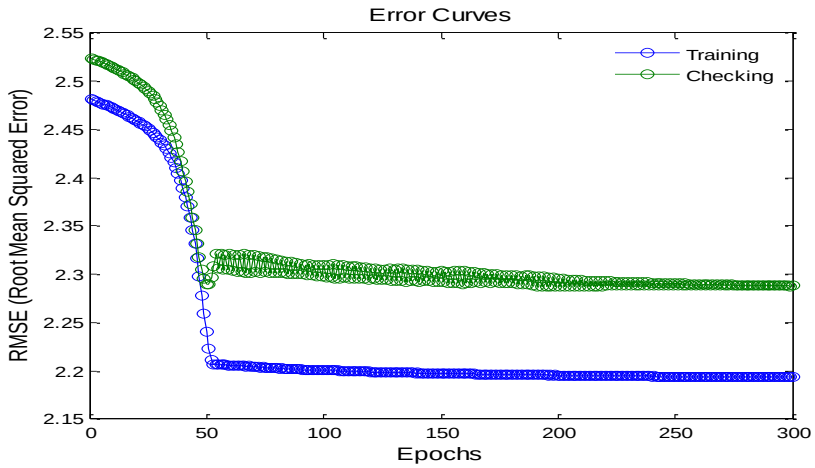

Figure 5.9.b: ANFIS V_{max} output RMSE (Training & checking the whole data base)

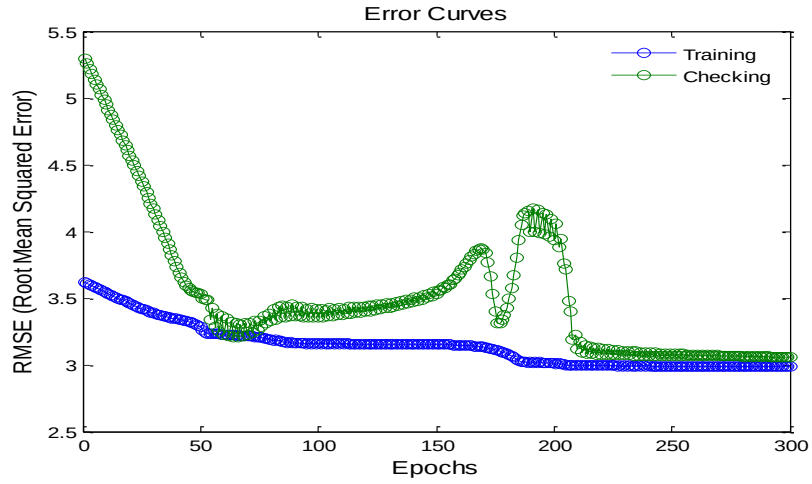

Figure 5.9.c: ANFIS V_{max} output RMSE (Training& checking the whole data base

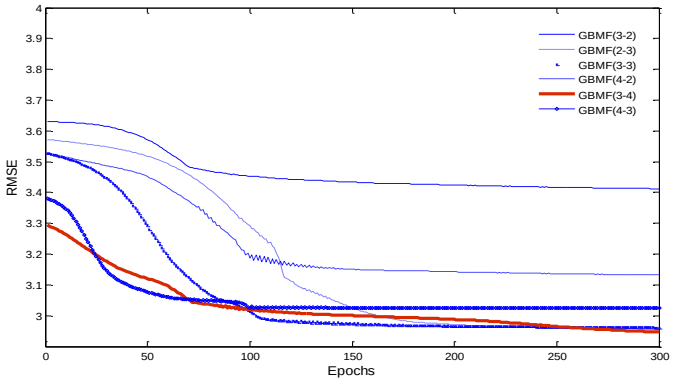

Figure 5.10: RMSE for differentGBell MFs the GBMF (3x4) fit well

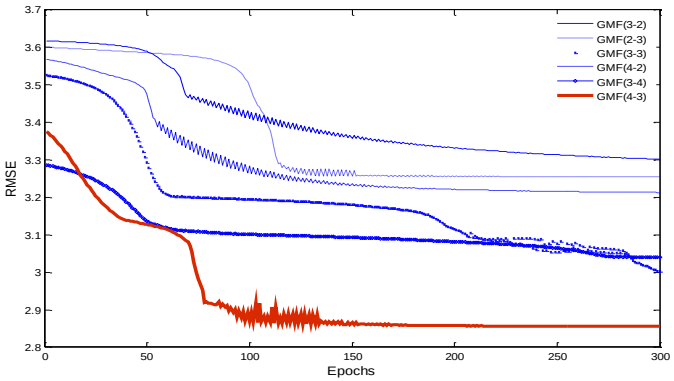

Figure 5.11: RMSE for different GMFs, the GMF (4x3) fit well

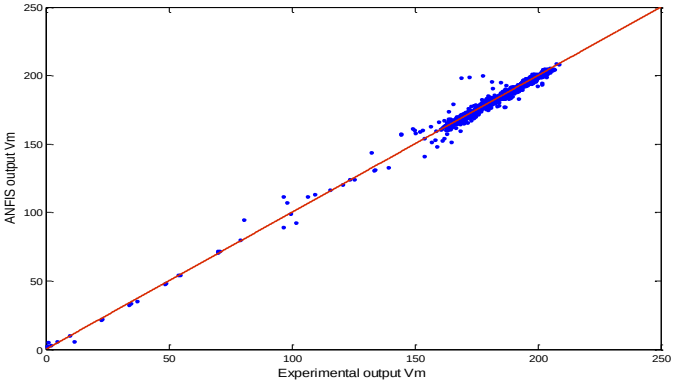

Figure 5.12:ANFIS V_{max} output (GBMF (3x4)) Vs the experimentalV_{max}

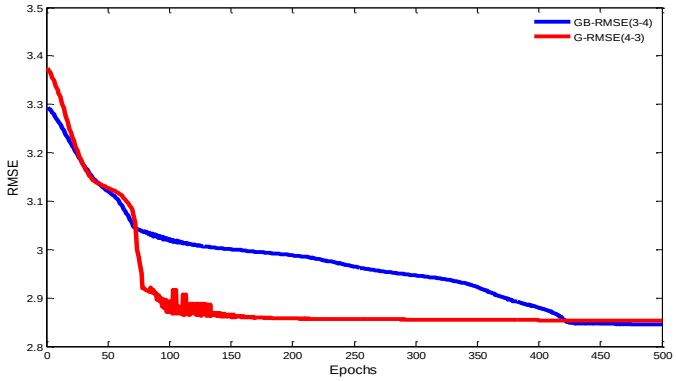

Figure 5.13: RMSE of both GBMF (3x4) and GMF(4,3), best RMSE ,GMF(4x3)

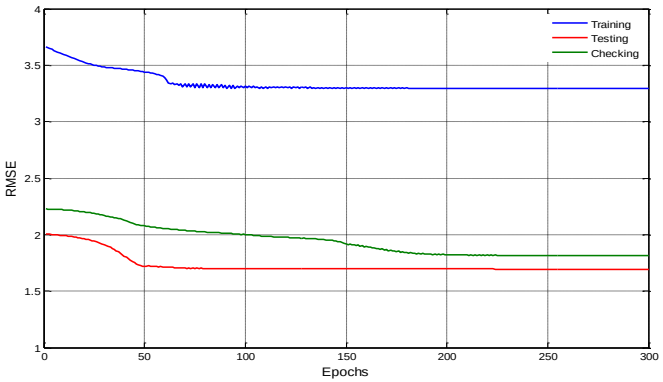

Figure 5.14.a: RMSE of ANFIS V_{max} (GMF (4x3), 1st (Training,testing, checking)

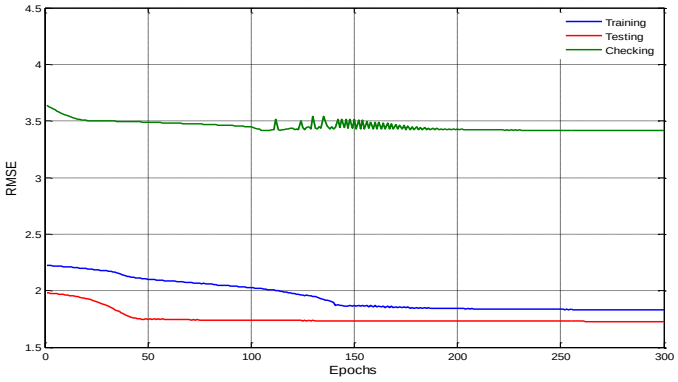

Figure 5.14.b: RMSE of ANFIS V_{max} (GMF (4x3)), 2nd (Training,testing, checking)

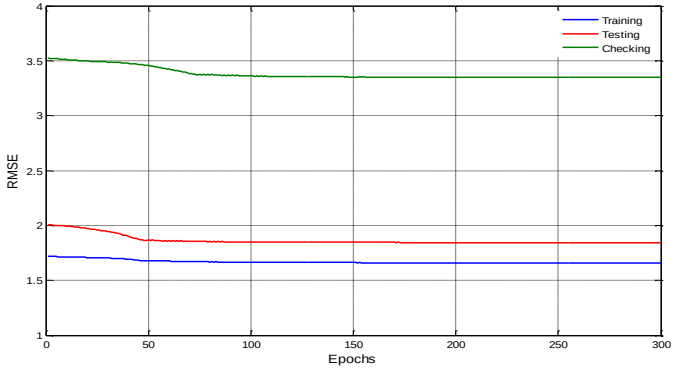

Figure 5.14.c: RMSE of ANFIS V_{max} (GMF (4x3)), 3rd (Training,testing, checking)

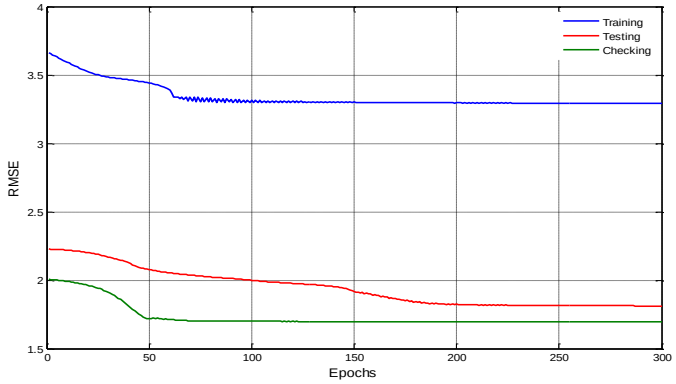

Figure 5.14.d: RMSE of ANFIS V_{max} (GMF (4x3)), 4th (Training ,testing ,checking)

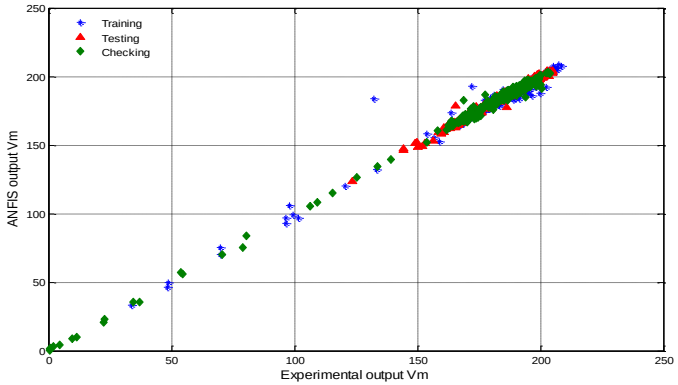

Figure 5.15.a: ANFIS V_{max} (GMF (4x3)) Vs Experimental V_{max},

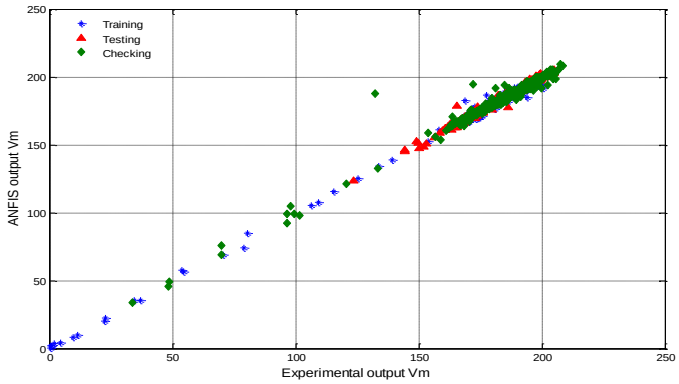

Figure 5.15.b: ANFIS V_{max} (GMF (4x3)) Vs Experimental V_{max}

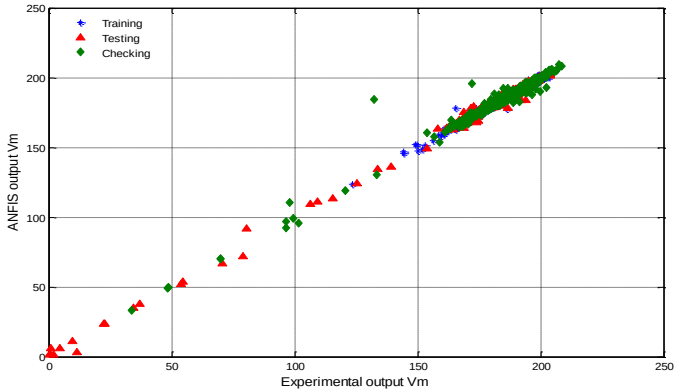

Figure 5.15.c: ANFIS V_{max} (GMF(4x3) Vs Experimental V_{max}

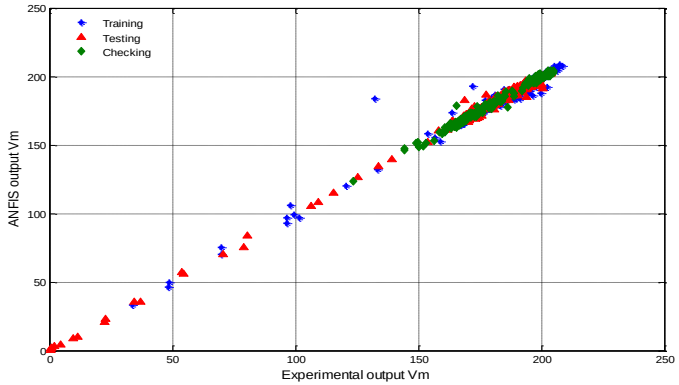

Figure 5.15.d: ANFIS V_{max} (GMF(4x3) Vs Experimental V_m

5.6 Maximum Power Point tracking (MPPT) using Fuzzy Logic Control (FLC)

5.6.1 Fuzzy Logic Controller (FLC)

Fuzzy Logic is an area of Set of Computing Techniques that enables a computer system to reason with uncertainty. Dealing with humanistic systems, whose behaviour is strongly influenced by human judgment, perception, and emotions,it characterized by its Membership Function (MF).Fuzzy inference systems consist of a set of "if-then" rules defined over fuzzy sets. Fuzzy sets are relations that can be used to model the linguistic variables that human experts use in their domain of expertise. The difference between fuzzy sets and logic (crisp) sets is that the membership functions for elements. The procedures in making the control designs are setting the constraints, assigning the linguistic variables and setting the rules for the controller [45].

The basic structure of fuzzy rule-based system involves four principal components: fuzzification interface, where the values of inputs are measured, fuzzified and the input range is mapped into the suitable universe of discourse, knowledge base, which involves a numeric ‘database’ section and a fuzzy (linguistic) rule-base section, fuzzy inference mechanism or engine, which constitutes the core of the fuzzy logic control,involves the decision making logic (fuzzy reasoning such as product, max-min composition etc) and defuzzification interface, which maps the range of output variables into corresponding universe of discourse and defuzzifies the results of fuzzy inference mechanism.

5.6.2 The proposed FLC

a- Fuzzification

At a certain I_{sc} and V_{oc} the ANFIS model will estimate the V_{max}, this reference voltage with I_{sc} are used as a crisp inputs on FLC to adjust the duty cycle of electronics switch of Buck-Boost converter to match between load voltage and V_{max} of PV panels. The reference voltage changes if either V_{oc} or I_{sc} has ample changes.The input and outputof FLC have been selected carefully to give sufficient and simple information for FLC. In addition, the fuzzy logic rules and MFs are assembled to solve the problem mentioned

previously. Firstly, ANFIS predicts V_{max} with Great changes in weather conditions. The maximum power point voltage predicted from ANFIS is used to calculate the first input of FLC as follow:

$$\Delta V = V_{in} - V_{max}$$

The second input is Isc value, which represents the level of irradiance. The power losses at high irradiance level are more than at low irradiance level due to V_{max} deviation. Therefore, a high precision is required at high Isc, however, at low Isc a high precision is not essential to attain more stability on the controlling system.

- First input variable "I_{sc}"
- Name: Short circuit current
- Universe of discourse: [0 7]
- Fuzzy sub set linguistic variables: B:Big, M: Medium, S: Small
- {B[3.5 7],M[2 5],S[0 3.5]}
- Membership Functions: see figure 5.16 (a)

- Second input variable "ΔV"
- Name: Error between ANFIS output and Cuk converter Input
- Universe of discourse: [-0.3 0.3]
- Fuzzy sub set linguistic variables: NB: Negative Big, NM: Negative Medium, NS: Negative Small, Z: Zero, PS: PositiveSmall, PM: Positive Medium, PB: Positive Big.
- {NB[-0.03 -0.02],NM[-0.04 -0.01],NS[-0.02 0.01],Z[-0.01 0.01],PS[0 0.02],PM[0.01 0.03],PB[0.02 0.03],}
- Membership Functions: See figure 5.16 (b)

b- Interpretation of If-then rules

Knowledge based decisions, according to the input conditions of (ΔV) and short circuit (I_{sc}), have been formulated as a fuzzy rule base To prevent instability due to small changes in V_{max} whichmake insignificant effect in generated power, as shown in Table 5.2.Also, the rules discriminate the level of Isc to prevent the oscillation in cloudy time. The output result controls the duty cycle of the Cuk converter. Type of load affects strongly on MFs design to determine the rate and limit of duty cycle at different value of Vin to help on designing the rules and MFs that control the Buck-Boost converter with constant voltage. Functions (MFs) are to be fuzzified, Depending on the actual membership degree values, $\mu\Delta V$(a) and μI_{sc}(b), where a and b represent the current conditions of both DeltaV and the short circuit current. The Min-Max method of

fuzzification is used to set the fuzzy rules of the controller according to the following decisions,

- If Isc is B And ΔV is NB Then D is NB
- If Isc is B And ΔV is NM Then D is NM
- If Isc is B And ΔV is NS ThenD is NS
- If Isc is B And ΔV is Z Then D is Z
- If Isc is B And ΔV is PS Then D is PS
- If Isc is B And ΔV is PM Then D is PS
- If Isc is B And ΔV is PB Then D is PM
- If Isc is M And ΔV is NB Then Dis NB
- If Isc is M And ΔV is NM Then Dis NM
- If Isc is M And ΔV is NS Then D is NS
- If Isc is M And ΔV is Z Then D is Z
- If Isc is M And ΔV is PS Then D is PS
- If Isc is M And ΔV is PM Then D is PM
- If Isc is M And ΔV is PBThenD is PM
- If Isc is S And ΔV is NB Then Dis NB
- If Isc is S And ΔV is NM Then Dis NM
- If Isc is S And ΔV is NS Then D is Z
- If Isc is S And ΔV is Z Then D is Z
- If Isc is S And ΔV is PS Then D is Z
- If Isc is S And ΔV is PMThenD is PM
- If Isc is S And ΔV is PBThen D is PB

The decision making results are concluded in the following table 5.2:

.....ΔV Isc	NB	NM	NS	z	PS	PM	PB
B	NB	NM	NS	z	PS	PS	PM
M	NB	NM	NS	z	PS	PM	PM
S	NB	NM	Z	z	Z	PM	PB

Table 5.2: The If-then rules

c- Defuzzification

The defuzzification module is in a sense the reverse of the fuzzification module: it converts all the fuzzy terms created by the rule base of the controller to crisp terms (numerical values) and then sends them to the physical system (process), so as to

execute the control of the system. The defuzzification module performs the following functions similarly; since the output of the pump cannot respond directly to the Book-booster, the fuzzy control sets generated by the fuzzy algorithm have to be converted to crisp values by using the method of defuzzification. Subsequently, the approximate centre of gravity (COG) method, supposed to be the most accurate method to get a crisp value is used for the defuzzification, as shown in equation 5.6

$$\mu_D = COG = (\sum w_i \mu(i))/\sum \mu_i \quad (5.6)$$

d- Fuzzy logic controller results

The duty cycle of Buck-Boost converter is adjusted using FLC in Matlab editor. Mamdani method is used in FLC with min-max composition. After the rules have been applied, the center of area as a deffuzification method is used to find the change in duty cycle as crisp output. The FLC that controlled the duty cycle of DC-DC Buck-Boost is simulated in MATLAB to track maximum power point voltage that predict by ANFIS model. The system is implemented with positive and negative values of ΔV and several values of short circuit current.

The following figure5.16 shows the different steps of controlling the duty cycle D of the Cuk converter by FLC, as follows:

(a): Short circuit current Isc input membership function

(b): ΔV input membership function

(c) : FLC output control signal

(d): If-then fuzzy rules

(e): Rule viewer results

(f): Surface viewer results

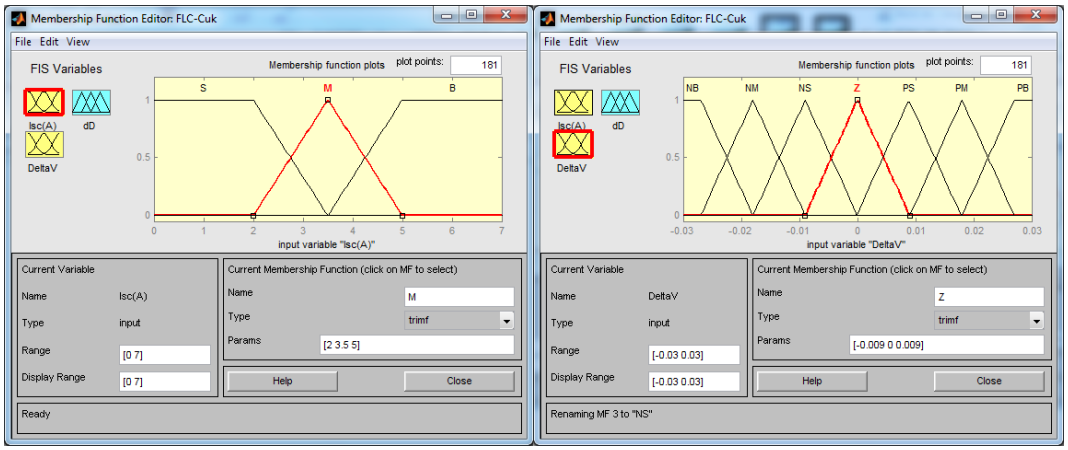

(a) (b)

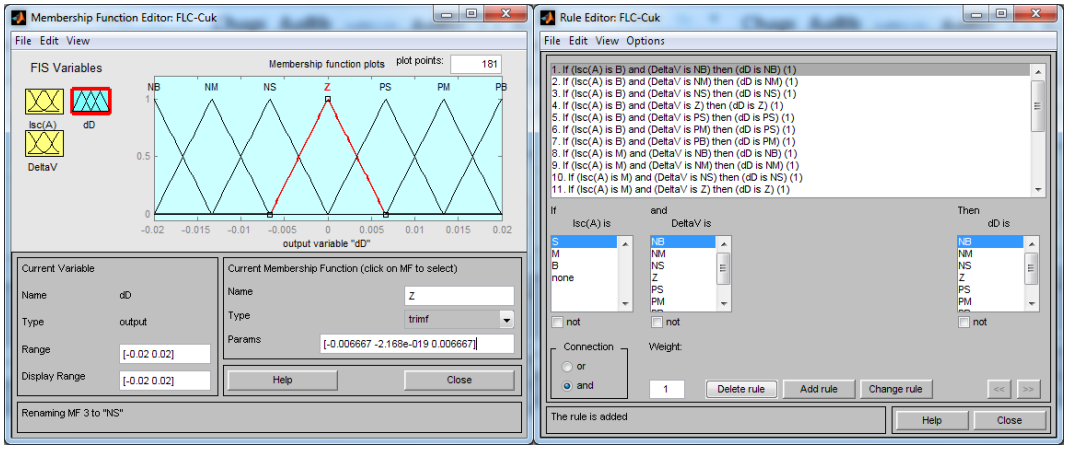

(c)(d)

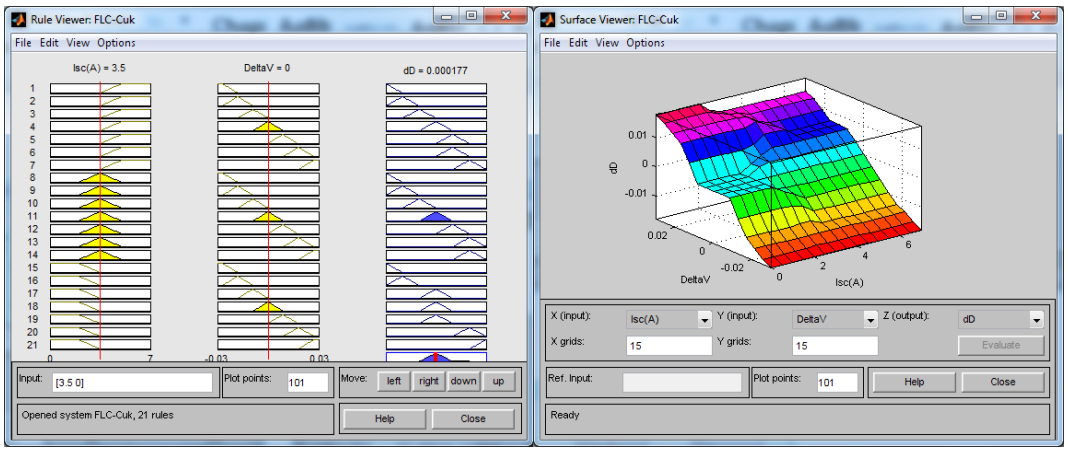

(e) **(f)**

Figure 5.16: The FLC-Cuk converter through Matlab simulation

General Conclusion

A direct coupling Photovoltaic Water Pumping System (PVPS) optimal design has been investigated in this thesis. The current work is a result of fruitful experiment test carried out in our Photovoltaic Water Pumping Laboratory, at Applied Research Unit for Renewable energies, in Ghardaia, Algeria. With a real data base of characterization tests under outdoor conditions of the local site, an optimal PVPS design has been sized and studied. Through different dimensioning steps, the PV generator peak power as well as its nominal configuration has been occurred. A simple but efficient mathematical model has been investigated in the aim to overcome the mismatch of the Demand/Supply energy in such system, which need to be developed. Theoretical studies of Maximum power point tracking using artificial intelligent algorithm techniques were used and then, through Matlab simulation, a proposed scheme has been discussed in the purpose to improve adaptation between the PV generator and the load (pump).This model is a method to investigate the performance of the whole PV water pumping system and verifies functionality and benefits of such dimensioning and modeling. The objective aim is to achieve an optimal low cost and adapted PVPSerection. The results validated averredthat this design cansignificantly increase the efficiency of energy production from PV and the performance of the PV water pumping system compared to the system with battery storage.

In this context the most realistic sizing and modeling options are reviewed and general design guidelines about optimal are given. The different part of the study verified the optional method to be usedinfinding optimal operation and control.

A methodology on how to perform a combined optimization of the system design and operation was outlined and recommended for future work.

Annexes

Training , testing , Checking program

```
clear all
load isofoton2x6.mat
Tot=[Dataglobal129;Dataglobal1568;Dataglobal1668;Dataglobal1768;Datagl
obal238;Dataglobal319;Dataglobal338;Dataglobal519;Dataglobal538;Datagl
obal728];
r=[3,5];
Tot(:,r)= [];
test=[Dataglobal1768;Dataglobal238;Dataglobal319;Dataglobal728];
check=[Dataglobal129;Dataglobal1668;Dataglobal338;Dataglobal519];
lairn=[test;Dataglobal1568;Dataglobal538];
lairn(:,r)= [];
test(:,r)= [];
check(:,r)= [];

x = lairn(:,1:2);
y = lairn(:,3);
trnData = [x y];
x1 = check(:,1:2);
y1 = check(:,3);
chkData = [x1 y1];
x2 = test(:,1:2);
y2 = test(:,3);
testData = [x2 y2];
numMFs = [4 3];
mfType = 'gaussmf';
epoch_n = 300;
in_fis = genfis1(trnData,numMFs,mfType);
[out_fis1,error1,ss,out_fis2,error2] =
anfis(trnData,in_fis,300,[],chkData);
figure(3)
axes1 = axes('Parent',figure(3));
box(axes1,'on');
hold(axes1,'all');
% plot([error1 error2]);
plot1 = plot(1:300,error1,'-ob', 1:300,error2,'-og');hold on;
xlabel('Epochs');
ylabel('RMSE (Root Mean Squared Error)');
title('Error Curves');

% Create axes


% Create multiple lines using matrix input to plot
set(plot1(1),'Color',[0 0 1],'DisplayName','Training');
set(plot1(2),'MarkerEdgeColor',[0 0.498 0],'Color',[0 0.498 0],...
    'DisplayName','Checking');
legend1 = legend(axes1,'show');
```

```
set(legend1,'EdgeColor',[1 1 1],'YColor',[1 1 1],'XColor',[1 1 1]);



% plot(error1)
% hold on
% figure(2)
% plot(y,evalfis(x,out_fis));
% % legend('Training Data','ANFIS Output');
% hold on
```

Learning program

```
clearall
loadisofoton2x6.mat
Tot=[Dataglobal129;Dataglobal1568;Dataglobal1668;Dataglobal1768;Datagl
obal238;Dataglobal319;Dataglobal338;Dataglobal519;Dataglobal538;Datagl
obal728];
r=[3,5];
Tot(:,r)= [];
test=[Dataglobal1768;Dataglobal238;Dataglobal319;Dataglobal728];
check=[Dataglobal129;Dataglobal1668;Dataglobal338;Dataglobal519];
lairn=[check;Dataglobal1568;Dataglobal538];
lairn(:,r)= [];
test(:,r)= [];
check(:,r)= [];

x = lairn(:,1:2);
y = lairn(:,3);
trnData = [x y];
x1 = check(:,1:2);
y1 = check(:,3);
chkData = [x1 y1];
x2 = test(:,1:2);
y2 = test(:,3);
testData = [x2 y2];
numMFs = [4 3];
mfType = 'gaussmf';
epoch_n = 300;
in_fis = genfis1(trnData,numMFs,mfType);
[out_fis1,error1,ss,out_fis2,error2] =
anfis(trnData,in_fis,300,[],chkData);
figure(3)
axes1 = axes('Parent',figure(3));
box(axes1,'on');
hold(axes1,'all');
% plot([error1 error2]);
plot1 = plot(1:300,error1,'-ob', 1:300,error2,'-og');hold on;


% Create axes


% Create multiple lines using matrix input to plot
set(plot1(1),'Color',[0 0 1],'DisplayName','Training');
set(plot1(2),'MarkerEdgeColor',[0 0.498 0],'Color',[0 0.498 0],...
'DisplayName','Checking');
xlabel('Epochs','FontSize',12);
ylabel('RMSE (Root Mean Squared Error)','FontSize',12);
```

```
title('Error Curves','FontSize',12);

legend1 = legend(axes1,'show');
set(legend1,'EdgeColor',[1 1 1],'YColor',[1 1 1],'XColor',[1 1 1]);




% plot(error1)
% hold on
% figure(2)
% plot(y,evalfis(x,out_fis));
% % legend('Training Data','ANFIS Output');
% hold on
```

Advantages and Disadvantages of PV powered System

System Type	Advantages	Disadvantages
PV Powered System	• Low maintenance • Unattended operation • Reliable long life • No fuel and no fumes • Easy to install • Low recurrent costs • System is modular and closely matched to need	• Relatively high initial cost • Low output in cloudy weather
Diesel (or Gas) Powered System	• Moderate capital costs • Easy to install • Can be portable • Extensive experience available	• Needs maintenance and replacement • Site visits necessary • Noise, fume, dirt problems • Fuel often expensive and supply intermittent
Windmill	• No fuel and no fumes • Potentially long-lasting • Works well in windy sites	• High maintenance • Seasonal disadvantages • Difficult find parts thus costly repair • Installation is labor intensive and needs special tools

PV module Isofoton (110/24) Characteristics

isofotón

I-110

Photovoltaic module

CHARACTERISTICS	I-110/12	I-110/24
PHYSICAL		
Dimensions	1310 x 654 x 39,5 mm	
Weight	11,5 kg	
Number of cells in series	36	72
Number of cells in parallel	2	1
NOCT (800 W/m², 20 ºC, AM 1.5, 1m/s)	47 ºC	
ELECTRICAL (1000 W/m², 25 ºC cell, AM 1.5)		
Nominal voltage (V_n)	12 V	24 V
Maximum power (P_{max})	110 W_P ± 10 %	
Short-circuit current (I_{sc})	6,76 A	3,38 A
Open circuit voltage (V_{oc})	21,6 V	43,2 V
Maximum power current (I_{max})	6,32 A	3,16 A
Maximum power voltage (V_{max})	17,4 V	34,8 V
CONSTRUCTIVE		
Cells	Single-crystal Si, textured and antireflectivity layered	
Contacts	Redundant contacts on each cell for circuit reliability	
Laminate	EVA (ethylene vinyl acetate)	
Front face	Tempered glass with improved light transmission	
Back face	Tough multi-layered backsheet Tedlar	
Frame	Anodised aluminium	
Connection boxes	IP 65 with built-in bypass diodes	
Grounding connection	Yes	
Specifications	IEC 61215 and Class II by TÜV certificate	
Cable section	4-10 mm2	
Connection box	Pression screw with possibility of soldering/ optional multi-contact	

6th Ed. 02/2002

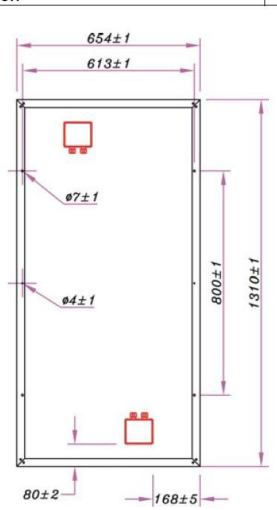

BACK VIEW I-110/12

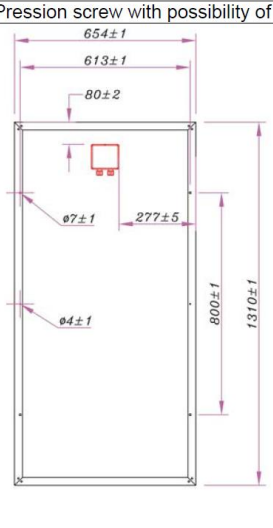

BACK VIEW I-110/24

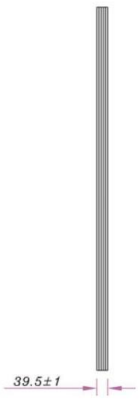

SECTION

Bibliography

[1] A. Maafi."A survey on photovoltaic activities in Algeria"; Renewable Energy, volume 20 year 2000.

[2] Azzedine BOUTELHIG 1, Yahia BAKELLI 1and Amar HADJ ARAB 2 :Promotion of Photovoltaic Water Pumping System (PVPS) for irrigation in Desert Regions (Ghardaia/Algeria)', "Journal of Agricultural Machinery Science", Turkey, Volume 4, Number2- ISSN 1306 – 0007 , Year 2008 ISSN 1306 – 0007 .

[3] Azzedine BOUTELHIG [1], Yahia BAKELLI [1]and Amar HADJ ARAB [2]: " Study and implementation of a stand-alone photovoltaic water pumping system (PVPS) in desert region, Ghardaia, Algeria.", 1st International Conference on Energy conversion and Conservation' Sousse/Tunisia' 11 – 13 April 2008.

[4] Azzedine BOUTELHIG [1], Yahia BAKELLI [1] , I. Hadj Mahammed[1] and Amar HADJ ARAB [2] "Performances study of different PV powered DC pump configurations for an optimum energy rating at different heads under the outdoor conditions of a desert area", Energy, volume 39, Mars 2012.

[5] L.C. Christ." Principles of Solar Energy Conversion", Energy, Volume 1, Pages 293–313, May 2012

[6] W.G.J.H.M Van Sark, "Introduction to Photovoltaic Technology", Utrecht university, Utrecht, The Netherlands, Energy, Volume 1, Pages 5- 11, May 2012.

[7] E. Antolín, A. Martí, A. Luque, "Intermediate Band Solar Cells", Comprehensive Renewable Energy, Volume 1, 2012, Pages 619-639, May 2012.

[8] A.H Lobbre Masters, Gilbert M. Renewable and Efficient Electric Power Systems John Wiley & Sons Ltd, 2004

[9] Yogi Goswami, "Principle of solar engineering", University of Colorado, USA

[10] Becquerel AE, Comt Rend. Academie d. Sciences 9 (1839) p. 561

[11] Renewable and efficient electric power systems. Gilbert M. Masters. ISBN 0-471 28060-7, 2004, John Wiley & Sons, Inc.

[12] Chapin DM, Fuller CS, Pearson GL, J. Appl. Phys. 25 (1954) p. 676

[13] A.H Lobbre Masters, Gilbert M. Renewable and Efficient Electric Power Systems John Wiley & Sons Ltd, 2004

[14] T. Muneer "Solar Radiation and Daylight Models". Napier University, Edinburgh - Elsevier copyright 1997, 2004, Elsevier

[15] Masters, Gilbert M. *Renewable and Efficient Electric Power Systems* John Wiley & Sons Ltd, 2004

[16] Florida solar energy center,"Photovoltaic system Design" ,April 1996.

[17] Messenger, Roger & Jerry Ventre Photovoltaic Systems Engineering 2nd Edition CRC Press, 2003

[18] A. Boutelhig, A. Guessoum and A. Hadjarab "New *model estimation for an optimum energy exploitation of a stand-alone photovoltaic water pumping system (PVPS)*", Seep2012 conference proceeding, Dublin City University, Ireland, June 2012.

[19] Castañer, Luis & Santiago Silvestre Modelling Photovoltaic Systems, Using PSpice John Wiley & Sons Ltd, 2002

[20] Green, Martin A. Solar Cells; Operating Principles, Technology, and System Applications Prentice Hall Inc., 1982

[21].Wei Chena,b, HuiShenc,_, BifenShuc, Hong Qind, Tao Dengc, *Evaluation of performance of MPPT devices in PV systems with storage batteries. Renewable Energy* 32 (2007) 1611–1622

[22].Robert Kroni, Gabi Friesen, Robert Kenny, Wilhelm Durisch, *Energy Rating for Solar Modules. Final Report PV P+D, DIS 47456 / 87538, Swiss Federal Office of Energy,* February 2005

[23] Friedrich Sick and Thomas Erge , " Photovoltaic in building" , International Energy Agency ' 1996

[24] F Lasnier and TG Ang., "Photovoltaic Engineering Handbook", IOP

[25] L. Kottas,S. Boutalis and D. Karlis, "New Maximum Power Point Tracker for PV Arrays Using Fuzzy Controller in Close Cooperation With Fuzzy CognitiveNetworks", IEEE Transaction on Energy Conversion, VOL. 21, NO. 3, September 2006,pp. 793-803.

[26] Bogdan M. Wilamowski and Xiangli Li, "Fuzzy System Based MPPT for PV System", IEEE2002 pp3280-3284

[27]Hussein, K. H., I. Muta, T. Hoshino, & M. Osakada "Maximum Photovoltaic Power Tracking: an Algorithm for Rapidly Changing Atmospheric Conditions" IEEEProceedings – Generation, Transmission and Distribution – v. 142 January 1995, page 59-64

[28] R. M. Hilloowala and A. M. sharaf, "A Rule-Based Fuzzy Logic Controller for A PWM Inverter in Photovoltaic Energy Conversion Scheme", Proceedings of the IEEE Industry Application Society Annual Meeting, Oct. 1992, pp. 762-769.

[29] A. Boutelhig, Y. Bakelli, I. Hadj mahammed, "performances study of PV powered

DC Shurflo pump model for an optimum energy use for different heads under outdoor conditions of desert area", Seep 2010, bari, Italy, June 2010.

[30]Mohamed M. Algazar a, Hamdy AL-monier b, HamdyAbd EL-halim a, MohamedEzzat El Kotb Salem " maximum power point using Fuzzy logic Control (FLC)", Electrical power and Energy systems, volume (39), 2012.

[31] N.Femia, G.Petrone. Optimization of perturb and observe maximum power point tracking method. IEEE Power Electron. , vol.20, no4, pp.963-973, Jul.2005.

[32] Anil K.Raia,n, N.D.Kaushika b, BhupalSingh a, NitiAgarwal b, "Simulation model of ANN based maximum power point tracking controller for solar PV system," , Solar Energy Materials & Solar Cells 95 (2011) 773–778.

[33] Amir Gheibi*, S.M.A.Mohammadi, M.maghfoori, "Maximum Power Point Tracking of Photovoltaic Generation Based on the Type 2 Fuzzy Logic Control Method" Energy Procedia 12(2011)538- 546.

[34] Mellit A, Kalogirou SA. Artificial intelligence techniques for photovoltaic applications: areview. Progr Energy Combust Sci 2008; 34:547–632.

[35] S. N. Singh ,Monika, K. PallaviJha, MadhuBala.,Sustainable Energy and Environmental Management in solar Powered Adaptative Fuzzy Control Model for Ground Water Conservation in Suburban Areas, International Journal of Engineering Science and Technology,Vol.3 N°.5 May 2011.

[36] Atlas IH, Sharaf AM. A novel maximum power fuzzy logic controller for photovoltaic solar energy systems. Renew Energy 2008;33:388–99.

[37] Z. Salameh, D. Taylor, Step-up maximum power point tracker for photovoltaic arrays, Solar Energy 44 (1990) 57–61

[38] Y.M. Chiang, L.C. Chang, M. J. Tsai, Y.F. Wang and F. G. Chang, "Auto-control of pumping operations in sewage systems by rule-based fuzzy neural networks," Hydrogen and earth system science., vol. 15, pp. 185–196, 2011

[39] C.-Y. Won, D.-H.Kim, S.-C.Kim, W.-S.Kim, and H.-S. Kim, "A new maximum power point tracker of photovoltaic arrays using fuzzy controller", in 25th Annu. IEEE PESC Jun. 20–25, 1994, vol. 1, pp.396–403

[40] A.H Lobbrecht and D.P. Solomatine., Control of Water Levels in Polder Areas using Neural Networks and Fuzzy Adaptative Systems, Water and Industry System. Baldock, UK, vol. 1.pp 509 – 518, 1999.

[41]Jang JSR. ANFIS: adaptive network-based fuzzy inference system. IEEE Transactions on Systems, Man and Cybernetics Part C 1993;23:665e85

[42] Patcharaprakiti and S. Premrudeepreechacharn,"Maximum Power Point Tracking Using Adaptive Fuzzy Logic Control for Grid-Connected Photovoltaic System", IEEE 2002, 372-376

[43]A.M.A. Mahmoud, H.M. Mashaly, S.A. Kandil, H. El Khashab, and M.N.F. Nashed, "Fuzzy Logic Implementation For Photovoltaic Maximum Power Tracking", Proceedings 9th IEEE International Workshop on Robot and Human Interactive Communication, pp. 155 –160, 2000

[44] M. Veerachary, T. Senjyu, K. Uezeto, Feed forward maximum power point tracking of PV systems using fuzzy controller, IEEE Transactions on Aerospace and Electronic System 38 (3) (2002) 969–981.

[45] V. Salas, E. Olias, A. Barrado, A. Lazaro, Review of the maximum power point tracking algorithms for stand-alone photovoltaic systems, Solar Energy Material and Solar Cells 90 (11) (2006) 1555–1578.